# 6: Interactions of *S*. Typhi and *S*. Paratyphi A with the hiPSC-derived iHO epithelium and macrophages

## Collaboration note:

The data in this chapter on supernatants from infected iHO and macrophages were generated jointly with Amber Barton, a PhD student from Oxford Vaccine Group. She has generated data from whole blood samples from those challenged with *S*. Typhi as part of the Vaccines Against Salmonella Typhi (VAST) study, (https://www.hra.nhs.uk/planning-and-improving-research/application-summaries/research-summaries/vaccines-against-salmonella-typhi-vast/), and it was felt best to use the same equipment and assay reagents in order to produce a comparable dataset from iHO and macrophage supernatants future analysis and publication. The TEM images for this chapter were produced by David Goulding and Claire Cormie, and analysis of the bulk RNA-Seq data was completed in collaboration with Artika Nath, a postdoctoral fellow with the Inouye group at the Baker Institute in Melbourne.

### 6.1 Introduction

Having used the hiPSC-derived iHO model to explore host-pathogen interactions with a number of enteric bacteria, and demonstrated its utility for untangling intracellular mechanisms during infection, the model was next used to explore interactions with human-restricted pathogens such as *S*. Typhi and *S*. Paratyphi A in the CL3 laboratory. Relatively few studies have been undertaken with these pathogens using human gut epithelium. Additionally, the availability of increasing amounts of *in vivo* data on *S*. Typhi and *S*. Paratyphi infections from the human challenge model, currently being carried out by the Oxford Vaccine Group, make comparisons between *in vivo* and *in vitro* approaches feasible.[1] These datasets could provide a valuable comparator to help intuit how much we can learn from the iHO model and how well this relates to *in vivo* infection. The bacterial strains chosen for the initial iHO and macrophage assays therefore match those used in the human

typhoid and paratyphoid challenge studies. The bacterial strain used for the human challenge typhoid work was *S*. Typhi Quailes, chosen for the fact that it is a well-phenotyped, virulent isolate, has been mapped on the *S*. Typhi phylogenetic tree,[2] expresses the Vi capsule,[3] is fully antibiotic sensitive[3,4] and the human infectious dose is known.[4] The isolate used for paratyphoid challenge was NVGH308, which is a Nepalese clinical isolate from 2006; it is susceptible to most commonly used antibiotics and is a contemporary circulating strain from an endemic setting.[5] Given that both *S*. Typhi and *S*. Paratyphi A show limited sequence diversity,[6] it was felt that the immune response to these isolates could translate to other wild type strains.

Having established the infection model in Kolf2 derived iHO, it was also of interest to use this same genetic background to look at interactions with elements of the immune system missing from the iHO model; in this case macrophages. Hale and colleagues have set up reliable methods of differentiating macrophages from hiPSC, phenotyping them via RNA-Seq, imaging and the analysis of cell surface markers and have simulated infections in this model.[7] In comparison to THP-1-derived macrophages, iPSC-derived macrophages demonstrate a more robust cytokine response and increased killing ability, and have proven a reliable model for study of *Salmonella* and *Chlamydia trachomatis* infections.[7]

Following the work using an antimicrobial sensitive clinical reference *S*. Typhi strain, the range of isolates investigated was expanded to include currently circulating and antibiotic resistant isolates. This was, in part, to assess whether the host response to Quailes was translatable to other wild-type isolates. These included the antibiotic sensitive *S*. Typhi E02-1180 SGB90, which is a clinical isolate from India in 2002. In addition, two representatives of the H58 clade were selected; both isolates were from Kenya in 2007, one from lineage 4.3.1.1 (2010K-0517 116TY) and one from lineage 4.3.1.2 (2010K-0515 101TY). H58 are frequently antibiotic resistant and this population initially expanded in South Asia, likely due to antibiotic selection.[8] The lineage has disseminated throughout Asia and into Africa, displacing antibiotic-susceptible strains and driving disease epidemics.[9] There are relatively few SNPs differences between the numerous H58 isolates that have been sequenced, fitting in with other evidence for their recent clonal expansion.[9] A major concern about H58 *S.* Typhi is their ability to gather additional resistance determinants via plasmids which provide

further mechanisms of resistance to antibiotics, such as has occurred in the recent extensively drug-resistant (XDR) typhoid outbreak in Pakistan.[10] Not all H58 strains have a gyrA mutation and other haplotypes which are antibiotic sensitive are persisting in many typhoid endemic regions. Of the H58 isolates sequenced in the study by Wong et al,[9] 68% harboured antibiotic resistance genes. There has recently been suggestion that increased severity of disease may be associated with H58 isolates, a phenotype which is not strictly related to antibiotic sensitivity. In a Vietnamese study, MDR status was not associated with severe disease, whereas intermediate sensitivity to Ciprofloxacin (and likely H58 status) was.[11] Similarly, there has been a recent outbreak of typhoid with severe complications in the Yucatan region of Mexico, in which strains were largely antibiotic sensitive. Sequencing of isolates to confirm whether they are of the H58 clade has not yet been reported.[12]

Here we investigate the hypothesis that it would be possible for *S*. Typhi and *S*. Paratyphi to invade IEC in the iHO model, with the expectation that typhoid-causing serovars would be less invasive than *S*. Typhimurium, given the limited local immune response that is thought to occur to these pathogens *in vivo*. We also thought it likely that transcriptional responses to these pathogens would vary depending on whether they were infecting IECs or macrophages, with a comparatively less inflammatory picture being produced in both compartments by the typhoid-causing serovars, although very little is known about the response to *S*. Paratyphi A from previous experimental models. Lastly, we hypothesised that H58 serovars of S. Typhi may generate a different transcriptomic response to non-H58 strains, given their apparent ability to cause severe disease beyond reliance on drug resistance mechanisms.

### 6.2 Generation and phenotyping of alternative iHO lines for use in assays

Given that this was the first occasion on which *S*. Typhi and *S*. Paratyphi isolates were being used in the iHO model, it was felt prudent to generate two further iHO lines from healthy volunteer hiPSC present in the HipSci consortium collection. This would assess if the response to infection exhibited in the Kolf2 iHO (whilst well phenotyped and widely used in multiple bioassays) was representative of human responses. Therefore, iHO were generated from the Sojd2 and Rayr2 cell lines, and phenotyped prior to infection, via RT-qPCR and

immunostaining, as outlined in 3.1 (**Figures 3.1-3.3**). No reproducible differences between the iHO generated from the different cell lines were detected during phenotyping.

## 6.3 Studies on the interactions of *S*. Typhi and *S*. Paratyphi A with hiPSC-derived iHO

### 6.3.1 Establishing infectivity in the iHO model

Given the information gleaned using *S*. Typhimurium SL1344 in the Kolf2 iHO, *S*. Typhi (Quailes) and *S*. Paratyphi (NVGH308) infections were first tested in iHO derived from this cell line. Microinjections were completed as outlined in 2.3, with iHO harvested at 1.5 hours and 3 hours after microinjection. Both microorganisms appeared to invade the epithelium, with viable CFU being recovered intracellularly following injection and incubation (**Figure 6.1**) . *S*. Typhi was less invasive than *S*. Paratyphi, which fits with literature from 2-D cell models.[13] Given the wealth of data already generated on *S*. Typhimurium SL1344 in the iHO, assays in this chapter do not include this pathogen but references to the numbers of *S*. Typhimurium SL1344 invading Kolf2 iHO across a number of experiments are included in **Figure 6.1.** Comparatively fewer *S*. Paratyphi A had invaded the iHO epithelium, compared to counts normally observed for SL1344, by the 1.5 hour timepoint, but this difference was lost at 3 hours. Starting inoculum was checked to be comparable across all groups by microinjecting directly into 100 μL DPBS, followed by dilution, incubation and colony counting (**Figure 6.1**).

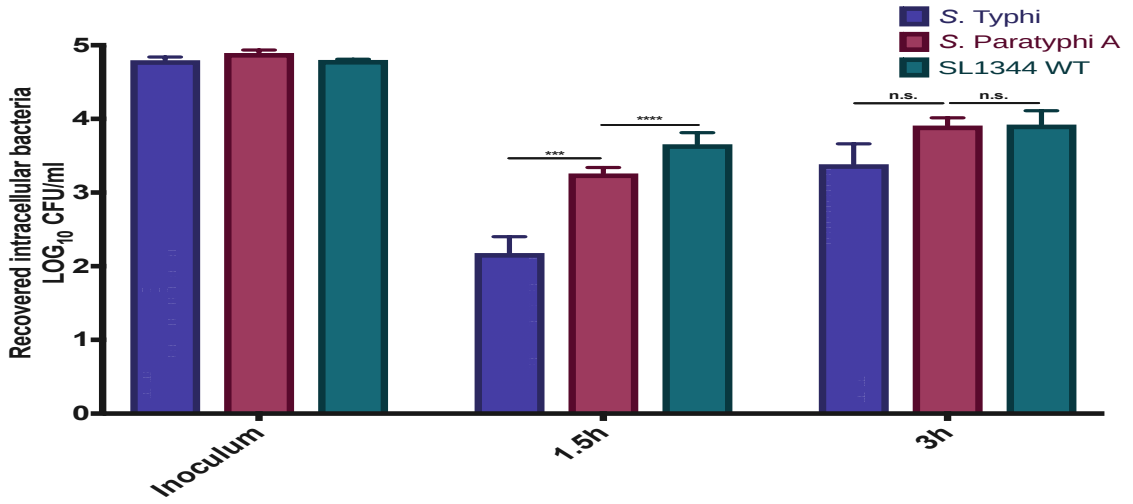


**Figure 6.1: Intracellular bacterial counts for *S.* Typhi and *S.* Paratyphi A in Kolf2 iHO.** Kolf2 iHO were injected with *S.* Typhi (Quailes) or *S.* Paratyphi A (NVGH308) and incubated for 1.5 or 3 hours, prior to undergoing modified gentamicin assays to recover intracellular bacteria. Data presented are for 3 biological replicates (each averaged from 3 technical replicates), with 30 iHO injected per replicate +/- SEM. Unpaired Mann-Whitney tests were used for all assays (n.s. – not significant, *** p< 0.001, **** p < 0.0001). There were significantly fewer intracellular *S.* Typhi recovered compared to *S.* Paratyphi A or SL1344 at the 1.5 hour timepoint, but by 3 hours post infection there were no differences in intracellular counts between these pathogens.

These assays were then performed in iHO generated from the Rayr2 and Sojd2 cell lines (**Figure 6.2**). Interestingly, a similar pattern of invasion was detected in the Sojd2 iHO to the Kolf2, with a difference in counts at 1.5 hours post-infection, which had resolved at 3 hours. In the Rayr2 iHO however, there was no initial difference in recovered counts, but by 3 hours, significantly more *S.* Paratyphi A were recovered from the iHO lumen.

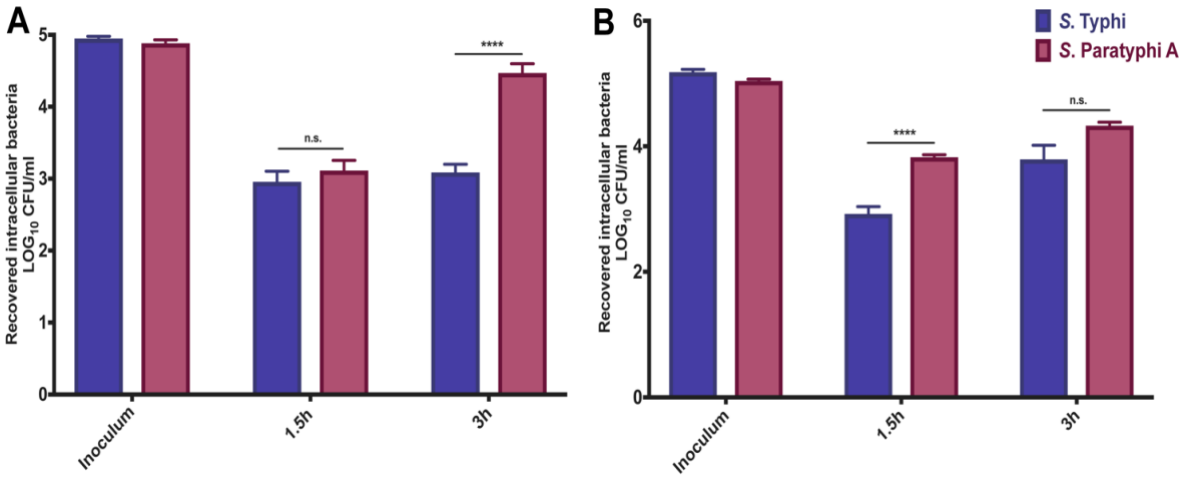


**Figure 6.2: Intracellular bacterial counts for *S.* Typhi and *S.* Paratyphi A in Rayr2 and Sojd2 iHO.** iHO generated from Rayr2 and Sojd2 hiPSC were injected with *S.* Typhi (Quailes) or *S.* Paratyphi A (NVGH308) and incubated for 1.5 or 3 hours, prior to undergoing modified gentamicin assays to recover intracellular bacteria. Data presented are for 3 biological replicates (each averaged from 3 technical replicates), with 30 iHO injected per replicate +/- SEM. Unpaired Mann-Whitney tests were used for all assays (**n.s.** – not significant, **** p < 0.0001). (**A**) In Rayr2 iHO, there was no significant difference between bacterial counts recovered at 1.5 hours post infection, but significantly more viable *S.* Paratyphi A at 3 hours. (**B**) The pattern observed in the Sojd2 iHO mirrors that in the Kolf2 line of an initial difference in counts which was lost by 3 hours post-infection.

Given these initial differences in invasion between the two isolates, assays were performed to assess the viable counts of bacteria in the lumen of the iHO following infection. These were performed by the bulk harvesting of the luminal contents at 1.5 and 3 hours post-infection in the Kolf2 cell line (**Figure 6.3A**). There was no significant difference in counts recovered from the lumen at 1.5 or 3 hours between the groups, and no large increase in counts within the lumen by 3 hours, suggesting an equilibrium between bacterial death and replication over this time period.

To establish whether the increase in intracellular *S*. Typhi observed at 3 hours was due to increased invasion or intracellular replication, a modified gentamicin protection assay was completed, with cells incubated for 1.5 hours post-infection. Cells were either lysed following the gentamicin incubation as normal, or washed and re-incubated for a further hour to check for any increase in counts over this time (**Figure 6.3B**). As previously observed in the Kolf2 iHO, there were significantly more intracellular *S*. Paratyphi A recovered at 1.5 hours post infection. There was no significant difference in counts recovered after the additional incubation period in either group, suggesting limited intracellular replication, and that the higher counts observed at the 3 hour timepoint were likely due to further invasion. Ideally, a longer additional incubation step could have been used, to try to allow more time for replication, but unfortunately it was not possible to extend this time point, given restrictions on working hours within the CL3 facility.

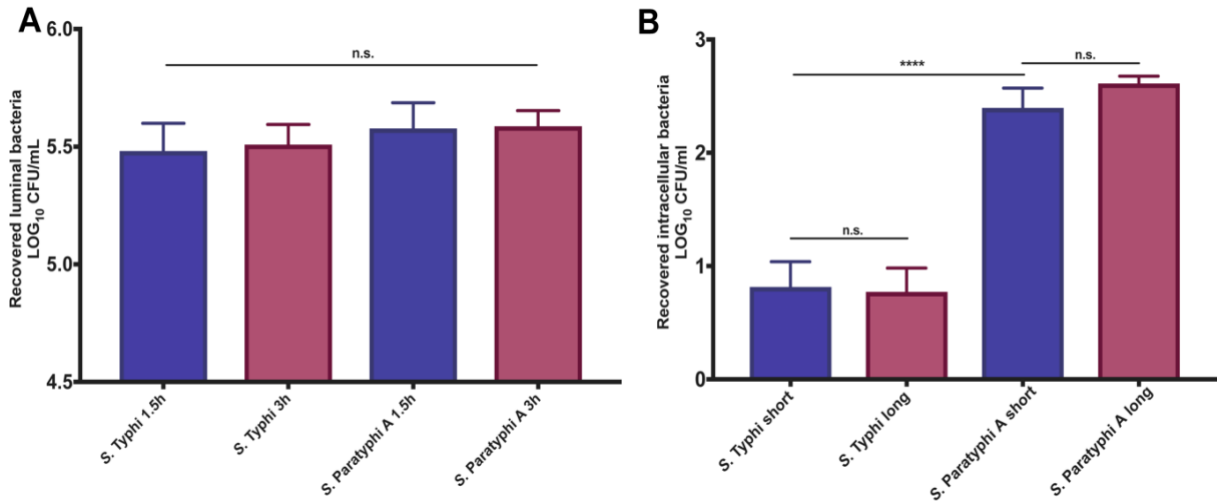


**Figure 6.3: Luminal bacterial counts and extended incubation counts for *S.* Typhi and *S.* Paratyphi A in Kolf2 iHO.** (**A**) Kolf2 iHO were injected with *S*. Typhi (Quailes) or *S*. Paratyphi A (NVGH308) and incubated for 1.5 or 3 hours, prior to recovery of luminal contents. (**B**) After injection with *S*. Typhi or *S*. Paratyphi A, iHO were harvested at 1.5 hours, and either underwent modified gentamicin assay and direct recovery of intracellular contents or were treated with gentamicin and incubated for a further hour prior to recovery of intracellular contents. Data presented are for 3 biological replicates (each averaged from 3 technical replicates), with 30 iHO injected per replicate +/- SEM. Unpaired Mann-Whitney tests were used for all assays (n.s. – not significant, **** $p < 0.0001$). (**A**) There was no significant difference between bacterial counts recovered from the lumen at 1.5 or 3 hours post-infection. (**B**) There was no significant difference in intracellular bacterial counts following an extended incubation period in either *S*. Typhi or *S*. Paratyphi A. As previously observed, there were significantly more intracellular *S*. Paratyphi recovered at the initial harvest 1.5 hours post-infection.

### 6.3.2 Imaging of interactions during infection

Following the intracellular infection assays, the next step towards obtaining information about what was happening within the iHO during infection was to utilise confocal imaging to demonstrate any interaction between the bacteria and epithelium. Images taken at 3 hours post-infection demonstrated the presence of bacteria in the lumen and their close interaction with the epithelium for both *S*. Typhi and *S*. Paratyphi A (**Figure 6.4**).

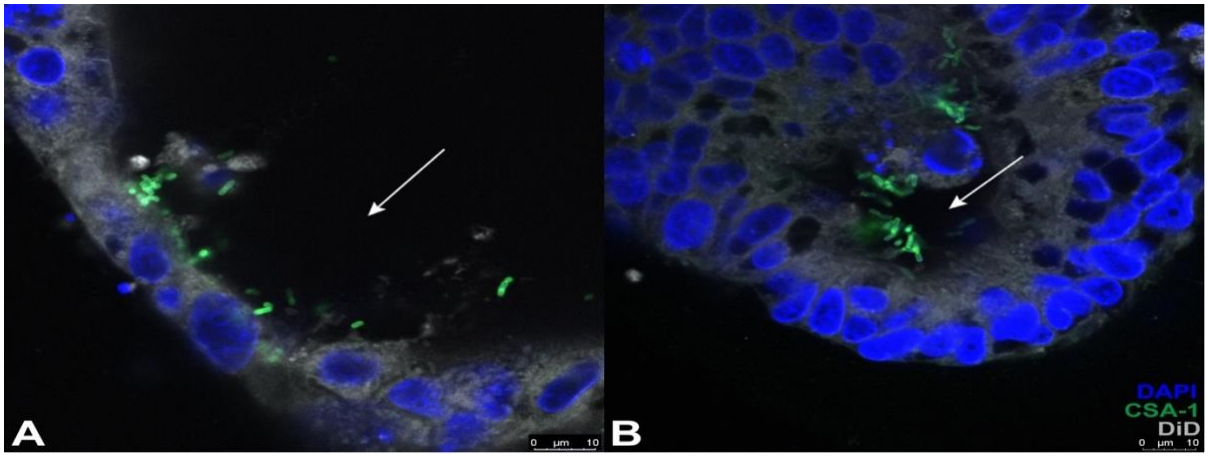


**Figure 6.4: Immunostaining for presence of *S*. Typhi and *S*. Paratyphi A in Kolf2 iHO.** iHO were injected with *S*. Typhi (Quailes) or *S*. Paratyphi A (NVGH308) and incubated for 3 hours prior to fixing and immunostaining. *S*. Typhi (**A**) and *S*. Paratyphi A (**B**) are demonstrated to be in the lumen of the iHO (lumen indicated by arrows), and interacting closely with the iHO epithelium, stained with DiD. Cell nuclei are stained with DAPI and bacteria with CSA-1. Images taken on the Leica SP8 confocal microscope at 20x magnification.

To study these interactions in more detail, TEM imaging was completed, with iHO again being fixed 3 hours after microinjection for both pathogens. Images for *S*. Typhi (**Figure 6.5**) demonstrated bacteria both within the mucus layer, and underneath it, interacting with and attaching to the epithelium. There was also evidence for division of bacteria in the lumen, expression of fimbriae, and expression of the Vi capsule.

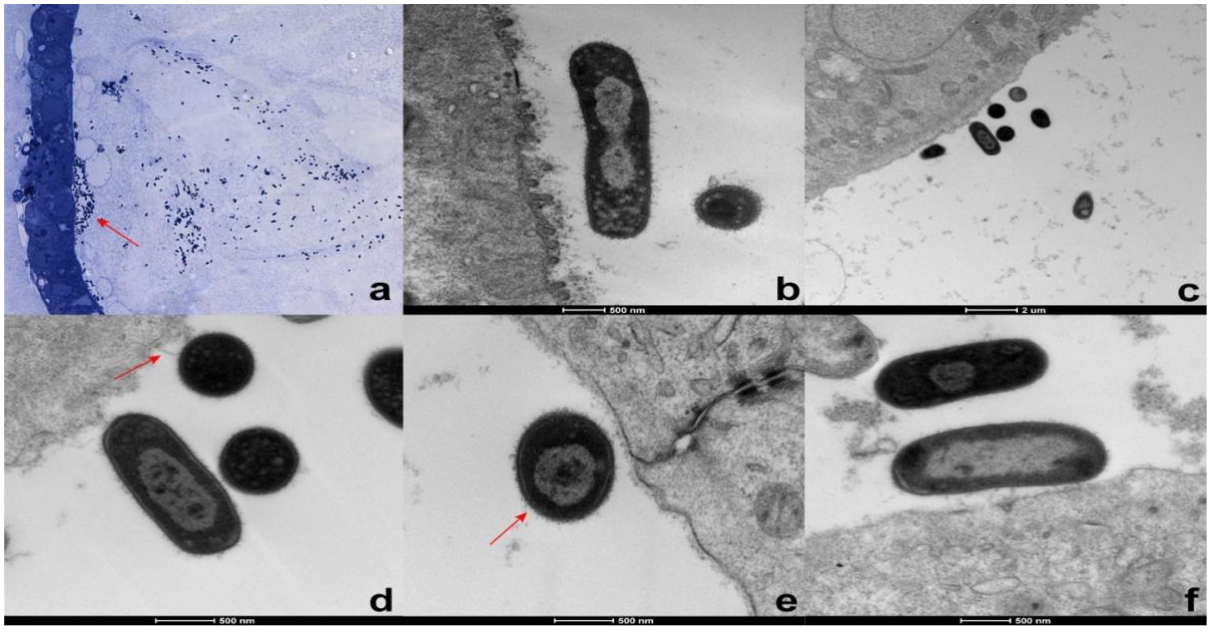


**Figure 6.5: Toluidine blue and TEM images of *S*. Typhi (Quailes) in the iHO lumen.** Kolf2 iHO were injected with *S*. Typhi and incubated for 3 hours prior to fixing. Panel (**a**) shows bacteria within the mucus layer in the lumen, and also having breached this layer, starting to attach to the epithelium (arrow). Shown in (**b**) is a bacterium dividing within the lumen. Panels (**c** & **d**) show bacteria interacting with the brush border of the apical surface of the epithelium, with fimbriae extending from one bacterium (arrow). *S*. Typhi in panel (**e** & **f**) demonstrate the putative Vi capsule being expressed by the bacteria as they interact with the epithelium. Toluidine blue images taken using AxioCam HRm via the Zeiss Axiovert 200M at 63x magnification. TEM images taken using FEI 120kV Spirit BioTWIN TEM and recorded on an F4.15 Tietz charge-coupled device camera.

Images of *S*. Paratyphi A also showed bacteria interacting with the epithelium, dividing within the lumen, expressing fimbriae and in some cases, bacteria expressed long pili, which is previously reported in *S*. Paratyphi C but not *S*. Paratyphi A strains.[14]

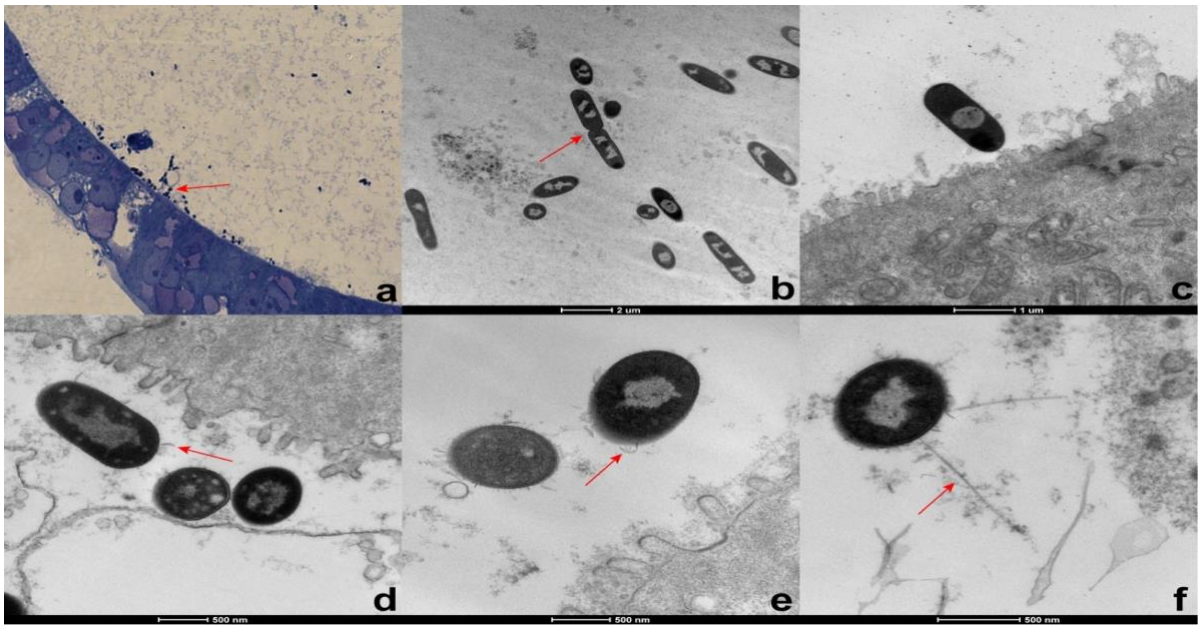


**Figure 6.6: Toluidine blue and TEM images of *S*. Paratyphi A (NVGH308) in the iHO lumen.** Kolf2 iHO were injected with *S*. Paratyphi A and incubated for 3 hours prior to fixing. Panel (**a**) shows bacteria starting to attach to the epithelium (arrow). Shown in (**b**) are bacteria dividing within the lumen. Panels (**c - e**) show bacteria interacting with the brush border of the apical surface of the epithelium, with fimbriae extending from bacteria (arrows). *S*. Paratyphi A in panel (**f**) demonstrates expression of long pili whilst potentially attempting to reach the epithelium. Toluidine blue images taken at 63x magnification.

### 6.3.3 Transcriptomic changes during iHO infection

Having witnessed interactions with iHO, and noted the differences in ability to infect cells between the encapsulated *S*. Typhi and unencapsulated *S*. Paratyphi A and *S*. Typhimurium SL1344, the next step was to analyse transcriptomic changes during each infection. Consequently, iHO were infected for 3 hours with *S*. Typhi (Quailes), *S*. Paratyphi A, *S*. Typhimurium SL1344 or PBS prior to harvesting, RNA extraction and submission for sequencing as outlined in 2.16. PBS replicates were completed as a control to ensure that any signatures were not simply due to the mechanical forces placed upon iHO by the microinjection process. These experiments were completed in iHO from the Kolf2, Rayr2 and Sojd2 lines. Detailed analysis for each line will be presented separately, but QC metrics

for all samples are outlined below (**Table 6.1, Figure 6.7**), demonstrating the similarities in terms of depth and alignment of reads for all cell lines and conditions.

| **Stimulation condition:** | **Cell line:** | **Read depth range:** (million reads) | **Read depth mean:** (million reads) | **Read depth median:** (million reads) |
|---|---|---|---|---|
| *S*. Typhi (Quailes) | Kolf2 | 18.53 – 20.00 | 19.44 | 17.81 |
| | Rayr2 | 17.58 – 19.55 | 18.39 | 18.04 |
| | Sojd2 | 18.52 – 21.20 | 19.88 | 19.90 |
| *S*. Paratyphi A (NVGH308) | Kolf2 | 20.05 – 21.27 | 20.72 | 20.85 |
| | Rayr2 | 17.88 – 19.36 | 18.51 | 18.30 |
| | Sojd2 | 19.35 – 20.89 | 19.90 | 19.46 |
| *S*. Typhimurium SL1344 | Kolf2 | 19.98 – 20.78 | 20.30 | 20.13 |
| | Rayr2 | 18.51 – 20.86 | 19.44 | 18.96 |
| | Sojd2 | 19.06 – 22.49 | 20.70 | 20.56 |
| PBS | Kolf2 | 18.77 – 24.14 | 21.10 | 20.39 |
| | Rayr2 | 19.34 – 20.16 | 19.64 | 19.43 |
| | Sojd2 | 19.82 – 22.17 | 20.91 | 20.75 |

**Table 6.1: Summary of raw RNA-Seq reads for each stimulation condition at sample level.** Kolf2, Rayr2 and Sojd2 iHO were injected with *S*. Typhi, *S*. Paratyphi A, *S*. Typhimurium or PBS and incubated for 3 hours prior to RNA extraction and sequencing, with 3 biological replicates completed per condition. Data were concatenated from lane-level reads and demonstrate similarities across groups in terms of depth of sequencing.

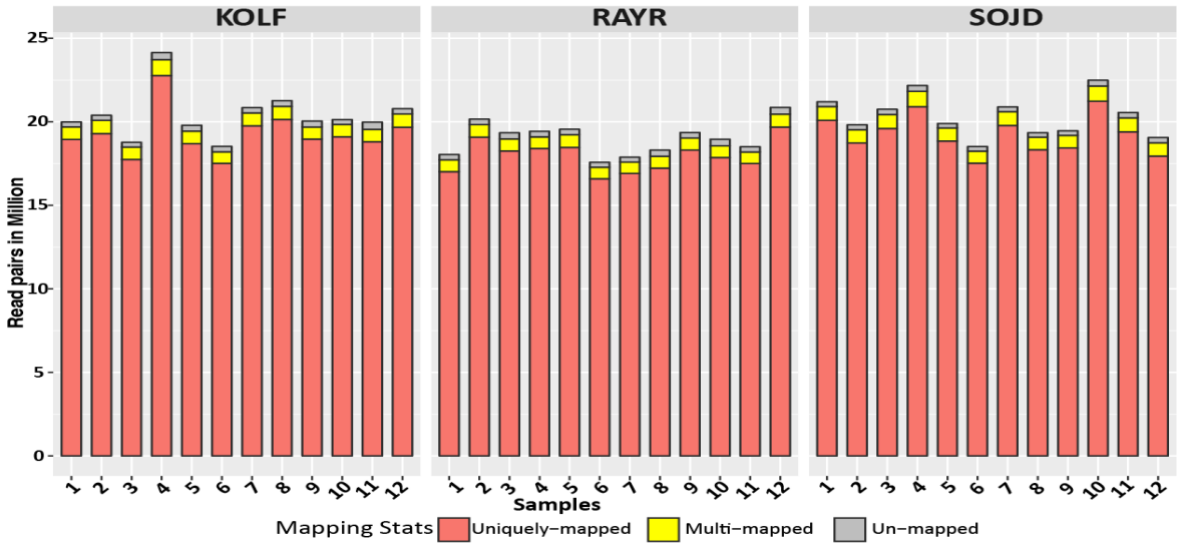


**Figure 6.7: Alignment summary.** Kolf2, Rayr2 and Sojd2 iHO were injected with *S*. Typhi, *S*. Paratyphi A, *S*. Typhimurium or PBS and incubated for 3 hours prior to RNA extraction and sequencing with 3 biological replicates completed per condition. Raw reads were aligned to hg19 genome. 94.13 – 95% of the reads uniquely mapped to the hg19 genome. This was consistent for all samples across all cell lines.

Count data for all samples were obtained from featureCounts,[15] which enumerated 26,364 genes**.** All lowly expressed genes across the 36 samples were removed, leaving 12,061 genes. Samples were normalised by library size and gene length, FPKM (Fragments Per Kilobase of transcript per Million mapped reads) values obtained and principal component analysis (PCA) performed (**Figure 6.8**). This demonstrated that the primary source of variance within the data was cell line (PC1 and PC2), explaining 50.10% and 35.4% of variation respectively.

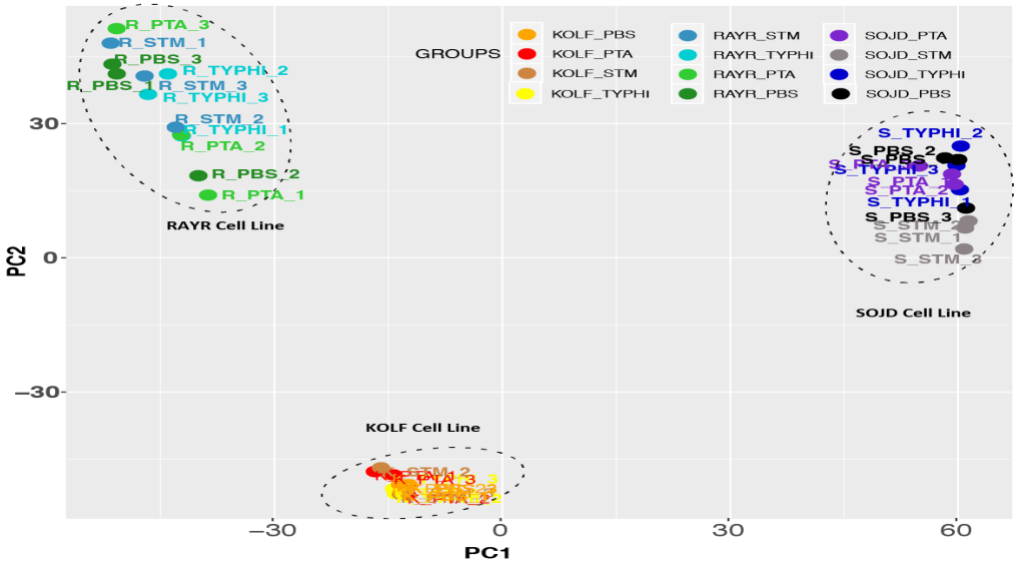


**Figure 6.8: Principal components analysis for all samples.** Kolf2, Rayr2 and Sojd2 iHO were injected with *S*. Typhi, *S*. Paratyphi A, *S*. Typhimurium or PBS and incubated for 3 hours prior to RNA extraction and sequencing, with 3 biological replicates completed per condition. Samples separate clearly by cell line, with PC1 explaining 50.1% and PC2 35.4% variation in the data. ***Key:*** STM = *S*. Typhimurium SL1344, Typhi = *S*. Typhi, PTA = *S*. Paratyphi A, PBS = control.

Differential gene expression analysis was therefore undertaken for each cell line, with results compared in **Table 6.2**. Total number of genes differentially expressed (DE) at a false discovery rate (FDR) < 0.05 are listed. This list was further narrowed down to FDR < 0.05 and log2 fold change (log2FC) > ± 1. The number of genes up and downregulated for each condition for the Kolf2 and Sojd2 cell lines look relatively similar, however there are markedly fewer genes differentially expressed for the *S*. Paratyphi A and *S*. Typhimurium stimulations in the Rayr2 cell line, and to a lesser extent for the *S*. Typhi stimulation in this cell line also.

| Cell line: | FDR: | Typhi vs. PBS (up / down) | PTA vs. PBS (up / down) | STM vs. PBS (up / down) |
|---|---|---|---|---|
| Kolf2 | < 0.05 | 748 / 550 | 1845 / 1523 | 1077 / 415 |
| | < 0.05 log2FC > ± 1 | 28 / 2 | 71/3 | 87/1 |
| Sojd2 | < 0.05 | 907 / 517 | 1481 / 1005 | 868 / 562 |
| | < 0.05 log2FC > ± 1 | 22 / 1 | 97 / 4 | 101 / 2 |
| Rayr2 | < 0.05 | 791 / 978 | 419 / 402 | 136 / 1 |
| | < 0.05 log2FC > ± 1 | 8/1 | 56 /0 | 53 / 0 |

**Table 6.2: Summary of the number of genes differentially expressed (DE) in each stimulation comparison across the three different cell lines.** Kolf2, Rayr2 and Sojd2 iHO were injected with *S*. Typhi, *S*. Paratyphi A, *S*. Typhimurium or PBS and incubated for 3 hours prior to RNA extraction and sequencing, with 3 biological replicates completed per condition. Differential expression was calculated for each infection condition compared to PBS injection. ***Key:*** STM = *S*. Typhimurium SL1344, Typhi = *S*. Typhi, PTA = *S*. Paratyphi A, PBS = control.

More detailed analysis of differentially expressed genes was then completed for each cell line and condition as outlined below.

### 6.3.3.1 Transcriptomic changes in Kolf2 iHO

PCA analysis was repeated for the Kolf2 cell line alone, which demonstrated that the primary source of variance was stimulation condition, with separation both between infected and uninfected samples, and encapsulated and non-encapsulated bacteria on PC1 (**Figure 6.9**).

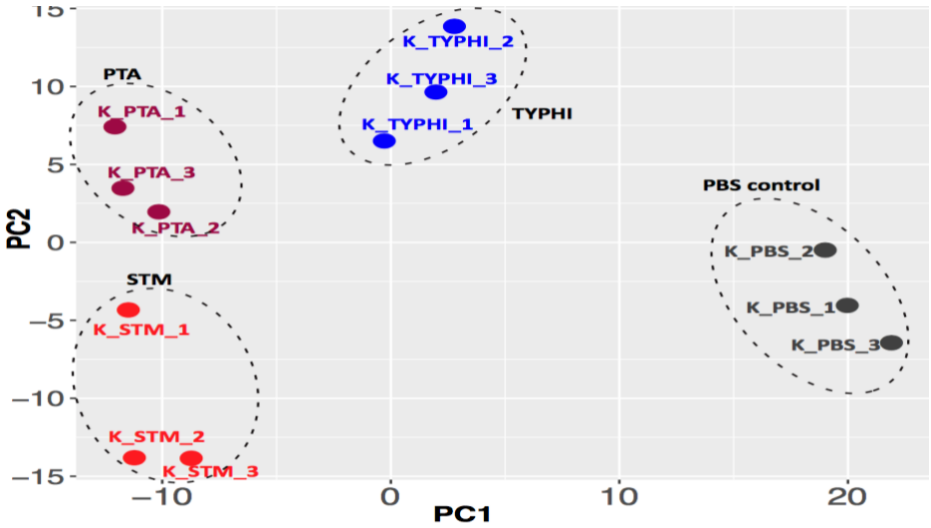


**Figure 6.9: Principal components analysis for Kolf2 samples.** Kolf2 iHO were injected with *S*. Typhi, *S*. Paratyphi A, *S*. Typhimurium or PBS and incubated for 3 hours prior to RNA extraction and sequencing, with 3 biological replicates completed per condition. Samples separate clearly by condition, with PC1 being separated both by infected vs. uninfected status and encapsulated vs. unencapsulated bacteria. ***Key:*** STM = *S*. Typhimurium SL1344, Typhi = *S*. Typhi, PTA = *S*. Paratyphi A, PBS = control.

The genes differentially expressed in each stimulation condition were calculated, and their overlap between conditions expressed as a Venn diagram (**Figure 6.10**). Interestingly, using FDR < 0.05 alone, there is a relatively large overlap of genes differentially expressed between *S*. Typhi and *S*. Paratyphi A stimulations. This is eliminated when adding the filter of log2FC > ± 1, but there remains a large overlap between genes upregulated in *S*. Typhimurium and *S*. Paratyphi A stimulations. Unsurprisingly, when the 22 genes differentially expressed for all groups (as illustrated below) were assessed using the g:Profiler tool (https://biit.cs.ut.ee/gprofiler/gost), the top 5 biological processes represented were: inflammatory response, cytokine-mediated signalling pathway, cellular response to cytokine, response to lipopolysaccharide and defence response.

The function of single genes highlighted in further analyses below were investigated with the GeneCards tool (https://www.genecards.org), which integrates data on gene annotation from ~150 online sources. Any gene functions not directly referenced were established from data available on this site.

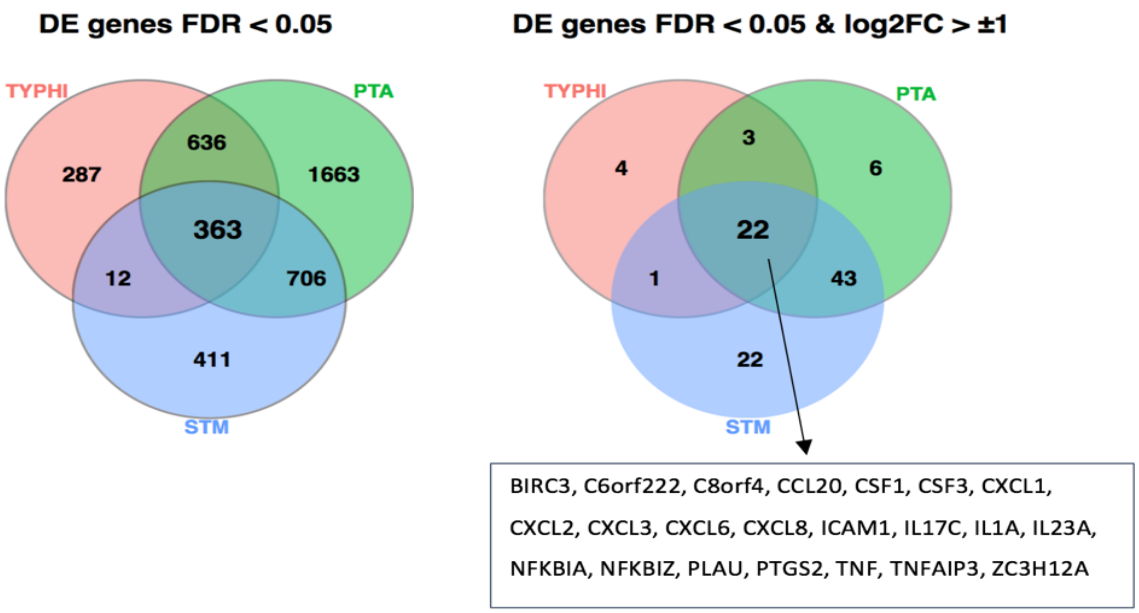


**Figure 6.10: Overlap between DE genes for each stimulation group.** Kolf2 iHO were injected with *S*. Typhi, *S*. Paratyphi A, *S*. Typhimurium or PBS and incubated for 3 hours prior to RNA extraction and sequencing, with 3 biological replicates completed per condition. Differential expression was calculated for each infection condition compared to PBS injection. There are 22 genes upregulated in all 3 stimulation conditions, with little overlap between *S*. Typhi and *S*. Paratyphi A or *S*. Typhimurium, but large amounts of overlap between both unencapsulated serovars. ***Key:*** STM = *S*. Typhimurium SL1344, Typhi = *S*. Typhi, PTA = *S*. Paratyphi A.

Volcano plots were then produced to visualise gene expression fold changes, for up and downregulated genes in each condition versus the PBS control (**Figure 6.11**). These plots clearly demonstrate differences between the *S*. Typhi stimulated and *S*. Paratyphi A / *S*. Typhimurium stimulated samples. There are fewer genes up-regulated in the *S*. Typhi stimulated iHO, suggesting a less inflammatory response, which would be consistent with the role of the Vi capsule in evasion of the immune response[16,17] and the lower numbers of intracellular bacteria seen in this condition.

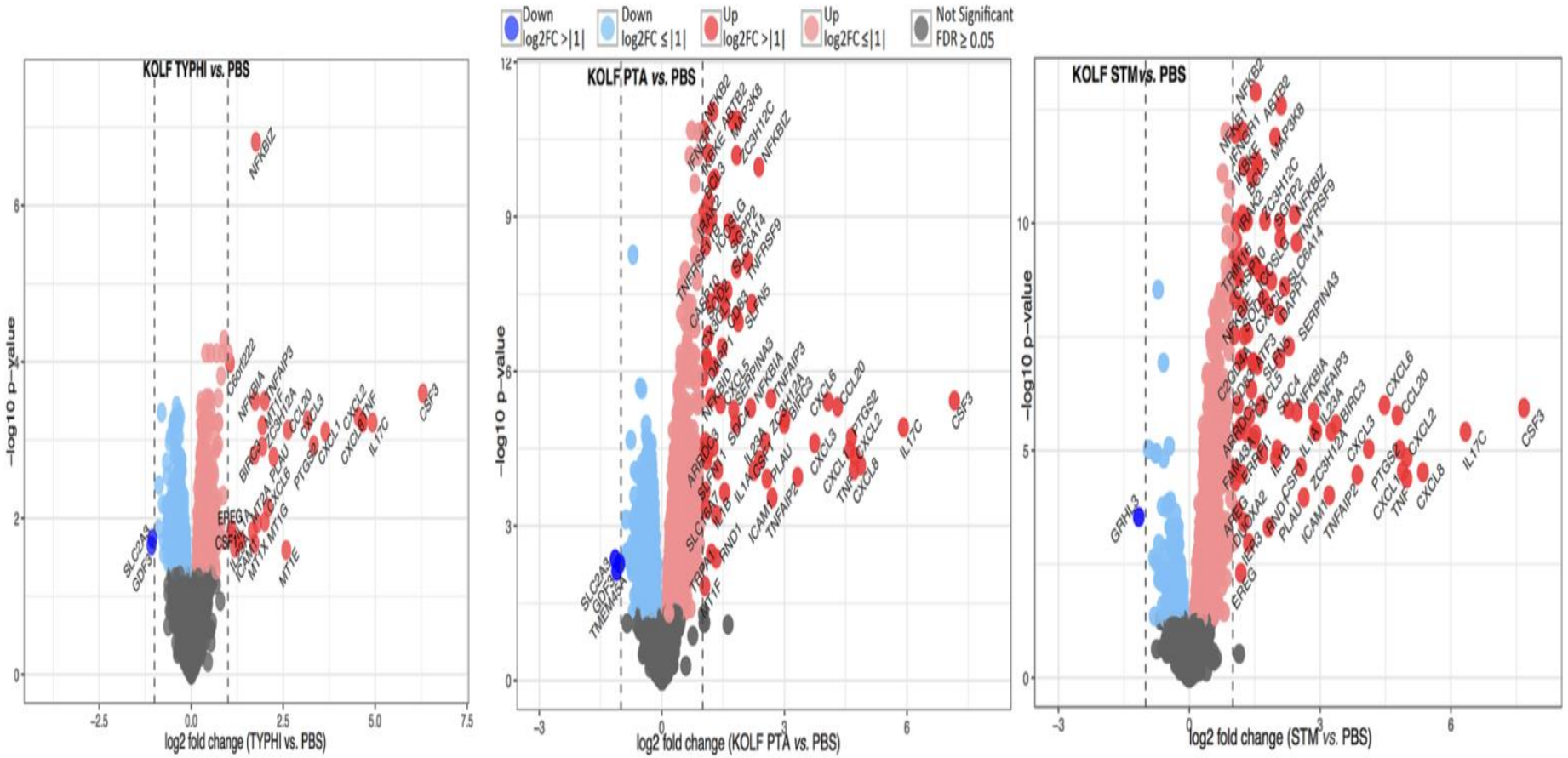


**Figure 6.11: Volcano plots for gene expression between stimulation conditions.** Kolf2 iHO were injected with *S*. Typhi, *S*. Paratyphi A, *S*. Typhimurium or PBS and incubated for 3 hours prior to RNA extraction and sequencing, with 3 biological replicates completed per condition. Differential expression was calculated for each infection condition compared to PBS injection. There are fewer genes upregulated in the *S*. Typhi infected iHO, with large similarities across the genes upregulated between the *S*. Paratyphi A and *S*. Typhimurium-infected samples. ***Key:*** STM = *S*. Typhimurium SL1344, Typhi = *S*. Typhi, PTA = *S*. Paratyphi A, PBS = control.

Genes which were upregulated with a log2FC of >2 in the *S*. Paratyphi A and *S*. Typhimurium, but not in the *S*. Typhi samples comprised the following list: CXCL6, TNFAIP2, BIRC3, ICAM1, PLAU, CSF-1, IL-23A, NFKBIA and SLFN5. CXCL6 is chemotactic for neutrophils, something which *S*. Typhi is able to subvert[17], TNFAIP2 mediates vesicular fusion, and CSF-1 promotes formation of membrane ruffles[18] and induces inflammatory response[19] which may be happening more frequently in *S*. Paratyphi A / *S*. Typhimurium infected cells, given higher intracellular counts. BIRC3 regulates caspases, apoptosis and inflammatory signalling, but interestingly is also upregulated in enteroendocrine cells infected with *Chlamydia trachomatis,*[20] suggesting that it may be possible to detect signatures from smaller cell populations on bulk RNA-seq. ICAM1 is involved in the regulatory pathways both of apoptosis and cellular architecture, with cytoskeletal rearrangement often being induced by *Salmonella* infection.[21,22] IL-23A initiates a T-cell dependent amplification of inflammatory response in the intestinal epithelium[23] and has previously been shown to be upregulated in *S*. Typhimurium infection,[24] but there is limited data on its role in *S*. Paratyphi A and *S*. Typhi infection.

The difference in intensity of inflammatory response is further demonstrated by a heat map of the top 100 genes differentially expressed between the stimulation conditions and PBS (**Figure 6.12**), with very clear similarities in genes differentially expressed between the encapsulated versus unencapsulated bacteria in comparison to PBS. Of note, the genes highly expressed in the PBS-stimulated condition are those related to cellular growth and differentiation (GDF3), solute carriage (SLC2A3) and migration of epithelial cells (GRHL3), suggesting that the upregulation of the infection response genes overwhelms the signature of this activity in the other conditions. This fits with the fact that as demonstrated in **Figure 6.11**, the most downregulated gene in the *S*. Typhimurium-infected group is GRHL3, and for *S*. Typhi and *S*. Paratyphi A, both GDF3 and SLC2A3 (a glucose transporter promoting cell proliferation[25]) are downregulated.

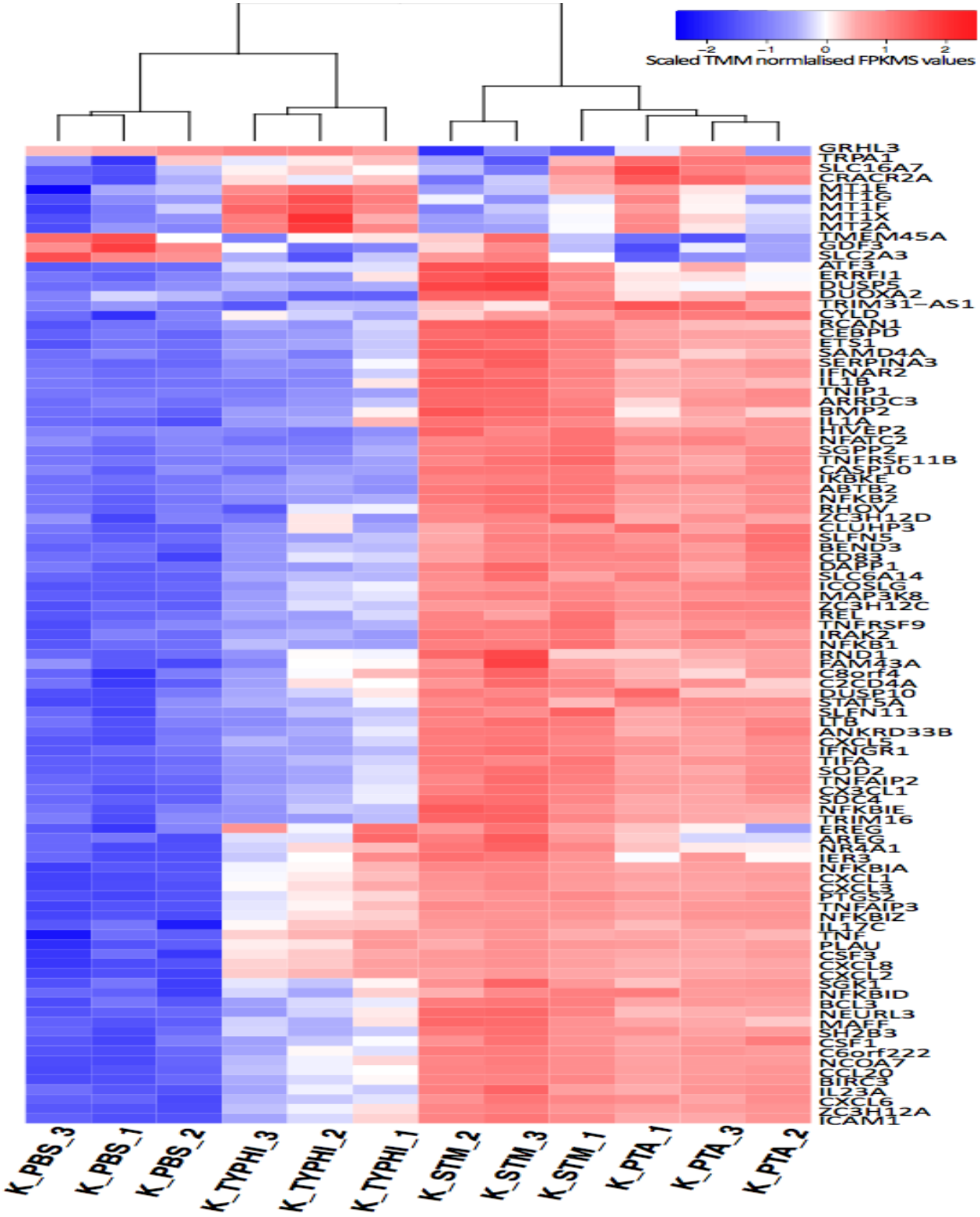


**Figure 6.12: Heatmap from the hierarchical clustering of top genes (FDR < 0.05 & log2FC > ± 1) differently expressed between stimulation conditions and PBS controls.** Kolf2 iHO were injected with *S*. Typhi, *S*. Paratyphi A, *S*. Typhimurium or PBS and incubated for 3 hours prior to RNA extraction and sequencing, with 3 biological replicates completed per condition. The normalised expression values for each gene across all samples were standardised (mean = 0 and SD = 1, such that red denotes increased expression and blue denotes decreased expression. 100 genes are mapped in total.

The genes most strikingly upregulated in the *S*. Typhi samples alone were metallothionein genes (MT1E, MT1G, MT1X and MT2A). These genes bind to heavy metals and control its homeostasis in the cell. This is intriguing, as *S*. Typhimurium is known to have mechanisms for scavenging heavy metals such as iron via production of 'stealth' siderophores which avoid binding by lipochalin-2, and zinc and magnesium via expression of transporters and uptake systems.[26] There is less information on whether this is the case in *S*. Typhi; however a recent paper which measured hepcidin (the hormone which controls systemic iron homeostasis) in participants in human typhoid challenge studies noted a marked increase in hepcidin levels during infection.[27] This hormone controls iron uptake into duodenal enterocytes and reduces circulating levels of iron by increasing its uptake into macrophages. This latter process is something which could in fact be beneficial for *S*. Typhi, as they differ from *S*. Typhimurium in their reliance on genes in the *fep* operon for growth; requiring ferric ($Fe^{3+}$) iron, which is the oxidation state found in the blood, where *S*. Typhi partially reside during the bacteraemic stage of typhoid fever pathogenesis.[28] Interestingly, MT1F was one of the 3 genes more highly expressed in both *S*. Typhi and *S*. Paratyphi A infections, but not *S*. Typhimurium infection.

Whilst there are many similarities between those genes upregulated in *S*. Typhimurium SL1344 and *S*. Paratyphi A infections, notable genes showing enhanced expression predominantly in SL1344 infection include DUSP5, which is a negative regulator of mitogen-activated protein kinases and EFFRI1 which negatively regulates EGFR signalling (and thus decreases cell proliferation), suggesting a suppressive effect on cellular growth and division during infection, perhaps relevant in defence against infection, as *S*. Typhimurium has been shown to preferentially target mitotic cells, due to their increased amounts of surface cholesterol.[29] Other highly upregulated genes in the SL1344 samples included DUOXA2, which generates hydrogen peroxide at the gut epithelial surface, and has an important role in the defence against cellular invasion[30] and dissemination[31] of *S*. Typhimurium. Lastly, RND1, a Rho GTPase which organises the actin cytoskeleton was highly upregulated, which is likely to be a response to the cytoskeletal re-arrangements induced by *S*. Typhimurium invasion.[21,22] Both *S*. Typhi and *S*. Paratyphi A should have the ability to induce similar changes, with actin inhibition preventing infection of iHO derived monolayers with *S*. Typhi in one study.[32] However, it is likely that the highest expression occurred in the *S*. Typhimurium sample, given that this was the most invasive pathogen studied; at least at the

1.5 hour timepoint. Of genes that were most highly upregulated in the *S*. Paratyphi A samples, these appeared to be involved in ion sensing and transport, with CRACR2A (a cytoplasmic calcium ion sensor) and TRPA1, a cation channel induced by LPS.[33] Again, there is no clear reason why these should be particularly relevant to pathogenesis of *S*. Paratyphi A alone.

### 6.3.3.2 Transcriptomic changes in Sojd2 iHO

PCA analysis was completed for the Sojd2 cell line, which demonstrated that the primary source of variance was stimulation condition, with separation here between encapsulated bacteria and PBS stimulations versus unencapsulated bacteria on PC1 (**Figure 6.13**).

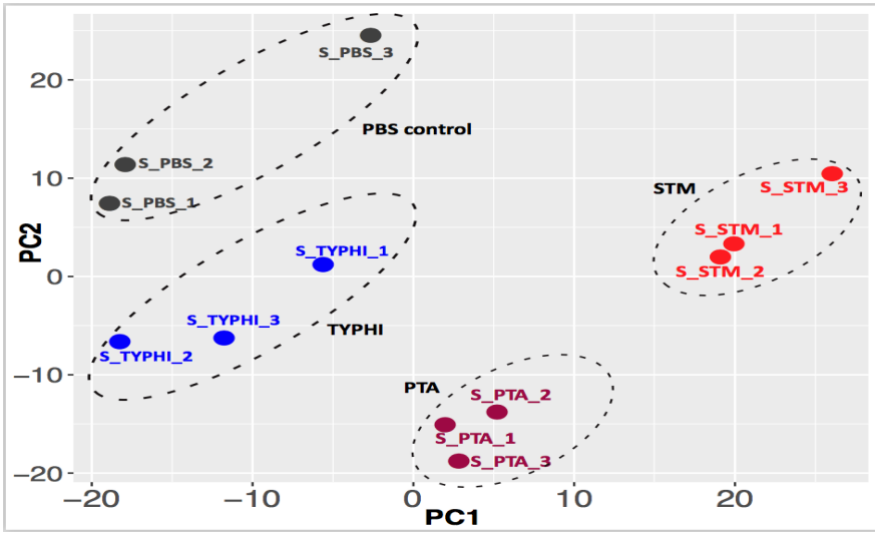


**Figure 6.13: Principal components analysis for Sojd2 samples.** Sojd2 iHO were injected with *S*. Typhi, *S*. Paratyphi A, *S*. Typhimurium or PBS and incubated for 3 hours prior to RNA extraction and sequencing, with 3 biological replicates completed per condition. Samples separate less clearly by condition here, with PC1 being separated by encapsulated bacteria + PBS vs. unencapsulated bacteria. ***Key:*** STM = *S*. Typhimurium SL1344, Typhi = *S*. Typhi, PTA = *S*. Paratyphi A, PBS = control.

The genes differentially expressed in each stimulation condition were calculated, and their overlap between conditions expressed as a Venn diagram (**Figure 6.14**). Again, the maximal overlap was seen between *S*. Typhimurium and *S*. Paratyphi A-infected iHO, with all similarities between *S*. Typhi and *S*. Paratyphi A being lost on filtering for biologically meaningful genes.

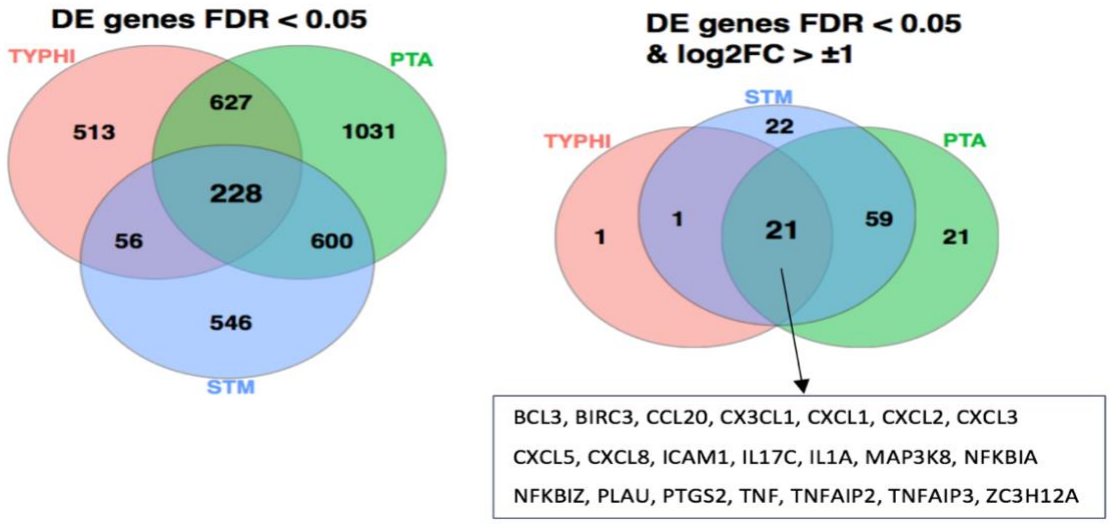


**Figure 6.14: Overlap between DE genes for each stimulation group.** Sojd2 iHO were injected with *S*. Typhi, *S*. Paratyphi A, *S*. Typhimurium or PBS and incubated for 3 hours prior to RNA extraction and sequencing, with 3 biological replicates completed per condition. Differential expression was calculated for each infection condition compared to PBS injection. There are 21 genes upregulated in all 3 stimulation conditions, with no overlap between *S*. Typhi and *S*. Paratyphi A, but large amounts of overlap between both unencapsulated serovars.

Of the 21 overlapping genes, there was a great deal of crossover with the genes universally DE in the Kolf2 stimulation, with only 5 genes overlapping in the Sojd2 stimulations that were not seen in the Kolf2 samples. These were: BCL3, CX3CL1, CXCL5, MAP3K8 and TNFAIP2, which g:Profiler places on the TNF signalling pathway; TNF$\alpha$ being a molecule well-known to be upregulated in the response to *Salmonellae* by the host epithelium.[34,35]

Volcano plots were produced (**Figure 6.15**) which again demonstrate a lot of overlap between *S*. Typhimurium and *S*. Paratyphi A stimulations, and many fewer upregulated genes in the *S*. Typhi samples. All of the genes with a log2 fold change >2 in the *S*. Typhi group were upregulated in both other conditions. Of note, TNF was highly upregulated in the *S*. Typhi stimulated iHO. Again, CXCL6 was highly upregulated in *S*. Typhimurium and *S*. Paratyphi A stimulations alone, but in the Sojd2 cell line, TNFAIP2, BIRC3, ICAM1, NFKBIA and PLAU were highly upregulated across all conditions, rather than just after stimulation with unencapsulated bacteria. Another SNARE-complex forming protein (SNPH) which mediates vesicular fusion, was highly upregulated only in the *S*. Typhimurium and *S*. Paratyphi A conditions, as were DUOXA2, CASP10 (an inducer of apoptosis[36]) and NF$\kappa$B2 which mediates a broad range of inflammatory processes,[37] fitting with the more inflammatory response seemingly occurring in the iHO with these pathogens.

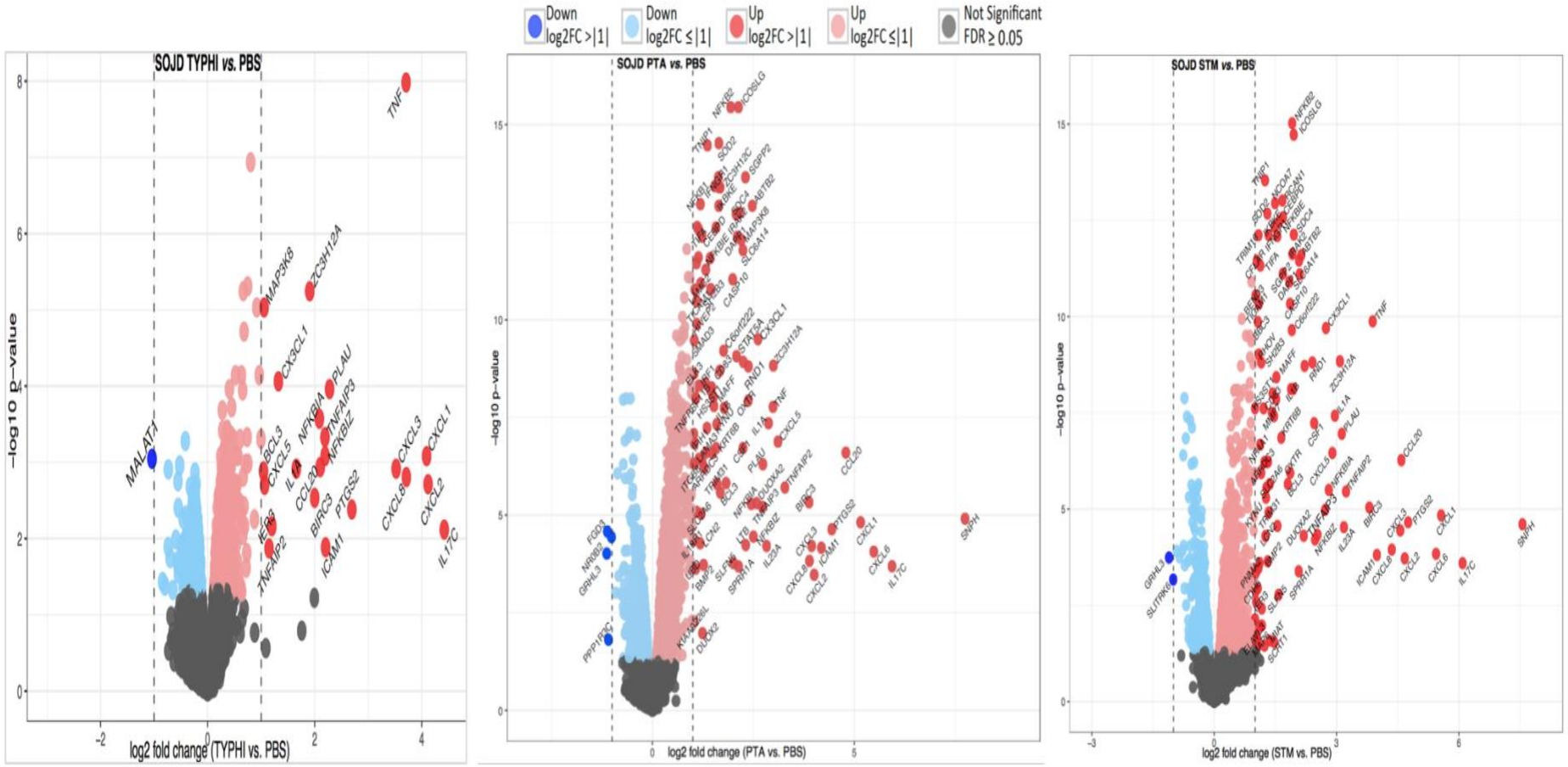


**Figure 6.15: Volcano plots for gene expression between stimulation conditions.** Sojd2 iHO were injected with *S*. Typhi, *S*. Paratyphi A, *S*. Typhimurium or PBS and incubated for 3 hours prior to RNA extraction and sequencing, with 3 biological replicates completed per condition. Differential expression was calculated for each infection condition compared to PBS injection. Again, there are fewer genes upregulated in the *S*. Typhi infected iHO, with large similarities across the genes upregulated between the *S*. Paratyphi and *S*. Typhimurium-infected samples. ***Key:*** STM = *S*. Typhimurium SL1344, Typhi = *S*. Typhi, PTA = *S*. Paratyphi A, PBS = control.

Production of a heat map (**Figure 6.16**) gives a clearer picture of the similarities of the inflammatory response in the unencapsulated versus encapsulated bacteria. Again, GHRL3 was highly upregulated in the PBS-stimulated group, and in this case the *S*. Typhi stimulated iHO, as was NR0B2, a transcriptional regulator. Of the genes most highly upregulated in the *S*. Typhimurium group there is no pathway which captures all of the genes, but a number of them (MAP6, RIMS3, CPLX2) were genes involved in vesicle exocytosis or endosome formation and apoptosis (NSG1), highlighting the phagolysosomal method for attempting to clear *Salmonella* infection in epithelial cells.

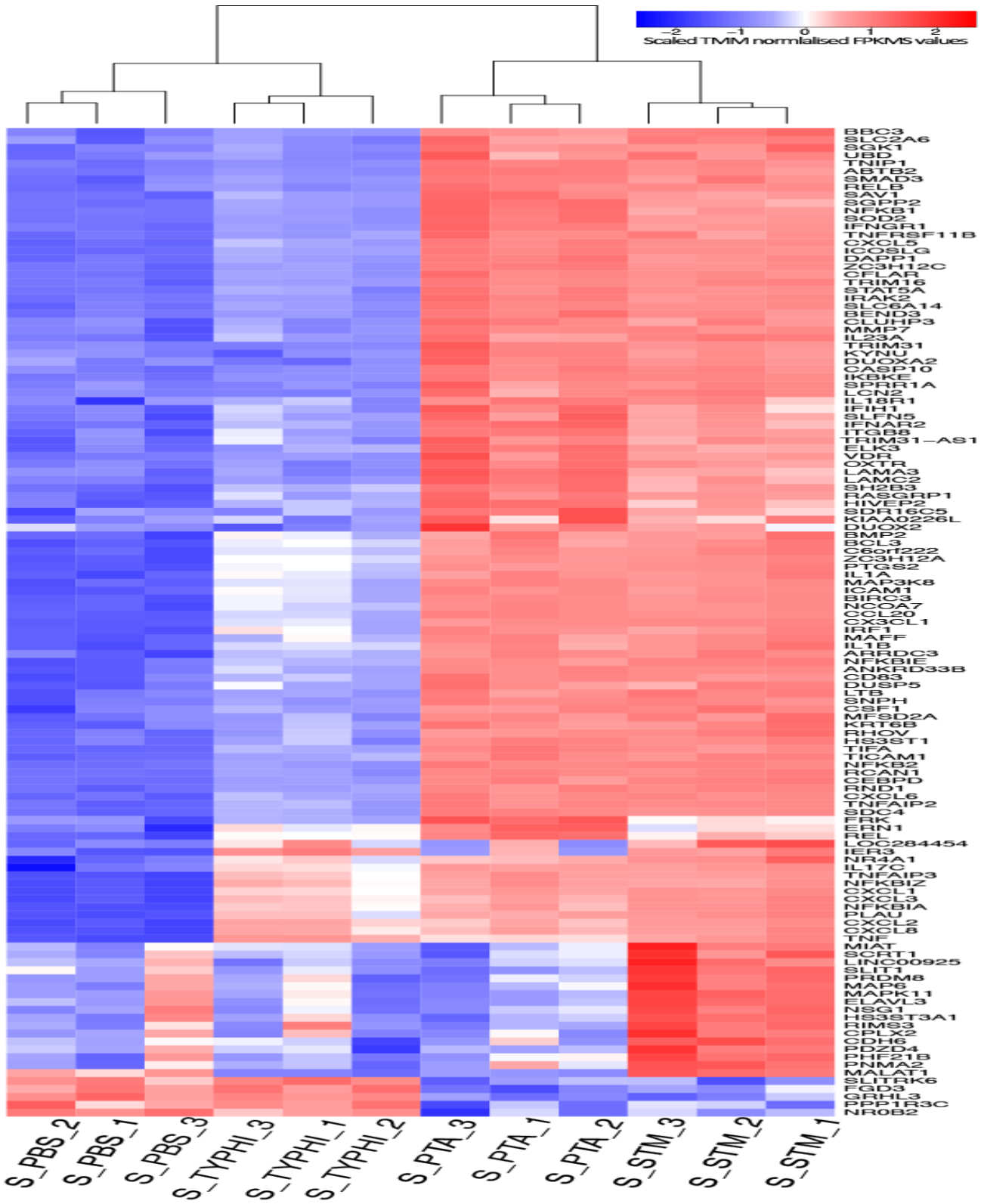


**Figure 6.16: Heatmap from the hierarchical clustering of top genes (FDR < 0.05 & log2FC > ± 1) differentially expressed between stimulation conditions and PBS controls.** Sojd2 iHO were injected with *S*. Typhi, *S*. Paratyphi A, *S*. Typhimurium or PBS and incubated for 3 hours prior to RNA extraction and sequencing, with 3 biological replicates completed per condition. The normalised expression values for each gene across all samples were standardised (mean = 0 and SD = 1, such that red denotes increased expression and blue denotes decreased expression. 125 genes are mapped in total. ***Key:*** STM = *S*. Typhimurium SL1344, Typhi = *S*. Typhi, PTA = *S*. Paratyphi A, PBS = control.

### 6.3.3.3 Transcriptomic changes in Rayr2 iHO

PCA plotting in the Rayr2 iHO demonstrated a slightly different picture, with infected versus non-infected iHO separating on PCs 1-2. On PCs 2-3 *S*. Typhi and PBS samples separate, but there is mixing of the *S*. Typhimurium and *S*. Paratyphi A samples (**Figure 6.17**).

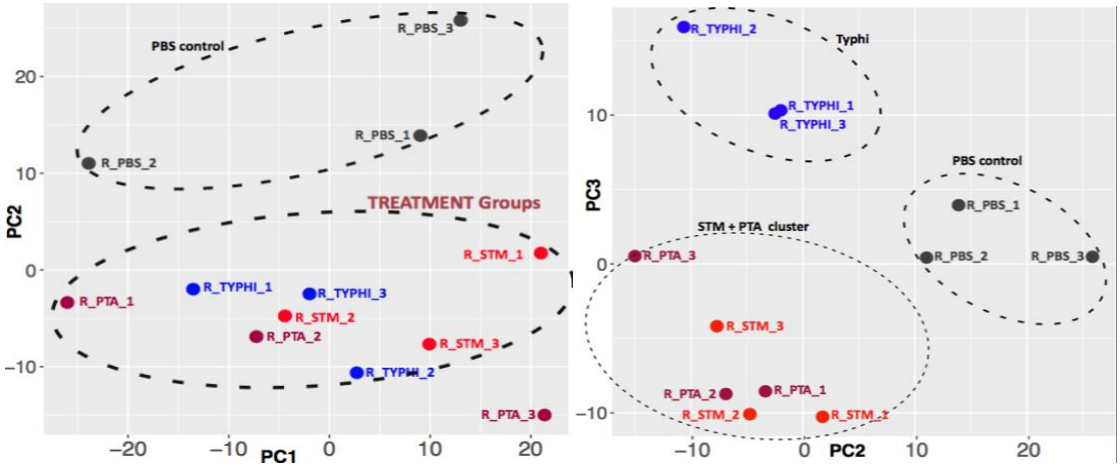


**Figure 6.17: Principal components analysis for Rayr2 samples.** Rayr2 iHO were injected with *S*. Typhi, *S*. Paratyphi A, *S*. Typhimurium or PBS and incubated for 3 hours prior to RNA extraction and sequencing, with 3 biological replicates completed per condition. Samples separate on PC2 by infected versus uninfected, however on PC2-3 there is mixing of the *S*. Typhimurium and *S*. Paratyphi A samples rather than their forming 2 discrete groups. ***Key:*** STM = *S*. Typhimurium SL1344, Typhi = *S*. Typhi, PTA = *S*. Paratyphi A, PBS = control.

Venn diagrams demonstrated that the similarities between the *S*. Typhimurium and *S*. Paratyphi A stimulated samples remained in this cell line, but in total there were fewer genes upregulated to FDR < 0.05 and log2FC > ± 1, and only 6 genes overlapping between all 3 bacterial conditions, with no overlap between *S*. Typhi and either unencapsulated strain (**Figure 6.18**).

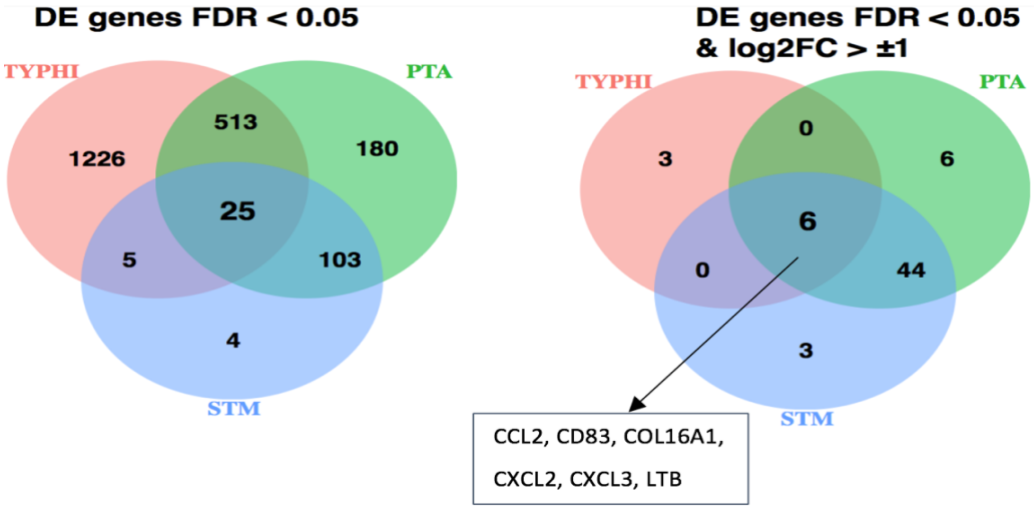


**Figure 6.18: Overlap between DE genes for each stimulation group.** Rayr2 iHO were injected with *S*. Typhi, *S*. Paratyphi A, *S*. Typhimurium or PBS and incubated for 3 hours prior to RNA extraction and sequencing, with 3 biological replicates completed per condition. Differential expression was calculated for each infection condition compared to PBS injection. There are only 6 genes upregulated in all 3 stimulation conditions, with no overlap between *S*. Typhi and *S*. Paratyphi A or *S*. Typhimurium, whereas overlap remains between both unencapsulated serovars. ***Key:*** STM = *S*. Typhimurium SL1344, Typhi = *S*. Typhi, PTA = *S*. Paratyphi A, PBS = control.

Volcano plots confirmed that there were relatively fewer highly up and down regulated genes for all conditions in the Rayr2 iHO (**Figure 6.19**). Genes upregulated across all 3 conditions were: CXCL2, CXCL3, CCL2 and CD83, all of which are related to the chemokine response to infection. Otherwise the other universally upregulated genes were: COL16A1, which is involved in causing alterations to cell morphology (which could be activated in response to *Salmonella* infection[38]) and LTB, an inducer of the inflammatory response. Genes highly upregulated in response to *S*. Typhi infection included: SPINK4, a serine-type endopeptidase inhibitor; members of which family are involved in the immune response[39] and FAR2P1, a pseudogene with no clear biological role in infection response. Only one gene was highly downregulated in the *S*. Typhi condition, with no genes being highly downregulated in either of the unencapsulated bacterial stimulations. This gene was NDNF, a promoter of cell-cell adhesiveness[40], something which may be lost with disruption of tight junctions by Salmonella invasion[38], but the fact that this was downregulated could perhaps suggest that lack of cytoskeletal modifications led to difficulties with invasion of these iHO for *S*. Typhi. There were minimal differences between the genes upregulated to log2 >2 in the *S*. Paratyphi A and *S*. Typhimurium conditions, with all genes related to chemokine activity or granulocyte migration (pathways defined using g:Profiler) and no dissimilarities to the genes upregulated in the Kolf2 or Sojd2 iHO.

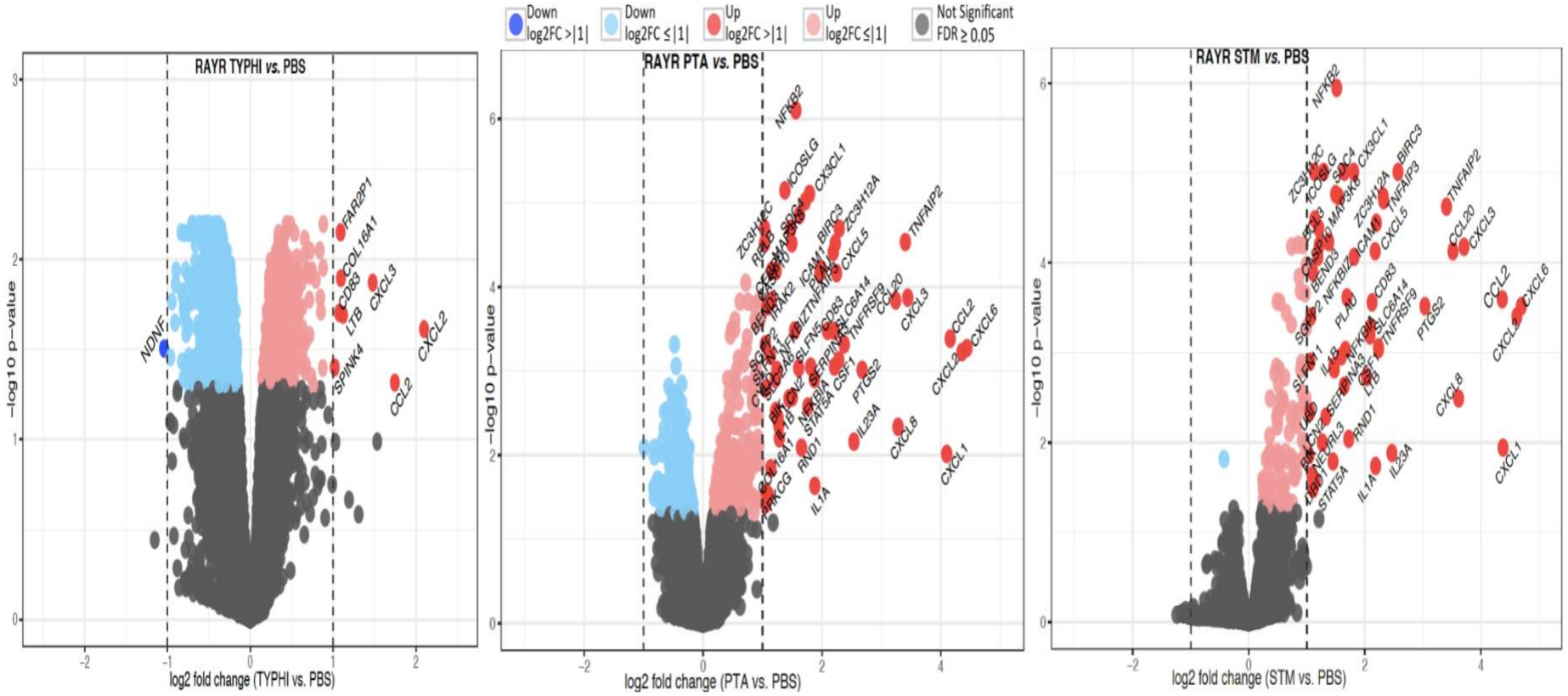


**Figure 6.19: Volcano plots for gene expression between stimulation conditions in Rayr2 iHO.** Rayr2 iHO were injected with *S*. Typhi, *S*. Paratyphi A, *S*. Typhimurium or PBS and incubated for 3 hours prior to RNA extraction and sequencing, with 3 biological replicates completed per condition. Differential expression was calculated for each infection condition compared to PBS injection. There are fewer genes upregulated in all conditions in this cell line, particularly in the *S*. Typhi infected iHO. Large similarities remain across the genes upregulated between the *S*. Paratyphi and *S*. Typhimurium-infected samples. ***Key:*** STM = *S*. Typhimurium SL1344, Typhi = *S*. Typhi, PTA = *S*. Paratyphi A, PBS = control.

A heatmap of top DE genes still demonstrated the difference in inflammatory response between the encapsulated versus unencapsulated bacteria (**Figure 6.20**), but there are fewer genes on display, and a much more generic response in terms of log2 fc from the *S*. Paratyphi A and *S*. Typhimurium stimulated iHO, with one *S*. Paratyphi A sample overlapping with the *S*. Typhimurium samples. NDNF was the only gene significantly upregulated in the PBS-stimulated group; and it is downregulated in many of the infected samples. There are no genes which stand out as being significantly upregulated in any condition alone versus control. Although the overall pattern of response to infection is the same, it is not clear why Rayr2 iHO are producing a less global inflammatory response to stimulation with the pathogens. A dampened inflammatory response to invasion could explain the increased *S*. Paratyphi A counts recovered in iHO from this cell line at 3 hours.

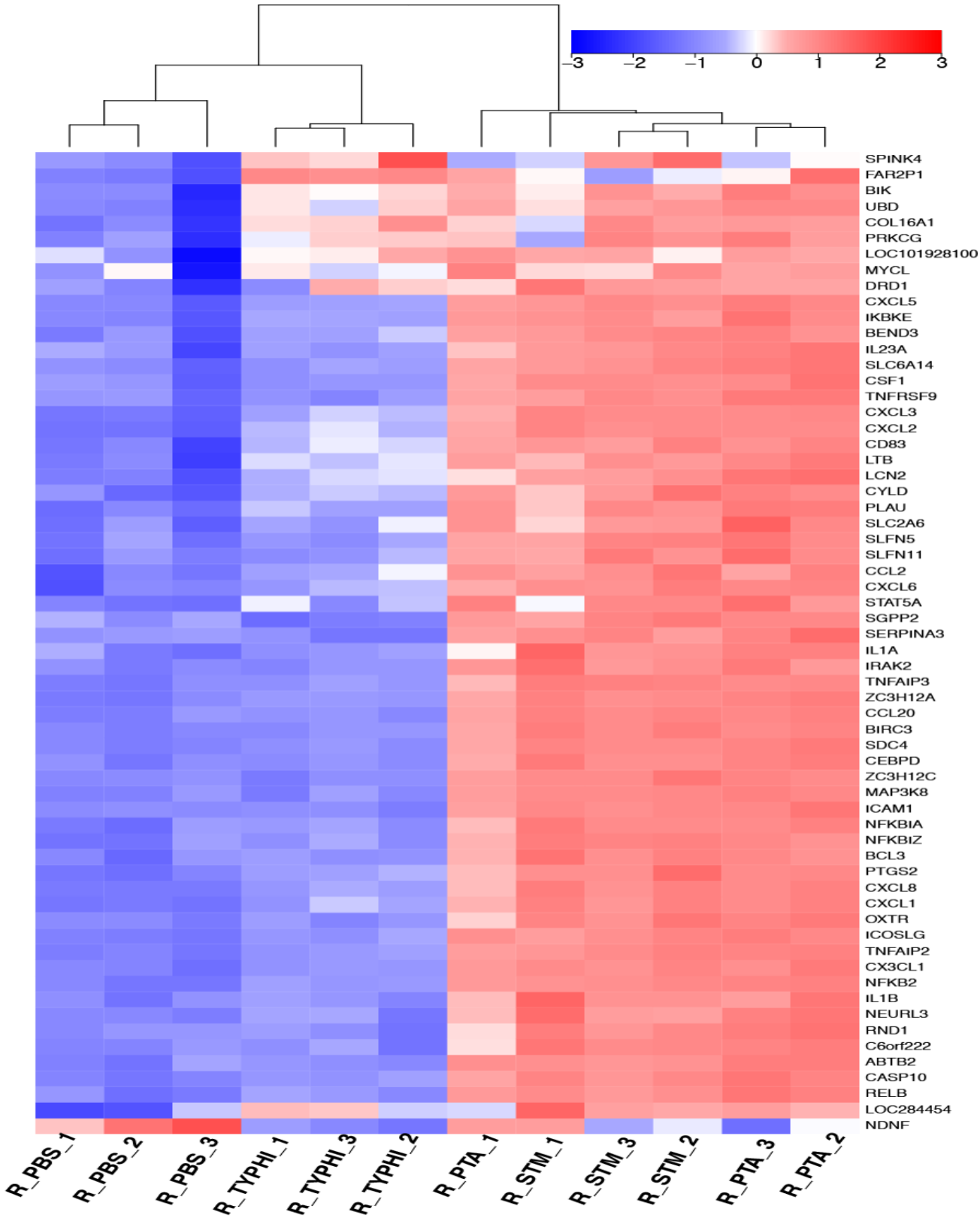


**Figure 6.20: Heatmap from the hierarchical clustering of top genes (FDR < 0.05 & log2FC > ± 1) differently expressed between stimulation conditions and PBS controls in Rayr2 iHO.** Rayr2 iHO were injected with *S*. Typhi, *S*. Paratyphi A, *S*. Typhimurium or PBS and incubated for 3 hours prior to RNA extraction and sequencing, with 3 biological replicates completed per condition. The normalised expression values for each gene across all samples were standardised (mean = 0 and SD = 1, such that red denotes increased expression and blue denotes decreased expression. 60 genes are mapped in total. ***Key:*** STM = *S*. Typhimurium SL1344, Typhi = *S*. Typhi, PTA = *S*. Paratyphi A, PBS = control.

Venn diagrams were used to make direct comparisons between each cell line for all pathogens (**Figure 6.21**). It appeared that the Rayr2 response to *S*. Typhi was equally as complex as in Sojd2 and Kolf2 iHO looking at genes differentially expressed with FDR < 0.05 alone, but when further filtering was put in place (FDR < 0.05 and log2 FC ± 1, this complexity was lost and fewer genes were differentially expressed in the Rayr2 iHO. Far more marked though was the lack of genes differentially expressed in response to the unencapsulated pathogens in the Rayr2 iHO, with far fewer genes differentially expressed for *S*. Paratyphi A and *S.* Typhimurium. Reassuringly, those genes which are differentially expressed in the Rayr2 iHO are those which are also expressed across the Kolf2 and Sojd2 cell lines; they are just fewer in number, suggesting a dampened response to these unencapsulated pathogens, which fits with the increased counts of *S*. Paratyphi A seen in iHO from this line.

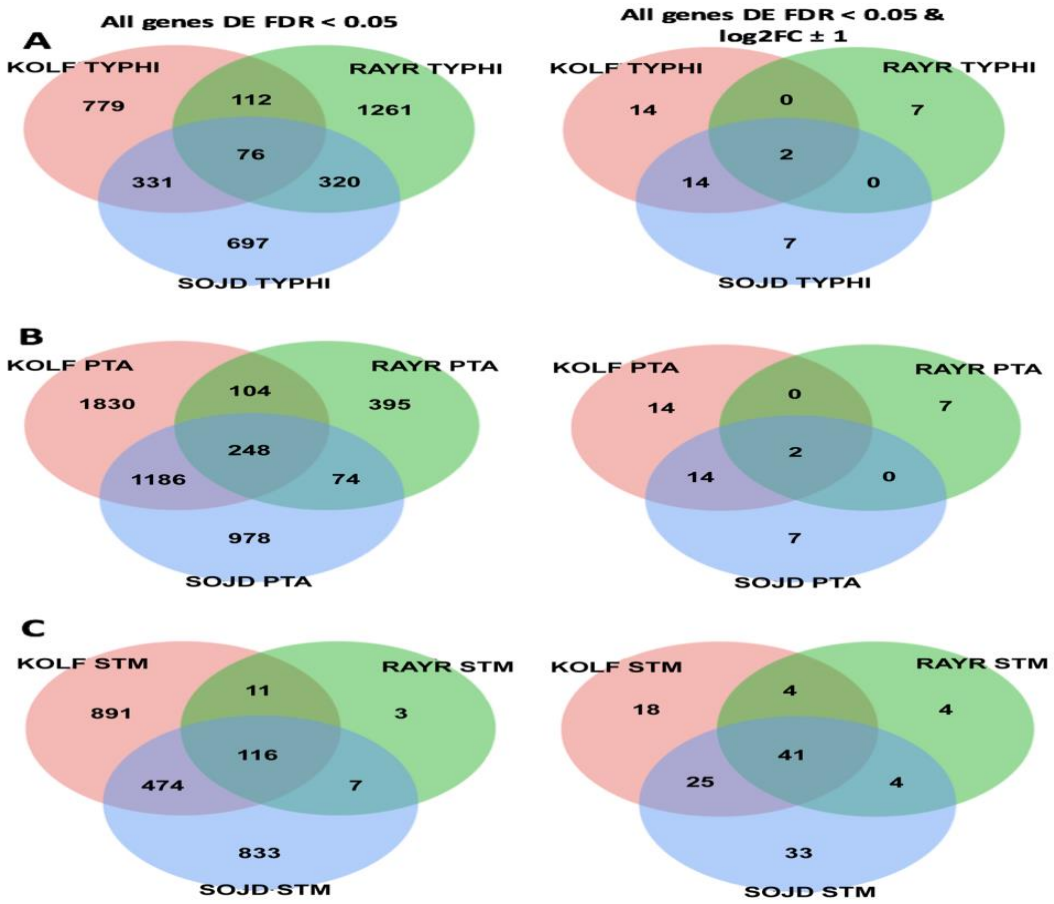


**Figure 6.21: Overlap between DE genes for each cell line and pathogen.** Kolf2, Sojd2 and Rayr2 iHO were injected with *S*. Typhi, *S*. Paratyphi A, *S*. Typhimurium or PBS and incubated for 3 hours prior to RNA extraction and sequencing, with 3 biological replicates completed per condition. Differential expression was calculated for each infection condition compared to PBS injection. In *S*. Typhi stimulated iHO (**A**), there are similar amounts of differentially expressed genes across all 3 cell lines, but for S. Paratyphi (**B**) and S. Typhimurium (**C**) stimulated iHO, the Rayr2 cell line exhibits many fewer differentially expressed genes. ***Key:*** STM = *S*. Typhimurium SL1344, Typhi = *S*. Typhi, PTA = *S*. Paratyphi A.

### 6.3.3.4 Transcriptomic differences between cell lines

To investigate these apparent differences in transcriptional response between the cell lines, expression of housekeeping genes across all cell lines and conditions was checked, and did not show any differences (**Figure 6.22**).

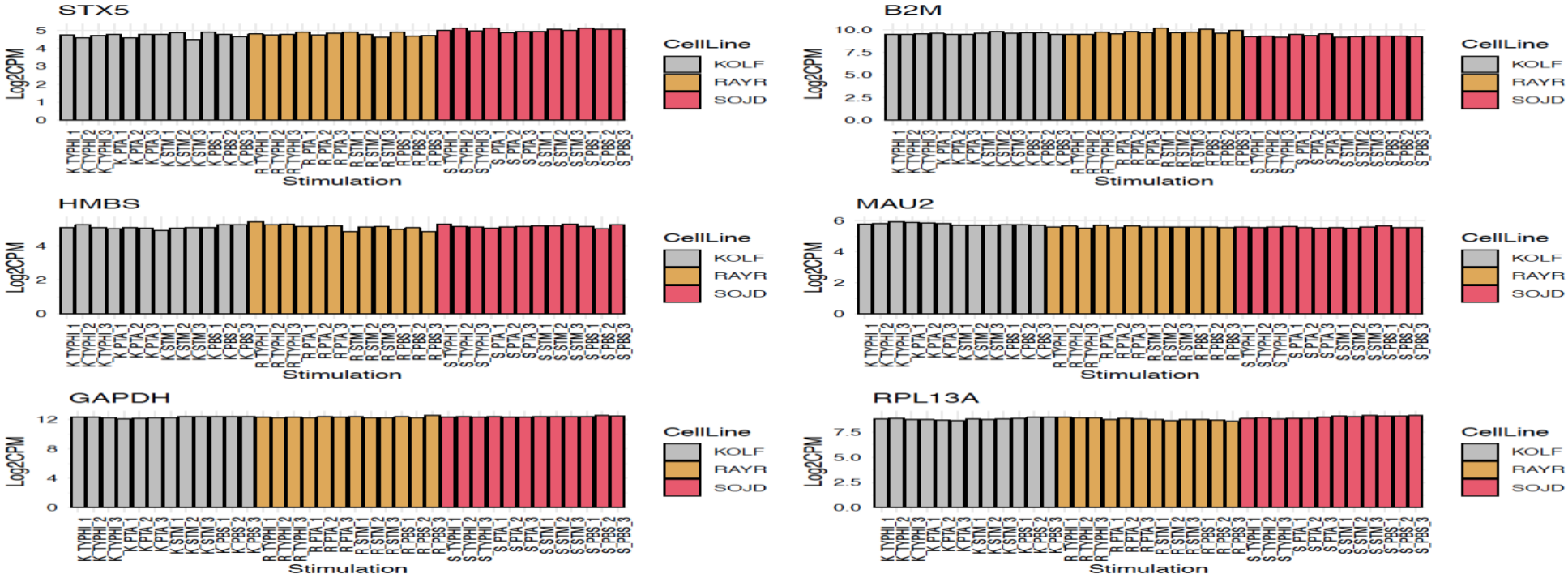


**Figure 6.22: Expression of housekeeping genes across all cell lines and conditions.** Kolf2, Sojd2 and Rayr2 iHO were injected with *S*. Typhi, *S*. Paratyphi A, *S*. Typhimurium or PBS and incubated for 3 hours prior to RNA extraction and sequencing, with 3 biological replicates completed per condition. Expression values are represented as Log2CPM (counts per million). ***Key:*** STM = *S*. Typhimurium SL1344, Typhi = *S*. Typhi, PTA = *S*. Paratyphi A, PBS = control.

Following this, a plot was completed to display the genes responsible for the most variance in the data between all cell lines. Of note, HOX genes (highlighted in **Figure 6.23**), such as HOXC10, HOXA10, HOXA9, HOXA11-AS, HOXA11, HOXA13 form a large proportion of the responsible genes, particularly appearing to be downregulated in the Rayr2 cell line. HOX genes are transcription factors which are part of the regulatory system organising cells along the anterior-posterior axis during development.[41] Although all iHO were injected on the same day post-splitting, given the downregulation of these genes in the Rayr2 cell line, it would appear that these iHO had completed more of their process of development than the other cell lines at the time of injection. Additionally, EDNRA and EDNRB; genes that play a role in cellular proliferation[42] are downregulated in the Rayr2 cell line. Those genes downregulated or upregulated in only the Kolf2 iHO do not perform a collective biological function, other than the upregulation of EDNRA and EDNRB, suggesting that the Kolf2 iHO were still proliferating at the time of infection.

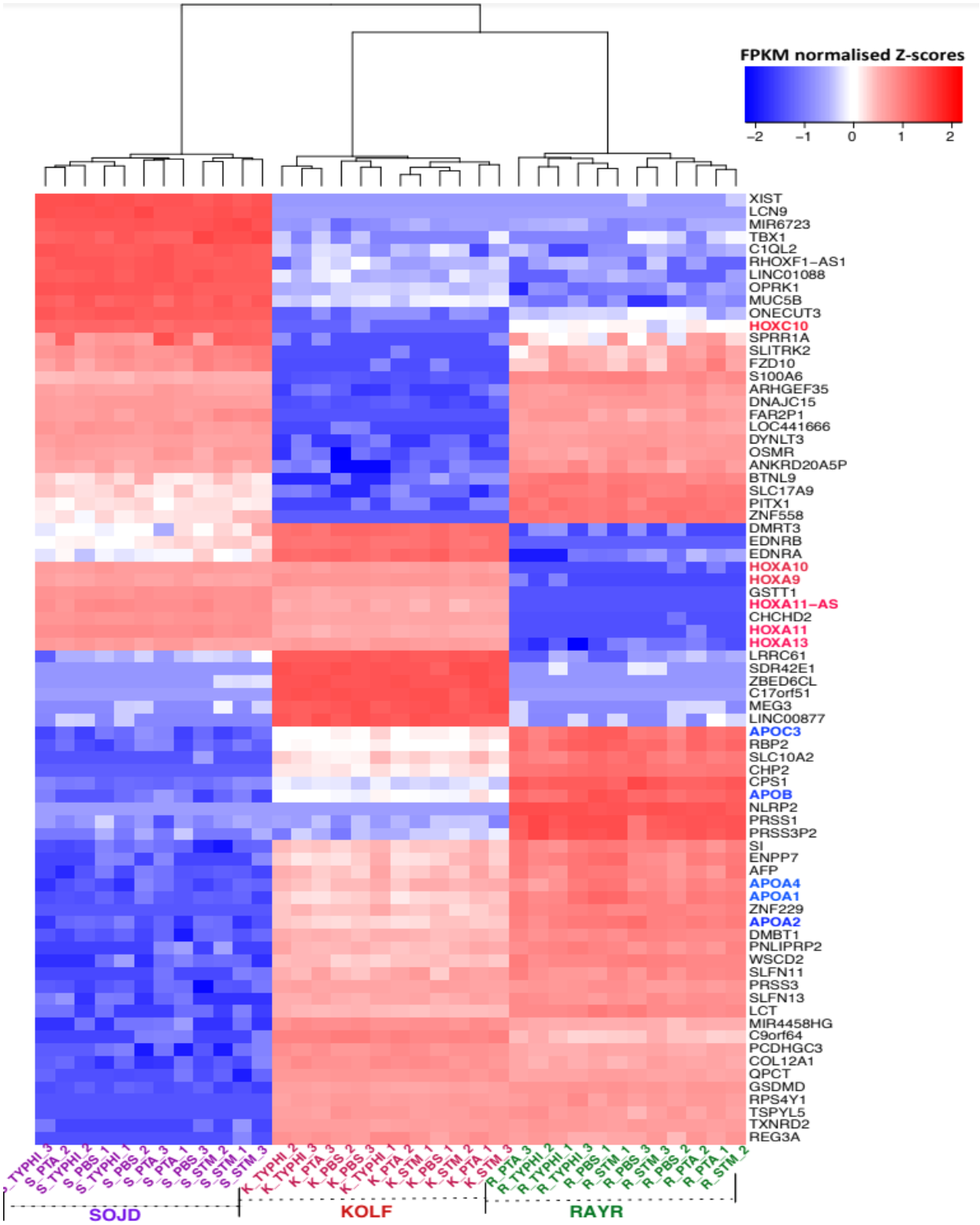


**Figure 6.23: Heatmap of genes explaining most variance in the transcriptome across all cell lines.** Kolf2, Sojd2 and Rayr2 iHO were injected with *S*. Typhi, *S*. Paratyphi A, *S*. Typhimurium or PBS and incubated for 3 hours prior to RNA extraction and sequencing, with 3 biological replicates completed per condition. Expression values for each gene were normalized by fragments per kilobase of exon model per million reads mapped (FPKM) and are expressed as Z-scores, with red denoting upregulated and blue downregulated. HOX genes are highlighted in red, apolipoprotein genes are highlighted in blue. ***Key:*** STM = *S*. Typhimurium SL1344, Typhi = *S*. Typhi, PTA = *S*. Paratyphi A, PBS = control.

There is also no particular pathway associated with the genes which are upregulated in Sojd2 iHO alone, but noteworthy given that this is the only cell line from a female volunteer; XIST (X-inactive specific transcript), a gene essential for X-inactivation is upregulated.[43] However, a number of apolipoprotein genes (highlighted in blue on **Figure 6.23**), including: APOC3, APOB, APOA4, APOA1 and APOA2 are down regulated in the Sojd2 line, particularly in comparison to the Rayr2 line where they appear highly expressed. In a large study of intra and inter-individual variation between iPSC lines, APOA2 was found to be a key driver of developmental pathways enriched in genes which varied the most between cell lines.[44] Genes highlighted as being on the 'digestion' pathway are also downregulated in the Sojd2 iHO, including: sucrase-isomaltase (SI), pancreatic lipase related protein 2 (PNLIPR2), serine protease 3 (PRSS3) and lactase (LCT), perhaps a reflector of relative immaturity versus the Rayr2 line. There are many potential reasons for these general differences in gene expression between cell lines, and these are considered further in the discussion.

### 6.3.4 Cytokine response in iHO infected with *S.* Typhi and *S.* Paratyphi

Cytokine assays on iHO supernatants were completed for all cell lines pre-infection, and post-infection at the 1.5 hour and 3 hour timepoints. Supernatants from each iHO line were run on the Luminex MAGPIX device using xPONENT software. Results were analysed separately and are presented in **Figure 6.24**.

There appeared to be little detectable cytokine response to *S*. Typhi by the iHO epithelium, with no significant elevation of cytokines in the Kolf2 line and only IL-1RA elevated in the Sojd2 line and GRO$\alpha$ and TGF$\alpha$ in the Rayr2 iHO.

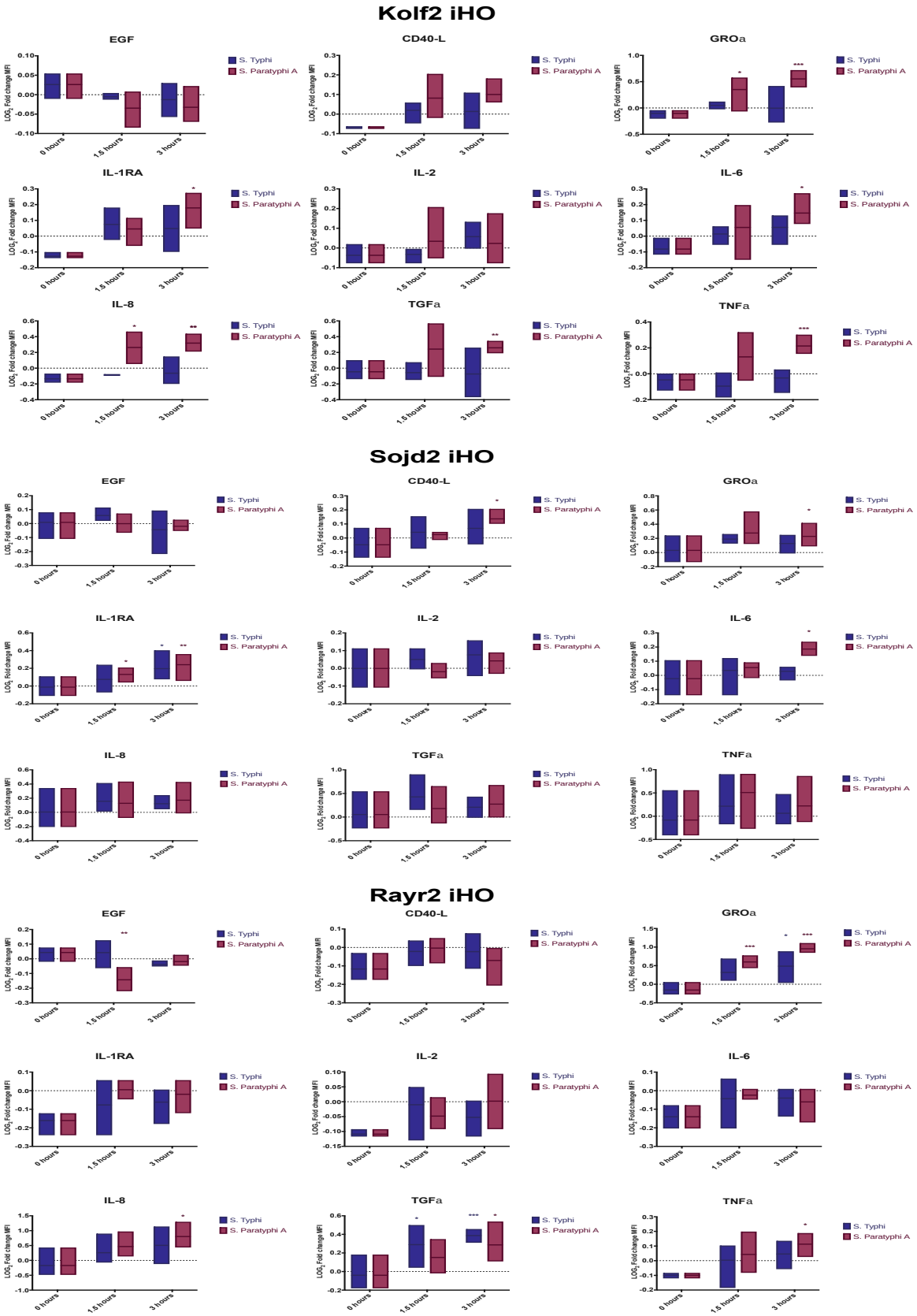


**Figure 6.24: Cytokine levels from iHO supernatants for all cell lines, infected with *S.* Typhi or *S.* Paratyphi A.** Kolf2, Sojd2 and Rayr2 iHO were injected with *S.* Typhi or *S.* Paratyphi A. Supernatant samples were taken pre-infection or after incubation for 1.5 or 3 hours post-infection. Data presented are from 3 biological replicates (containing 2 technical replicates). Unpaired student's t-test was used to compare results (* $p < 0.05$, ** < 0.01, *** < 0.001).

GROα and IL-1RA were significantly upregulated by the 3 hour timepoint in iHO from all lines infected with *S*. Paratyphi A. IL-6 levels were elevated in Kolf2 and Sojd2 iHO, and TGFα, TNFα and IL-8 in Kolf2 and Rayr2 iHO. In addition, CD40-L was elevated in Sojd2 iHO. Kolf2 iHO appeared to have the most robust pro-inflammatory picture in response to *S*. Paratyphi A, with the most numerous and significantly elevated cytokine levels. Cytokine levels bore good resemblance to those genes determined to be significantly upregulated in the transcriptomic work, with GROα and IL-1RA again significantly upregulated in all 3 cell lines after *S*. Paratyphi A infection. Additionally, IL-8 (CXCL8) was detected in Kolf2 and Rayr2 iHO, alongside numerous TNF-induced proteins.

A significant elevation of GROα, IL-1RA and CD40L was observed in the blood of volunteers 12 hours after *S*. Typhi and *S*. Paratyphi A challenge. As described above, significant elevation of GROα was observed for all iHO stimulated with *S*. Paratyphi A and in Rayr2 iHO challenged with *S*. Typhi. IL-6 has been shown previously to be induced by *S*. Typhi infection of intestinal epithelial cells[45], and IL-8 following *S*. Paratyphi infection of Caco2 cells.[46] In short, there appears to be overlap in the cytokine response produced by epithelial cells to both *S*. Typhi and *S*. Paratyphi, but as observed in transcriptomic data, there was some variation in the intensity and range of that response between cell lines.

## 6.4 Study of interactions of *S*. Typhi and *S*. Paratyphi A with hiPSC-derived macrophages

### 6.4.1 Assessing infectivity of *S*. Typhi and *S*. Paratyphi A in macrophages

Having established that *S*. Typhi (Quailes strain) and *S.* Paratyphi A are both able to invade the epithelium in iHO derived from iPSC-derived cell lines, infection assays were also completed for macrophages derived from one of these cell lines. The Kolf2 line was chosen, given that this line is well phenotyped and has been used in assays with multiple pathogens[7,47,48] by both our group and others. This also presented an opportunity to investigate the individual host response to *S*. Typhi and *S*. Paratyphi A at both the epithelial and macrophage (systemic) levels. Gentamicin protection assays using an MOI of 10 were completed with cells being harvested and lysed at 6 hours. *S*. Typhimurium SL1344 was used as a comparator, as it was known that this isolate is reliably taken up into these

macrophages.[7] As has been demonstrated previously in THP-1 and hiPSC[7] or bone marrow-derived macrophages,[16] *S*. Typhimurium SL1344 was recovered intracellularly at a higher level than *S*. Typhi, with *S*. Paratyphi A uptake falling somewhere in between in this study (**Figure 6.25**). Thus, both of the unencapsulated pathogens were phagocytosed more effectively than the Vi-expressing *S*. Typhi.

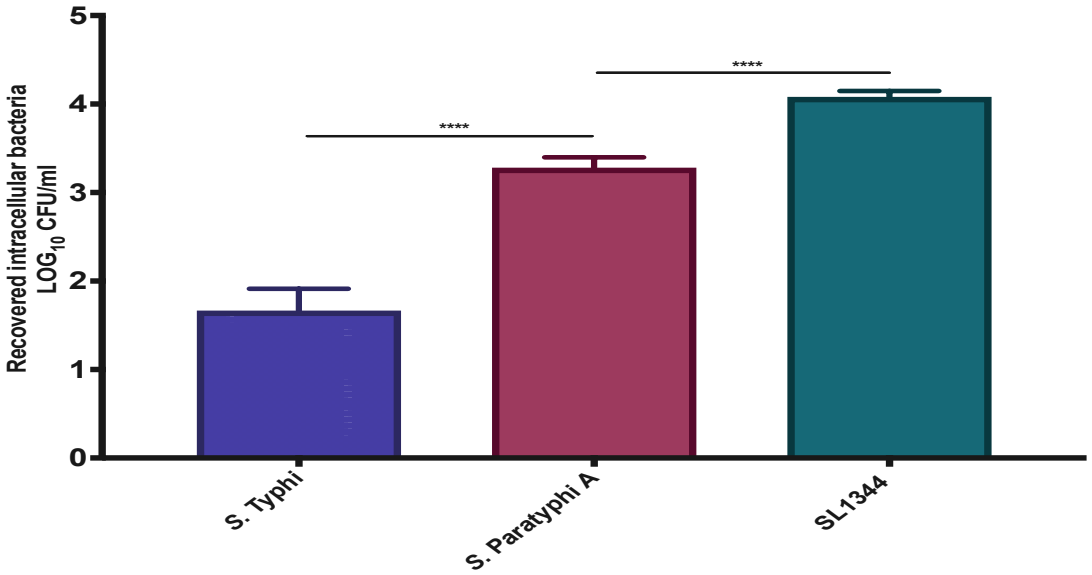


**Figure 6.25: Intracellular bacterial counts for infections in iPSC-derived macrophages from the Kolf2 cell line.** Kolf2 macrophages were infected with *S*. Typhi, *S*. Paratyphi A or *S*. Typhimurium at MOI of 10 for 6 hours prior to gentamicin protection assay and recovery of intracellular bacteria. Data presented are for 3 biological replicates (each averaged from 12 technical replicates) +/- SEM. Unpaired Mann-Whitney tests were used for all assays (**** $p < 0.0001$). *S*. Typhi was phagocytosed less efficiently than *S*. Paratyphi A and *S*. Typhimurium SL1344. SL1344 was recovered at significantly higher intracellular counts compared to *S*. Paratyphi A.

### 6.4.2 Imaging of interactions during infection

These findings were confirmed using immunostaining and confocal imaging, with representative images captured for each condition (**Figure 6.26**). Bacteria were visible within macrophages from each infection assay. Bacterial counts per cell were taken for 150 randomly-selected macrophages from each infection assay and these yielded a pattern of infectivity similar to that obtained by direct viable counts, with most bacteria being demonstrated within the cells infected with SL1344.

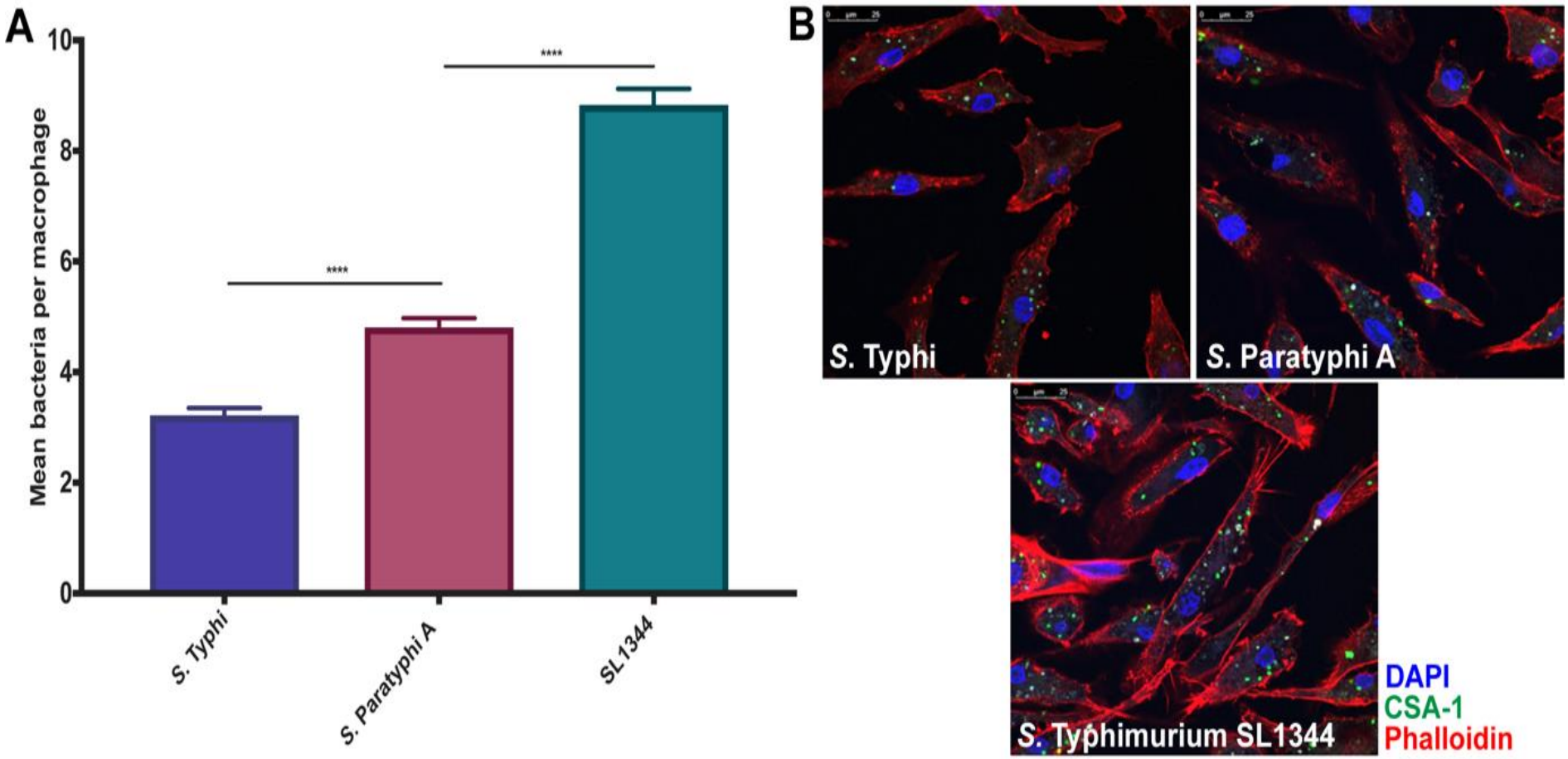


**Figure 6.26: Intracellular bacterial counts using confocal imaging in Kolf2 macrophages.** Kolf2 macrophages were infected with *S*. Typhi, *S*. Paratyphi A or *S*. Typhimurium at MOI of 10 for 6 hours prior to fixation for immunostaining. (**A**) Results confirmed that *S*. Typhi was found intracellularly at significantly lower counts compared to *S*. Paratyphi A and *S*. Typhimurium SL1344. Data presented are for 3 biological replicates (each of 150 cells) +/- SEM. Unpaired Mann-Whitney tests were used for all assays (**** $p < 0.0001$). (**B**) Representative images from each condition, with highest numbers of bacteria visible in *S*. Typhimurium SL1344-infected macrophages. Cell nuclei are stained with DAPI, bacteria with CSA-1 and macrophage membranes with phalloidin. Images taken on the Leica SP8 confocal microscope at 63x magnification.

TEM images were also obtained for all 3 strains, with cells being infected at MOI of 50 for 6 hours prior to fixing. It was clear that macrophages imaged were responding to the infection, with high numbers of vesicles and phagosome/membrane formations witnessed inside cells, alongside cytoskeletal actin rearrangement and presence of membrane ruffes. Bacteria were visible inside cells from all 3 conditions. (**Figure 6.27-6.29**).

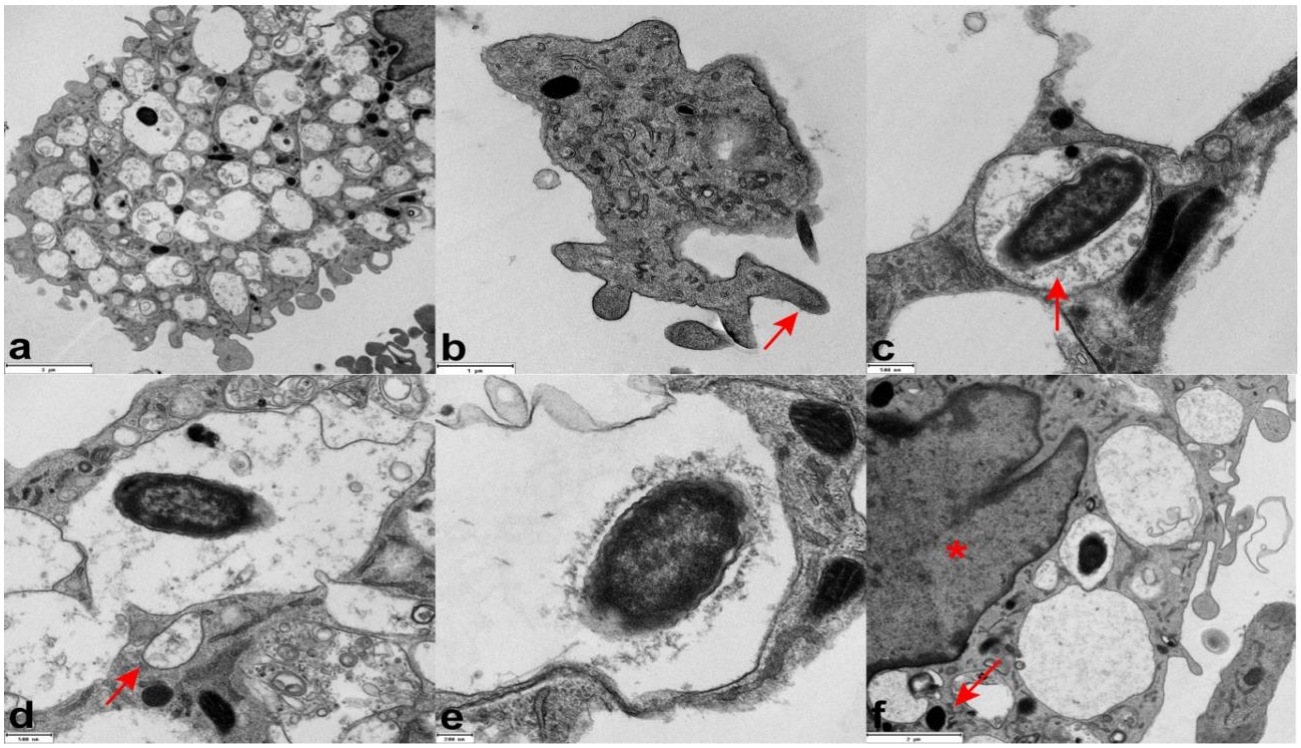


**Figure 6.27: TEM images of *S*. Typhi infected Kolf2 macrophages.** Kolf2 macrophages were infected with *S*. Typhi at MOI of 50 for 6 hours prior to fixation. Panel **a** depicts a whole macrophage containing numerous vesicles and phagosomal complexes, indicating response to infection. Panel **b** demonstrates membrane ruffling (arrow). Panel **c** shows *S*. Typhi inside an SCV; and demonstrates expression of the Vi capsule (arrow). Panel **d** represents S. Typhi inside SCV in proximity to additional early phagosome (arrow), **e** shows possible degradation/shedding of Vi capsule inside of SCV and **f** an SCV in close proximity to the nucleus (asterisk) with lysosome also present (arrow).

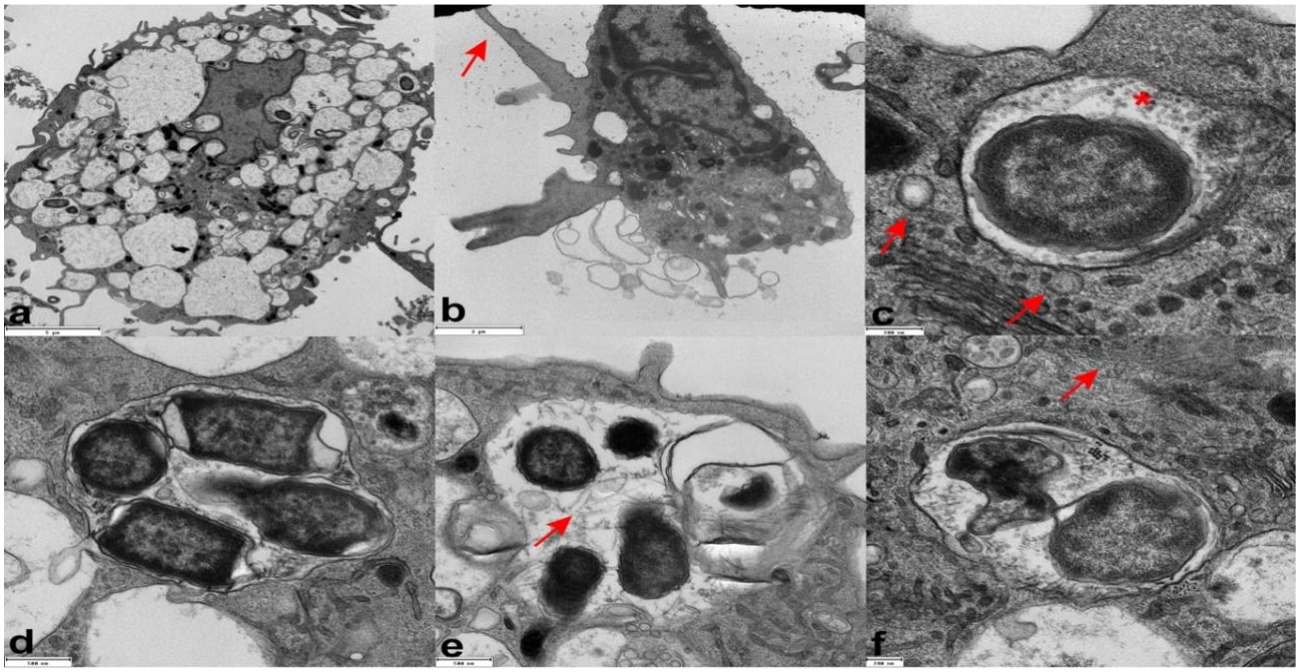


**Figure 6.28: TEM images of *S*. Paratyphi A infected Kolf2 macrophages.** Kolf2 macrophages were infected with *S*. Paratyphi A at MOI of 50 for 6 hours prior to fixation. Numerous vesicles and phagosomal complexes are visible in panel **a,** some containing bacteria, indicating response to infection. Panel **b** demonstrates membrane ruffling (arrow). Panel **c** shows *S*. Paratyphi A inside an SCV; and demonstrates outer membrane vesicles being formed from bacteria (asterisk) and likely endosomes being formed by Golgi apparatus (arrows). Panel **d** represents multiple S. Paratyphi A inside SCV with degradation of some bacteria, **e** shows further bacterial degradation inside SCV with multiple flagellae visible (arrow). Panel **f** displays bacteria inside an SCV in close proximity to actin bundles (arrow).

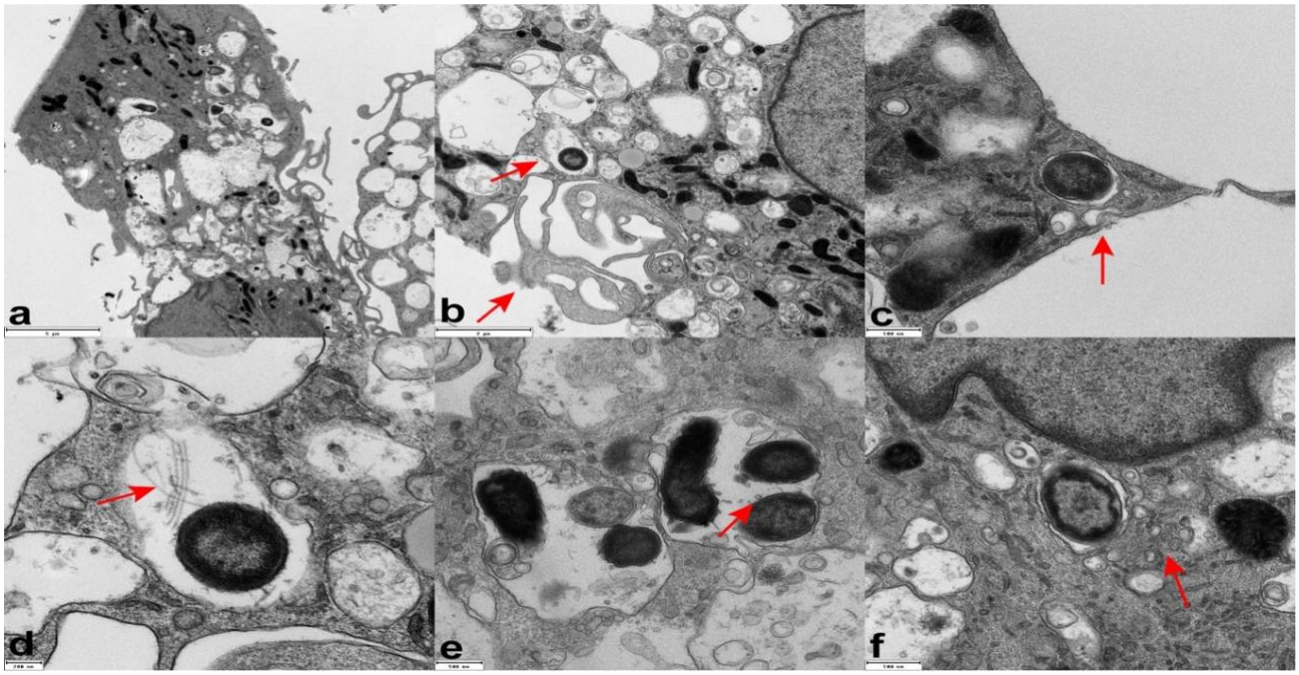


**Figure 6.29: TEM images of *S*. Typhimurium infected Kolf2 macrophages.** Kolf2 macrophages were infected with *S*. Typhimurium at MOI of 50 for 6 hours prior to fixation. Numerous vesicles and phagosomal complexes are visible in panel **a,** some containing bacteria, with ragged appearance of macrophage. Panel **b** demonstrates membrane ruffling (arrow), with bacteria inside SCV above the area of ruffling (asterisk). Panel **c** shows *S*. Typhimurium inside an SCV; likely shortly after entry to cell (arrow). Panel **d** represents *S.* Typhimurium inside SCV with flagellae (arrow), **e** shows multiple bacteria inside SCV with outer membrane vesicle formation occurring (arrow). Panel **f** displays bacteria inside an SCV in close proximity to the nucleus and multiple endosomes (arrow).

### 6.4.3 Transcriptomic changes witnessed during macrophage infection

Kolf2 macrophages were infected for 6 hours at MOI 10 with *S*. Typhi (Quailes), *S*. Paratyphi A, *S*. Typhimurium SL1344 or PBS prior to harvesting, RNA extraction and submission for sequencing as outlined in 2.16. PBS replicates were completed as a control to ensure that any signatures were not simply due to media and chemicals used during the infection assay and harvesting process. QC metrics for all samples are outlined below (**Table 6.3, Figure 6.30**), demonstrating the similarities in terms of depth and alignment of reads for all cell lines and conditions.

| **Stimulation condition:** | **Read depth range:** (million reads) | **Read depth mean:** (million reads) | **Read depth median:** (million reads) |
|---|---|---|---|
| *S*. Typhi | 16.20 – 22.43 | 18.86 | 17.94 |
| *S*. Paratyphi A | 18.30 – 20.63 | 19.10 | 18.36 |
| *S*. Typhimurium SL1344 | 20.19 – 21.14 | 20.52 | 20.24 |
| PBS | 18.30 – 20.63 | 19.10 | 18.36 |

**Table 6.3: Summary of raw RNA-Seq reads for each stimulation condition at sample level.** Kolf2 macrophages were infected with *S.* Typhi, *S.* Paratyphi A, or *S*. Typhimurium at MOI of 10, or treated with PBS for 6 hours, with 3 biological replicates completed per condition. Data were concatenated from replicate-level reads and demonstrate similarities across groups in terms of depth of sequencing.

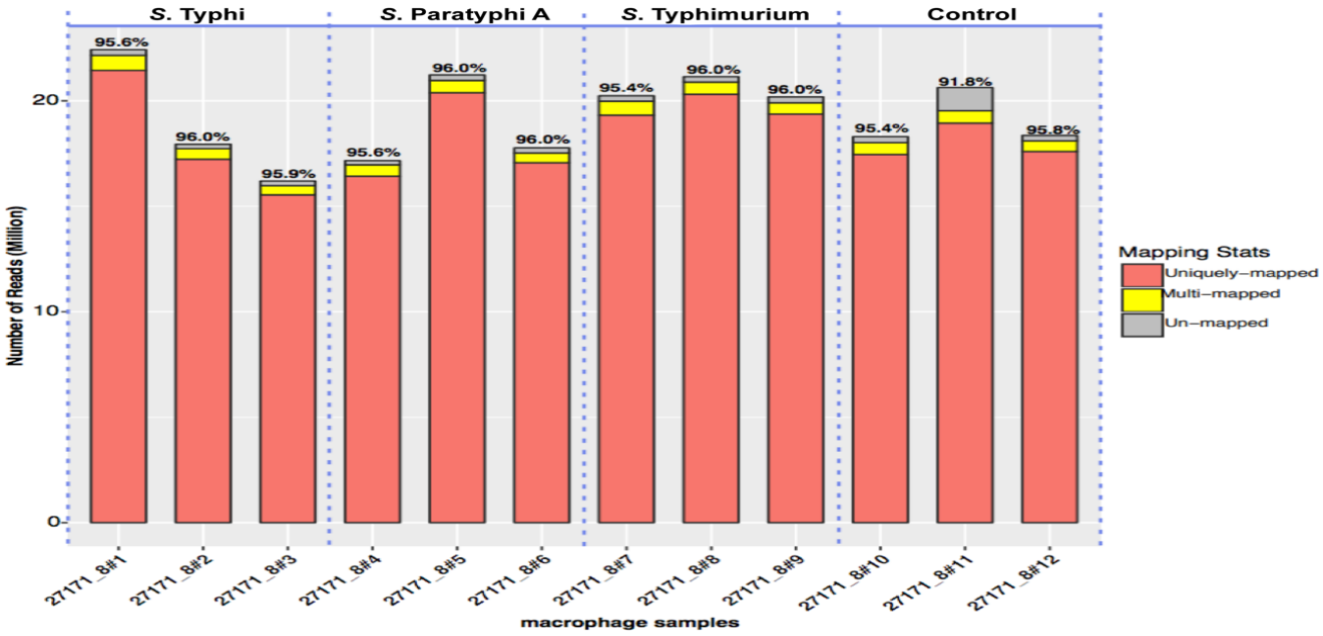


**Figure 6.30: Alignment summary.** Kolf2 macrophages were infected with *S.* Typhi, *S.* Paratyphi A, or *S*. Typhimurium at MOI of 10, or treated with PBS for 6 hours, with 3 biological replicates completed per condition. Raw reads were aligned to hg19 genome. 91.8 – 96% of the reads uniquely mapped to the hg19 genome. This was consistent for samples across all conditions.

All lowly expressed genes across the 12 samples were removed, leaving 11,473 genes. Samples were normalised by library size and gene length, FPKM (Fragments Per Kilobase of transcript per million mapped reads) values obtained and principal component analysis (PCA) performed (**Figure 6.31**). This demonstrated that the primary source of variance within the data was control versus stimulation/infection, followed by replicate number (PC1 and PC2), explaining 62% and 28% of variation respectively.

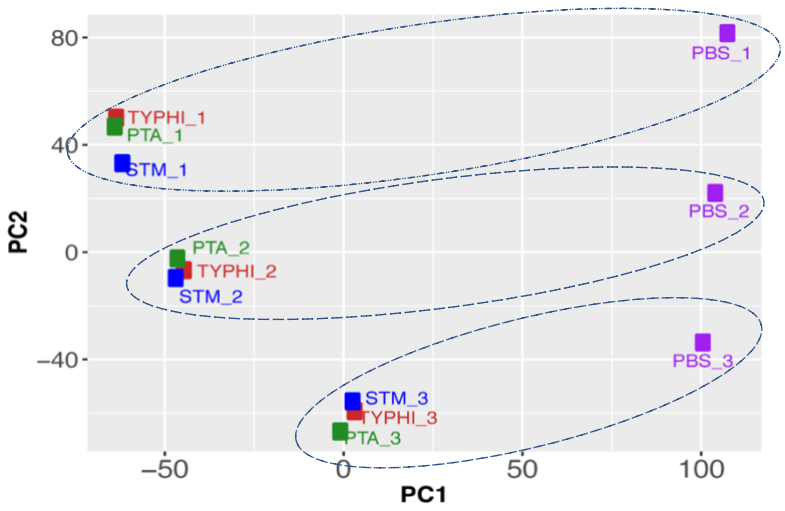


**Figure 6.31: Principal components analysis for macrophage samples.** Kolf2 macrophages were infected with *S.* Typhi, *S.* Paratyphi A, or *S.* Typhimurium at MOI of 10, or treated with PBS for 6 hours, with 3 biological replicates completed per condition. Samples separate on PC1 by infected versus uninfected, then on PC2 by replicate number (circled). ***Key:*** STM = *S.* Typhimurium SL1344, Typhi = *S.* Typhi, PTA = *S.* Paratyphi A, PBS = control.

In these macrophage samples, the variation in gene expression between replicates was higher than between the infection types. This is largely because the macrophages had to be freshly differentiated each week; and whilst culture conditions were the same for each set of samples, plated counts of macrophages aimed to be the same, experiments were performed on the same day post-differentiation, and using the same MOI of bacteria; these are all sources of potential variation. Having detected potential differentiation-related effects between iHO cell lines, analysis was performed to look at surface markers and transcription factors associated with macrophage differentiation and maturation (**Figure 6.32**).

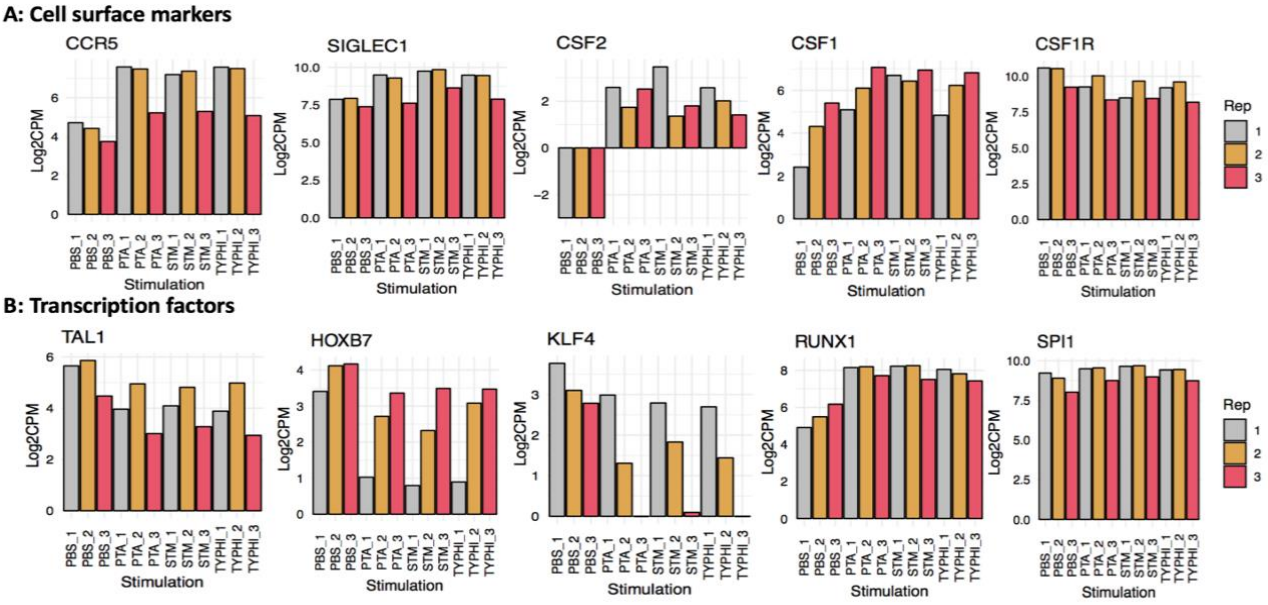


**Figure 6.32: Expression of cell surface markers and transcription factors associated with macrophage differentiation and maturation.** Kolf2 macrophages were infected with *S.* Typhi, *S.* Paratyphi A, or *S*. Typhimurium at MOI of 10, or treated with PBS for 6 hours, with 3 biological replicates completed per condition. Data are presented as log2 transformed counts per million values (Log2CPM) and normalised by library depth. Similarities in counts are seen across pathogens, but within replicates. ***Key:*** Rep = replicate number

The most striking feature was that expression levels were largely very similar across pathogens. The differences in expression occurred between replicates, and in the case of some genes, expression varied mostly in the uninfected versus infected conditions. Given that the replicate (batch) effect was very consistent, i.e. the same bias was present for each sample within a batch, it was decided to use the batches as a covariate in the design when fitting the data to a linear model. This did not yield large differences in genes expressed between the 3 infection conditions, therefore a normalization process called 'remove unwanted variation', (RUV)[49] was trialed, which removes unwanted technical effects on the data (such as batch effects), by performing factor analysis on suitable control genes or samples. In this case, the RUV method was used to estimate the factors of nuisance variation using the biological replicate samples for each stimulation condition for which the covariates of interest are constant (i.e. the effect of bacterial stimulation is constant between the replicates). When running RUV, the number of factors of unwanted variation (*k*) is decided by the user, and is based on considerations of sample size and extents of technical effects captured by each *k* factor. RUV is relatively robust to the *k* used.[49] In this case, *k* = 4 was chosen for the analysis. PCA plots were reproduced following RUV (**Figure 6.33**), and demonstrated that PC1 now separated samples by infected / uninfected status

and PC2 by pathogen. Hence, RUV efficiently removed the batch effect between replicates, whilst retaining the bacterial stimulation variation. Interestingly on these analyses, *S*. Typhi and *S*. Paratyphi A clustered closely, in comparison to the similarities seen between *S*. Paratyphi A and *S*. Typhimurium in infected iHO.

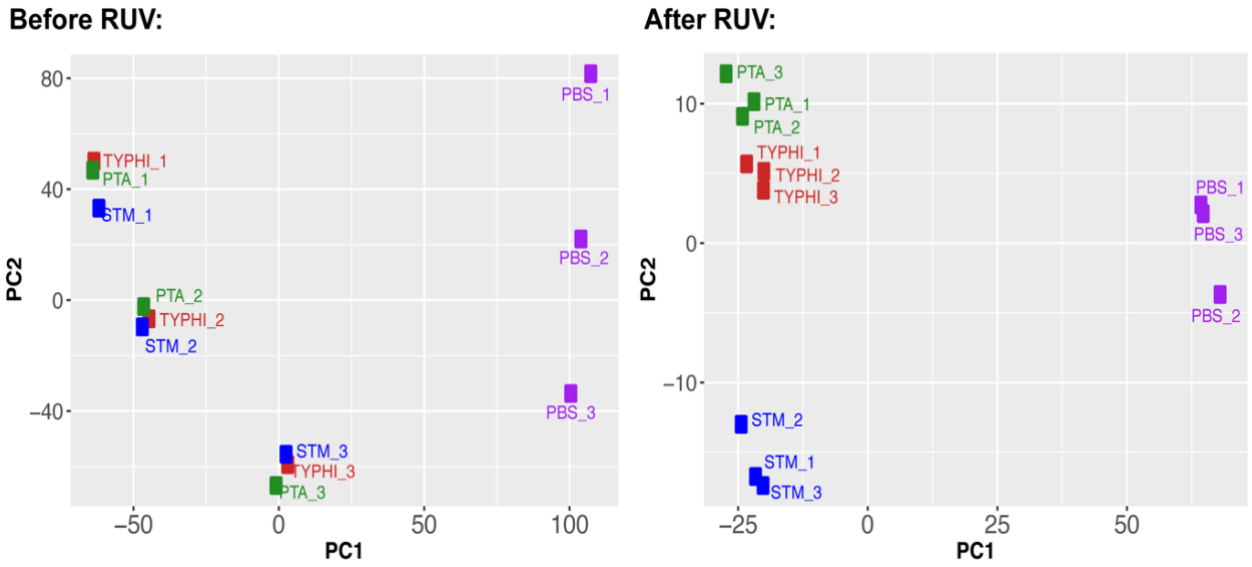


**Figure 6.33: Principal components analysis for infected Kolf2 macrophage samples before and after RUV.** Kolf2 macrophages were infected with *S.* Typhi, *S.* Paratyphi A, or *S*. Typhimurium at MOI of 10, or treated with PBS for 6 hours, with 3 biological replicates completed per condition. Samples initially separated on PC2 by replicate number, but following RUV, separate by pathogen, with clustering of typhoidal vs. non-typhoidal bacteria. ***Key:*** STM = *S*. Typhimurium SL1344, Typhi = *S*. Typhi, PTA = *S*. Paratyphi A, PBS = control.

Following these adjustments, differential expression analysis was run for all infection groups versus PBS (control), using the 4 *k* factors obtained from the RUV analysis as covariates in the model (**Table 6.4**). Total number of genes differentially expressed (DE) at a false discovery rate (FDR) < 0.05 are listed. To obtain biologically meaningful genes, this list was further narrowed down to FDR < 0.05 and log2 fold change (log2FC) > ± 2 (4 fold change) and log2 fold change (log2FC) > ± 3 (8 fold change). Numbers of up / downregulated genes were consistent across all 3 infections.

| Cell line: | FDR: | Typhi vs. PBS (up / down) | PTA vs. PBS (up / down) | STM vs. PBS (up / down) |
|---|---|---|---|---|
| Kolf2 | < 0.05 | 856 / 458 | 929 / 566 | 944 / 421 |
| | < 0.05 log2FC > ± 2 | 215 / 86 | 227 / 103 | 229 / 81 |
| | < 0.05 log2FC > ± 3 | 117 / 27 | 118 / 32 | 126 / 30 |

**Table 6.4: Summary of the number of genes differentially expressed (DE) in each stimulation comparison.** Kolf2 macrophages were infected with *S.* Typhi, *S.* Paratyphi A, or *S.* Typhimurium at MOI of 10, or treated with PBS for 6 hours, with 3 biological replicates completed per condition. ***Key:*** STM = *S.* Typhimurium SL1344, Typhi = *S.* Typhi, PTA = *S.* Paratyphi A, PBS = control.

Differentially expressed genes for each condition were calculated and compared between each stimulation condition in the form of a Venn diagram (**Figure 6.34**). Venn diagrams confirmed that in the macrophage stimulations, the greatest overlap in DE genes was between the two typhoid-causing serovars (*S.* Typhi and *S.* Paratyphi A), rather than between the unencapsulated bacteria as was the case in the iHO stimulations. There were also many fewer genes DE in *S.* Typhi stimulated macrophages alone than for either of the other pathogens, suggesting that beyond the commonalities between serovars in host response to genes bacteria are modulating for intracellular survival and replication, *S.* Typhi is able to go relatively unnoticed by the host macrophage.

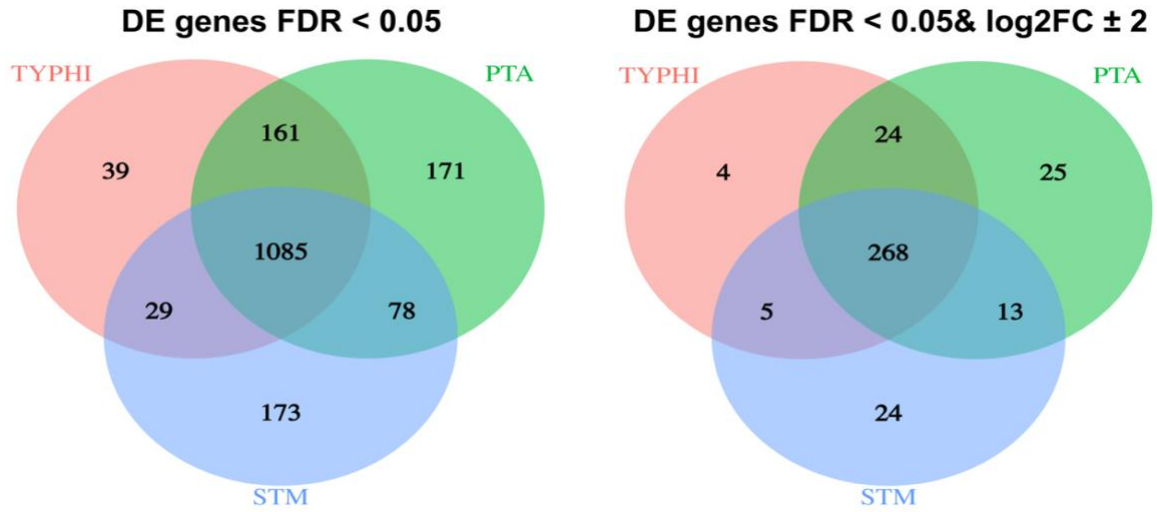


**Figure 6.34: Overlap between DE genes for each stimulation group.** Kolf2 macrophages were infected with *S.* Typhi, *S.* Paratyphi A, or *S.* Typhimurium at MOI of 10, or treated with PBS for 6 hours, with 3 biological replicates completed per condition. Differential expression was calculated for each infection condition versus PBS treatment. There are 1085 genes upregulated in all 3 stimulation conditions, with greater overlap between *S.* Typhi and *S.* Paratyphi A than for either of those pathogens and *S.* Typhimurium. Fewer genes are upregulated for *S.* Typhi alone than for any other pathogen.

Volcano plots were then produced to visualise differential expression for relatively up and down-regulated genes in each infection condition versus the PBS control (**Figure 6.35**), with very similar plots being observed in each condition. Gene ontology resource (http://geneontology.org) was used to generate plots of the top 10 biological pathways DE in the macrophages for each pathogen (using a cut off of logFC >2), with the number of genes DE per pathway (**Figure 6.36**). These were exactly the same for the top nine pathways for each pathogen, with the tenth pathway for *S*. Typhi and *S*. Paratyphi A being 'immune response' and for *S*. Typhimurium 'cellular response to organic substance'. The response to stimulation with both encapsulated and unencapsulated pathogens was uniform within the macrophages. Perhaps an additional harvest at an earlier timepoint of infection would garner more detail about initial interactions.

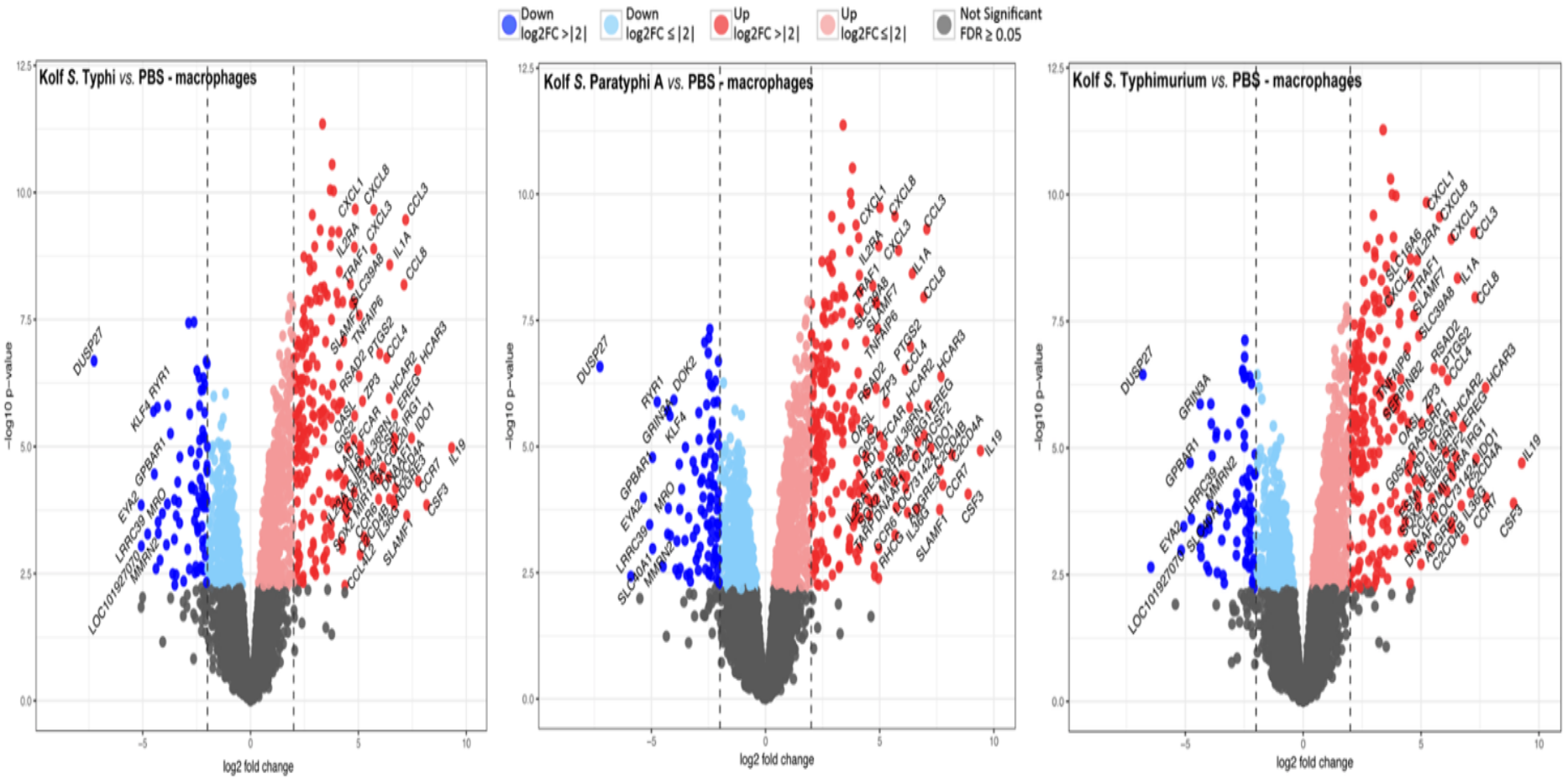


**Figure 6.35 Volcano plots for gene expression between macrophage stimulation conditions.** Kolf2 macrophages were infected with *S.* Typhi, *S.* Paratyphi A, or *S.* Typhimurium at MOI of 10, or treated with PBS for 6 hours, with 3 biological replicates completed per condition. Differential expression was calculated for each infection condition versus PBS treatment. There is a large degree of similarity between macrophage responses for all 3 pathogens.

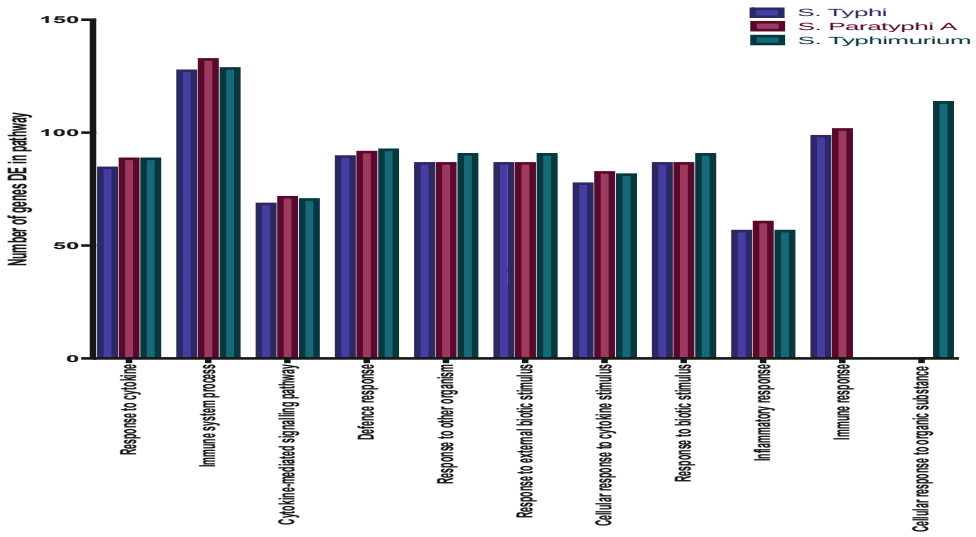


**Figure 6.36: Top 10 pathways upregulated in response to each pathogen.** Kolf2 macrophages were infected with *S.* Typhi, *S.* Paratyphi A, or *S*. Typhimurium at MOI of 10, or treated with PBS for 6 hours, with 3 biological replicates completed per condition. Differential expression was calculated for each infection condition versus PBS treatment. Data are presented are for the 10 most significantly DE biological pathways for each pathogen, with columns representing the number of genes per pathway upregulated.

In contrast to the commonalities seen between the serovars in terms of response to infection, with expected genes upregulated (e.g. CXCL1, CXCL8, CCL3, CXCL3, CCL8, IL19, CSF3) there were interesting differences witnessed when investigating genes DE solely for one pathogen. In *S*. Typhi, these genes were fewer than for either of the unencapsulated serovars and mapped to the Gene ontology (GO) component 'late endosomal membrane'. This suggests modification of phagolysosomal fusion; examples of genes downregulated for macrophages infected with *S*. Typhi were: MICALL1 (a lipid binding protein enriched in endosomal membranes), ARL8B (which has a role in lysosomal mobility), and CYB561A3 (which reduces $Fe^{3+}$ to $Fe^{2+}$ before transport from the endosome to the cytoplasm). Interestingly, SOCS1 is also downregulated in *S*. Typhi infection, which could mean loss of inhibition of the JAK/STAT pathway and increased inflammation, something which is unexpected with S. Typhi infection.

Genes which were solely DE for *S*. Paratyphi A, were associated with the GO component 'cytoplasm' and may provide some insight into how this serovar evades the immune response without the expression of SPI-7. Downregulated for macrophages infected with *S*. Paratyphi A were: CD28 (involved in T cell activation, proliferation and production of IL-4 and IL-10), BMP4 (a ligand of TGFβ required for Th17 differentiation) and SIGLEC11 (which

mediates anti-inflammatory signalling). In addition, cell survival-related proteins were downregulated, such as NEIL1 (involved in DNA repair) and PIK3C2b (involved in cell proliferation and survival). Upregulated were genes that would appear to be involved in phagolysosomal fusion such as: SYT6 (involved in exocytosis), and PPAP2V (associated with synthesis of the membrane component glycerolipids) and SLC1A2 (an amino acid / ion transporter). Intriguingly SOCS3 was upregulated in this condition, meaning negative regulation for the JAK/STAT pathway and modulated levels of inflammation.

Lastly, genes solely DE in *S*. Typhimurium infection were associated with the GO processes 'vesicle mediated transport, intracellular signal transduction and regulation of cell communication'. Genes downregulated included: MAML3 (involved in expansion of haematopoietic stem cells) and TBC1D4 (a GTPase-activating protein for members of the Rab family). Genes upregulated were inflammatory in nature, including: THBS (a platelet binding protein), LAT (involved in T cell activation, cytoskeletal change and MAPK pathway activation), CXCR4 (which binds to LPS and mediates inflammatory response, including TNF$\alpha$ secretion and the MAPK1/3 response) and CEACAM3 (which binds to certain pathogens to induce phagocytosis and pathogen clearance). CXCR4 is not well documented as a factor involved in *S*. Typhimurium infection[50], but Vi is known to reduce signalling via the MAPK pathway, with loss of activation of this pathway when HeLa cells were infected with a Vi expressing *S*. Typhimurium.[51] CEACAM3 proteins are known to be bound by *S*. Typhimurium[52] but it is interesting that there is no evidence of this in *S*. Paratyphi A or *S*. Typhi infection; with *S*. Typhi thought to be bound by CEACAM5 and CEACAM6.[53]

A heatmap for top genes DE at log2FC > 4 and FDR < 0.05 was constructed (**Figure 6.37**).

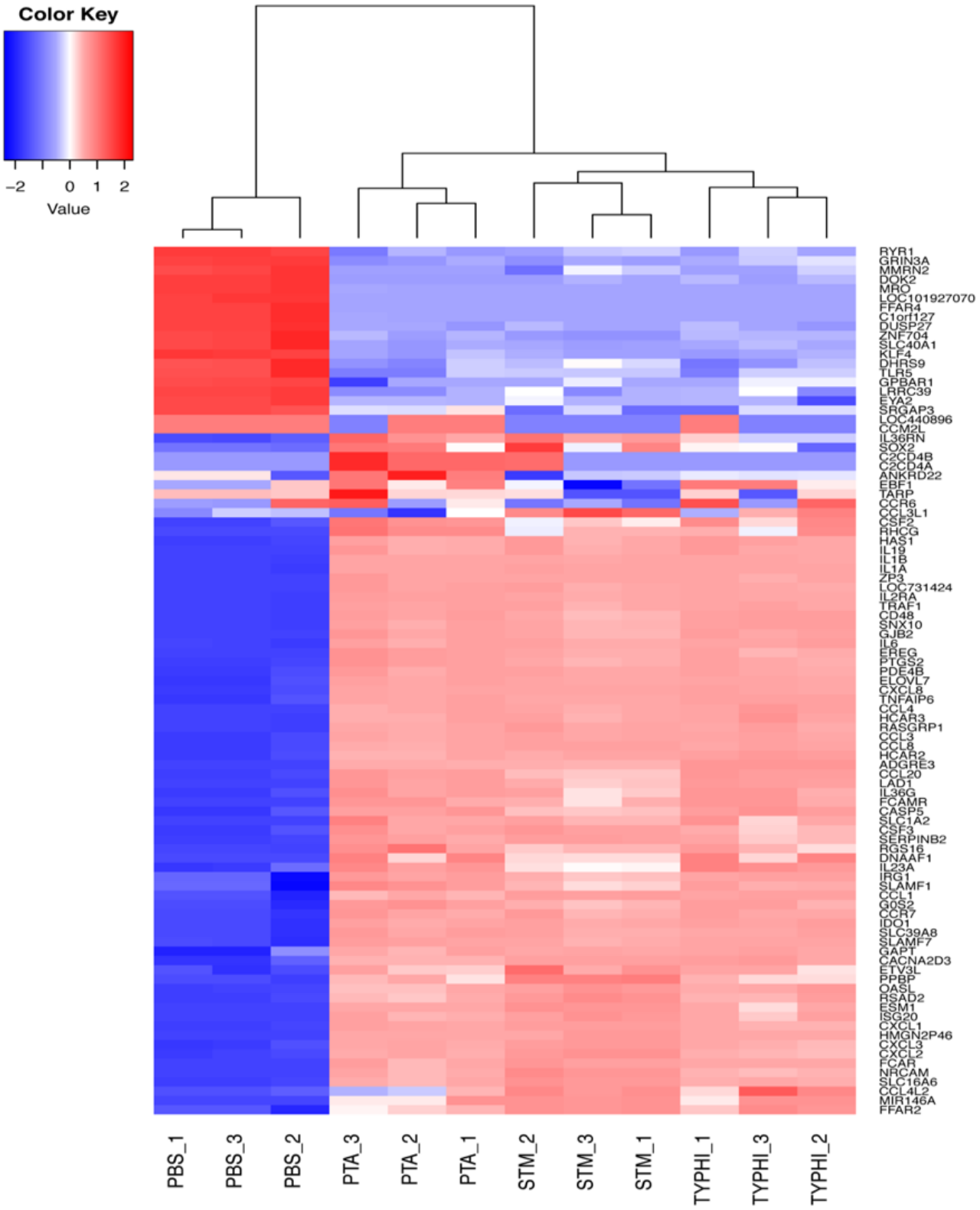


**Figure 6.37: Heatmap of top genes differentially expressed between infection conditions in macrophages.** Kolf2 macrophages were infected with *S.* Typhi, *S.* Paratyphi A, or *S.* Typhimurium at MOI of 10, or treated with PBS for 6 hours, with 3 biological replicates completed per condition. Expression values for genes DE at log2FC > 4 and FDR < 0.05 were normalized by fragments per kilobase of exon model per million reads mapped (FPKM) and are expressed as Z-scores, with red denoting upregulated and blue downregulated. ***Key:*** STM = *S.* Typhimurium SL1344, Typhi = *S.* Typhi, PTA = *S.* Paratyphi A, PBS = control.

This plot demonstrates both the similarities between all infected groups and the genes which are downregulated in all infection conditions in comparison to the control. These included RYR1 (involved in calmodulin binding), DOK2 (which attenuates MAPK activation), FFAR4 (a free fatty acid receptor that attenuates the inflammatory response), EYA2 (involved in DNA repair) and intriguingly, TLR5 which is one of the primary activators of NFκB via the MyD88 pathway in response to flagellin. TLR5 signalling is an essential part of the epithelial response to *Salmonella*, and has certainly been implicated in response to *S*. Typhimurium in murine macrophages,[54] but evidence for its role in *S*. Typhi infection is less pronounced.[55] The relative downregulation of TLR5 following infection in these samples may be due to the use of a timepoint at which bacteria should all be intracellular (especially following gentamicin treatment to kill external bacteria) and TLR5 related activation of the inflammatory response would likely already have occurred.

Venn diagrams were constructed to check whether there were any similarities between genes upregulated in macrophages versus those in iHO for all pathogens (**Figure 6.38**). This was the case for 20 genes in cells stimulated with *S*. Typhi, 47 for *S*. Paratyphi A and 55 for *S*. Typhimurium SL1344; with these genes representing very similar biological pathways for all pathogens, including: 'cytokine-mediated signalling pathway', 'inflammatory response', 'response to bacterium', 'response to LPS', 'regulation of signal transduction', 'cellular chemotaxis' and 'regulation of cell communication' (pathways generated using g:Profiler). The top 3 KEGG pathways upregulated for all pathogens were all known to be important early responders to Salmonella infection: TNF signalling pathway[56], IL-17 pathway[57] and NFκB signalling pathway.[58]

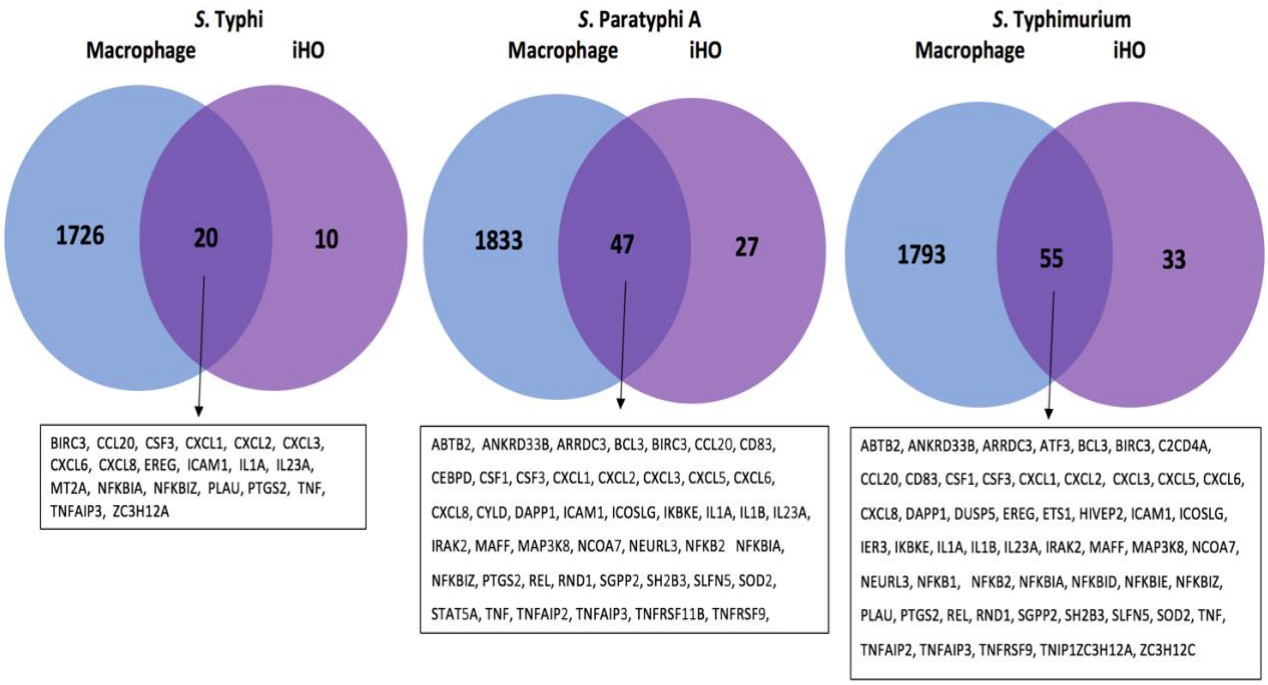


**Figure 6.38: Overlap between DE genes for each pathogen in iHO and macrophage.** Kolf2 iHO were infected with *S.* Typhi, *S.* Paratyphi A, or *S*. Typhimurium or injected with PBS and incubated for 3 hours prior to RNA extraction, with 3 biological replicates completed per condition. Kolf2 macrophages were infected with *S.* Typhi, *S.* Paratyphi A, or *S*. Typhimurium at MOI of 10, or treated with PBS for 6 hours, with 3 biological replicates completed per condition. Differential expression was calculated for each infection condition versus PBS treatment. There is less crossover between differentially expressed genes in macrophages and iHO infected with *S*. Typhi, given that there were fewer upregulated genes in iHO for this pathogen. Biological pathways activated for all 3 pathogens were very similar.

### 6.4.4 Cytokine response in macrophages infected with *S*. Typhi and *S*. Paratyphi A

Supernatants were collected from macrophages prior to, and at 6 hours post infection with *S*. Typhi, *S*. Paratyphi A and *S*. Typhimurium SL1344. Strong cytokine responses were demonstrated against all pathogens with responses of a similar magnitude for each cytokine with all pathogens (**Figure 6.39**).

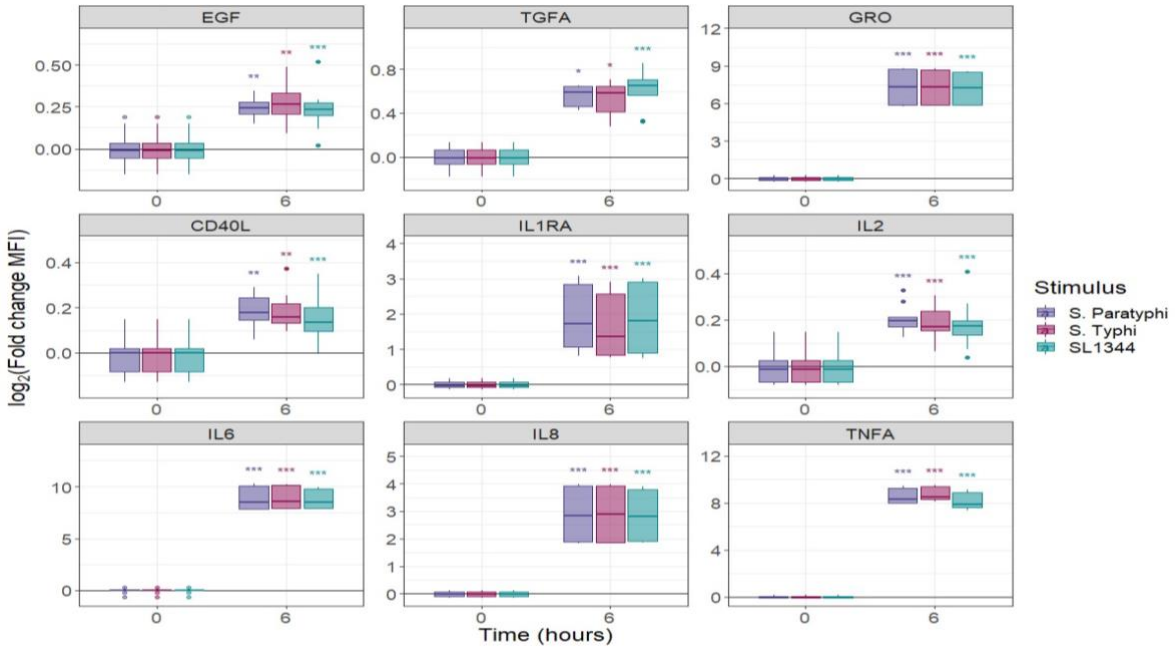


**Figure 6.39: Macrophage cytokine responses for all pathogens pre- and post-infection.** Kolf2 macrophages were infected with *S.* Typhi, *S.* Paratyphi A, or *S.* Typhimurium at MOI of 10, or treated with PBS for 6 hours. Supernatant samples were taken pre-infection and at 6 hours post-infection. Data presented are from 3 biological replicates (containing 2 technical replicates). Unpaired student's t-test was used to compare results (* $p < 0.05$, ** $p < 0.01$, *** $p < 0001$). Significant elevation of all cytokines occurred post-infection, with similar magnitudes of response across pathogens.

These similarities between pathogens fit with what was noted on transcriptomic analysis, and demonstrate overlap between the transcriptomic and cytokine responses. Particularly highly upregulated were IL1-RA and IL-6, with $log_2FC$ >10, and TNF$\alpha$, IL-8, GRO$\alpha$ with $log_2FC$ >5. It appears that once inside the macrophage, all pathogens initiated a similar inflammatory response, which was surprising given the differences in intracellular counts recovered, and the expectation that *S.* Typhi and to an extent *S.* Paratyphi A may be able to subvert the host's immune response to infection.

## 6.5 Preliminary studies of the interactions of clinical (H58) *S.* Typhi with the iHO epithelium

### 6.5.1 Assessing the infectivity of H58 *S.* Typhi in the iHO model

Both *S.* Typhi Quailes and *S.* Paratyphi A NVGH308 were selected for use in human challenge studies[59] due to their antimicrobial sensitivities, well-characterised nature and presumed similarities to circulating strains. However, as individual isolates, that they do not fully represent overall serovar diversity, for example the spread of the H58 clade[9] and increase in

multidrug resistant and XDR *S*. Typhi.[10] Therefore, experiments were performed with additional isolates of *S*. Typhi, as outlined in **Table 6.5.** These included 2 H58 isolates, one from Lineage 1 and one from Lineage 2, and one additional non-H58 clinical isolate.

| **Name:*** | **Country and year of origin:** | **H58?** | **Genotype:** | **Relevant mutations / plasmids:** |
|---|---|---|---|---|
| E02-1180 SGB90 (**SGB90**) | India, 2002 | No | 0.0.3 | gyrA-D87G |
| 2010K-0515 101TY (**Ty101**) | Kenya, 2007 | Yes | 4.3.1.2 | None |
| 2010K-0517 116TY (**Ty116**) | Kenya, 2007 | Yes | 4.3.1.1 | None |

**Table 6.5: List of additional S. Typhi utilised in the iHO model** *abbreviated name used in this study in brackets

All isolates were tested using slide agglutination assays, with anti-Salmonella Vi monoclonal antibody (Sifin Diagnostics GmbH) and were demonstrated to be expressing Vi capsule prior to use in experiments. The isolates were microinjected independently into Kolf2 iHO, with *S*. Typhi Quailes acting as a control. Intracellular assays demonstrated that in the initial stages of infection, Ty116; the Lineage 1 H58 isolate appeared to be most infective, but by 3 hours post-infection, all isolates had been overtaken by *S*. Typhi Quailes in terms of intracellular counts. As in previous assays, Quailes appeared to be invading and surviving within cells more effectively up until the 3 hour time point (**Figure 6.40**).

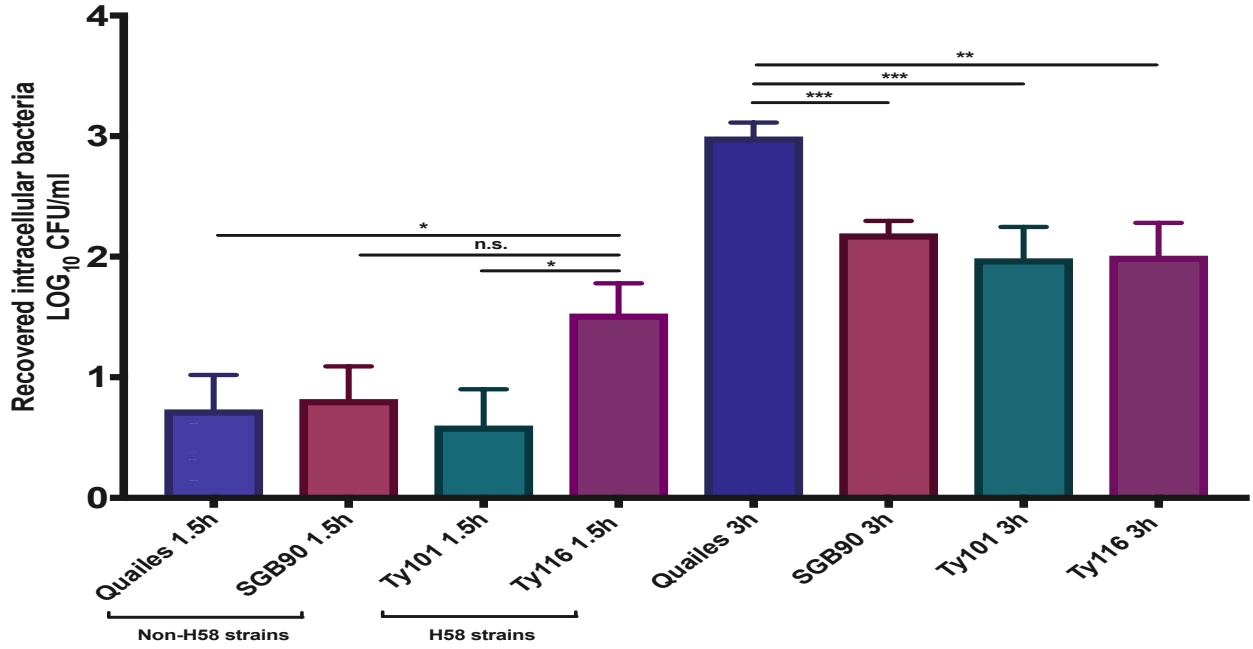


**Figure 6.40: Intracellular assays for H58 versus non-H58 *S*. Typhi in Kolf2 iHO.** Kolf2 iHO were injected with *S*. Typhi Quailes, SGB90, Ty101 or Ty116 strains and incubated for 1.5 or 3 hours prior to undergoing modified gentamicin protection assays and recovery of intracellular bacteria. Data presented are for 3 biological replicates (each averaged from 3 technical replicates), with 30 iHO injected per replicate +/- SEM. Unpaired Mann-Whitney tests were used for all assays (**n.s.** not significant, * $p < 0.05$, ** $p < 0.01$, *** $p < 0.001$). In the initial stages, the lineage 1 H58 isolate Ty116 was significantly more invasive than Quailes and Ty101. However, by 3 hours post-infection, Quailes had overtaken the other 3 isolates with significantly more Quailes being recovered.

Given the differences in numbers of bacteria invading the epithelium, assays were completed to assess whether there was any difference in numbers of bacteria surviving in the lumen post-infection (**Figure 6.41**). Results demonstrated that all isolates were able to survive in the lumen, with significantly more of the non-H58 bacteria being present at 3 hours post-infection. In particular, SGB90 appeared to replicate well in the iHO lumen, with counts at 3 hours being significantly higher than at 1.5 hours. Counts of *S*. Typhi Quailes were marginally higher at 3 hours than 1.5 hours, and both the H58 isolates appeared to be in equilibrium at this point. Given their propensity to cause disease in vivo, it was interesting that the H58 isolates were neither significantly better at invading the epithelium nor at surviving in the luminal environment of the iHO at 3 hours post infection.

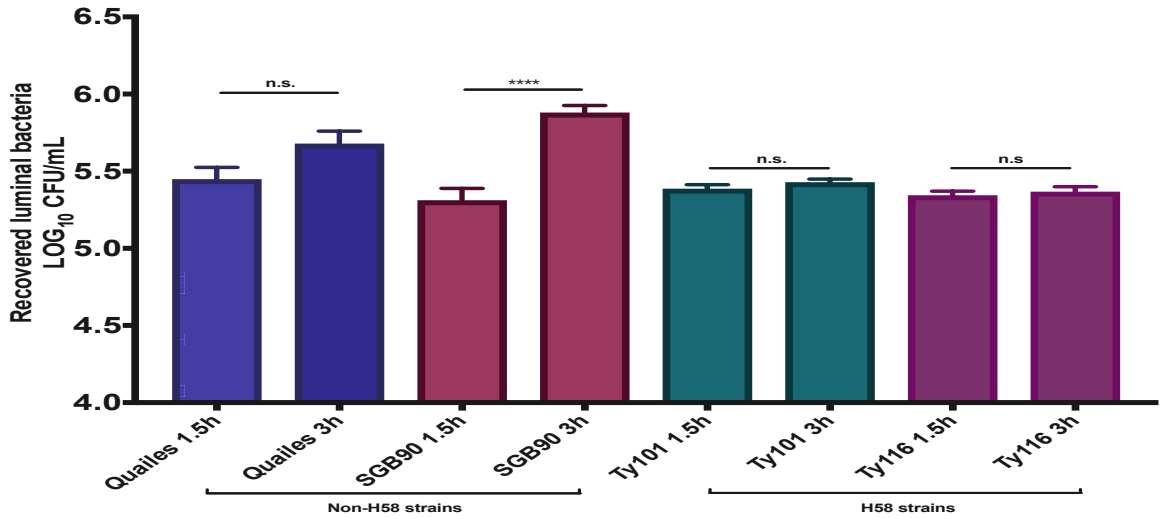


**Figure 6.41: Luminal assays for H58 versus non-H58 *S.* Typhi in Kolf2 iHO.** Kolf2 iHO were injected with *S*. Typhi Quailes, SGB90, Ty101 or Ty116 strains and incubated for 1.5 or 3 hours prior to recovery of luminal contents. Data presented are for 3 biological replicates (each averaged from 3 technical replicates), with 30 iHO injected per replicate +/- SEM. Unpaired Mann-Whitney tests were used for all assays (n.s. – not significant, **** $p < 0.0001$). Both of the non-H58 isolates, in particular SGB90 were able to survive and replicate in the lumen of the iHO, with counts of SGB90 at 3 hours being significantly higher than at 1.5 hours post-infection. Counts of both Quailes and SGB90 were significantly higher than Ty101 and Ty116 at 3 hours post-infection ($p < 0.05$ for all comparisons).

### 6.5.2 Transcriptomic changes witnessed during H58 iHO infection

Given the differences in iHO epithelial response to pathogens observed with different *Salmonella* serovars, and the differences in invasion between the *S*. Typhi isolates, bulk RNA-Seq was completed as described in 2.16 for iHO infected with SGB90, Ty101 and Ty116, with Quailes-infected iHO as the control. QC metrics for all samples are outlined below (**Table 6.6, Figure 6.42**), demonstrating the similarities in terms of depth and alignment of reads for all cell lines and conditions, and higher total read counts than those observed in the iHO experiment outlined earlier in this chapter.

| **Stimulation condition:** | **Cell line:** | **Read depth range:** (million reads) | **Read depth mean:** (million reads) | **Read depth median:** (million reads) |
|---|---|---|---|---|
| Quailes | Kolf2 | 27.18 – 32.43 | 30.08 | 30.62 |
| SGB90 | Kolf2 | 29.55 – 32.59 | 31.08 | 31.09 |
| Ty101 | Kolf2 | 26.23 – 31.37 | 29.65 | 31.34 |
| Ty116 | Kolf2 | 26.33 – 29.71 | 28.33 | 28.95 |

**Table 6.6: Summary of raw RNA-Seq reads for each stimulation condition at sample level.** Kolf2 iHO were injected with *S*. Typhi Quailes, SGB90, Ty101 or Ty116 strains and incubated for 3 hours prior to RNA extraction and sequencing, with 3 biological replicates completed per condition. Data were concatenated from replicate-level reads and demonstrate similarities across groups in terms of depth of sequencing.

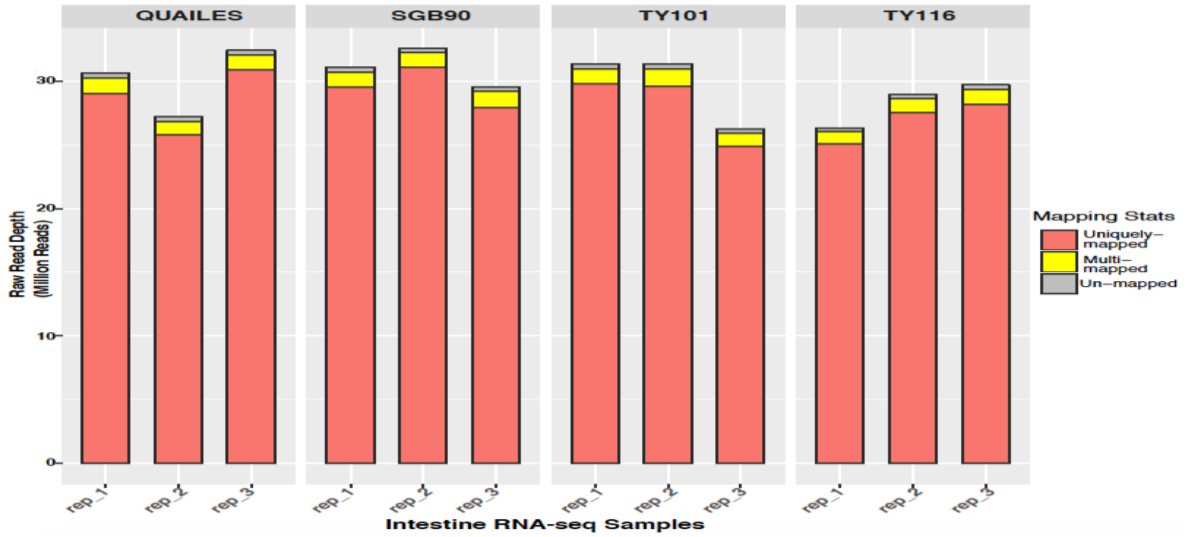


**Figure 6.42: Alignment summary.** Kolf2 iHO were injected with *S*. Typhi Quailes, SGB90, Ty101 or Ty116 strains and incubated for 3 hours prior to RNA extraction and sequencing, with 3 biological replicates completed per condition. Raw reads were aligned to hg19 genome. 94.38 – 95.49% of the reads uniquely mapped to the hg19 genome. This was consistent for samples across all conditions.

All lowly expressed genes across the 12 samples were removed, leaving 11,396 genes. Samples were then normalised by library size and gene length, FPKM (Fragments Per Kilobase of transcript per Million mapped reads) values obtained and principal component analysis (PCA) performed (**Figure 6.43**). In this case, samples did not cluster clearly into groups in any of the first 3 PCs, either by pathogen or by replicate number.

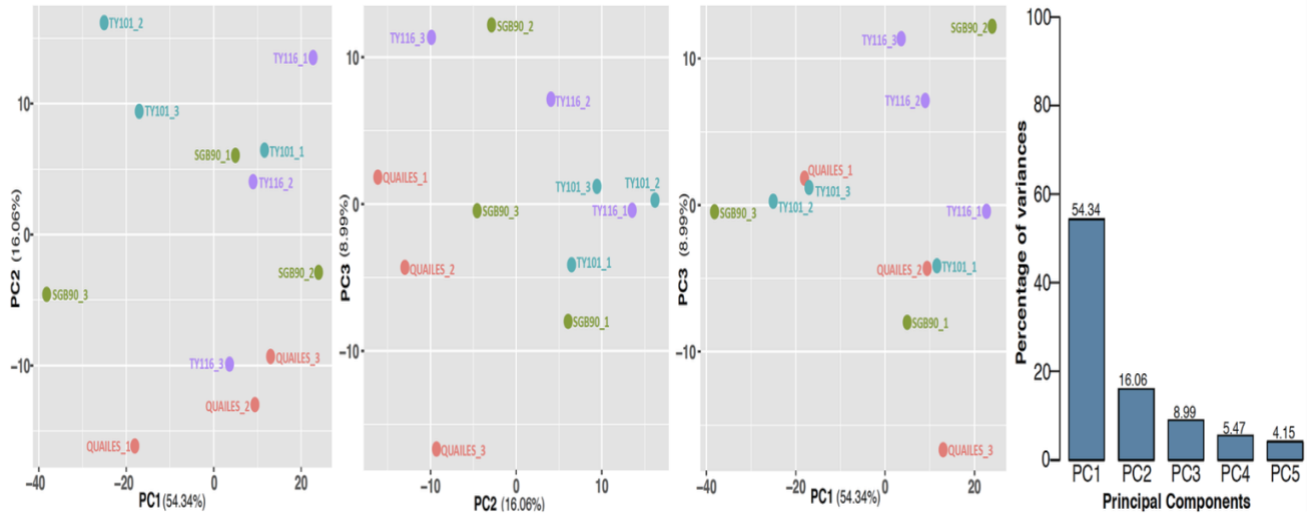


**Figure 6.43: Principal components analysis for H58 versus non-H58 isolates.** Kolf2 iHO were injected with *S*. Typhi Quailes, SGB90, Ty101 or Ty116 strains and incubated for 3 hours prior to RNA extraction and sequencing, with 3 biological replicates completed per condition. Samples do not clearly separate by PC in terms of pathogen or replicate. The top 5 PCs were responsible for 89.01% of variance between samples.

Examining the top 20 genes contributing to PC1, a large proportion of these are involved in transcriptional regulation, differentiation or the WNT pathway (CTNND1, DDI2, KIAA0754, RBM5-AS1, REL, TRIM71, TTBK2, ZBED6, ZNF121 and ZNF354C). Genes associated with immune regulation (THRIL) and metal ion transport (NIPAL1) were upregulated, as was a gene associated with natural-killer cell activation (NCR3LG1). Interestingly, study of the blood transcriptome following challenge with oral typhoid vaccines (Ty21a (unencapsulated) and M01ZH09 (encapsulated)) showed upregulation of NK-activating genes and cell cycle blood transcription modules (BTMs) respectively,[60] suggesting that we may be capturing an early epithelial signature which mimics what is happening in vivo. Results suggested that cell cycle BTMs may be predictive of humoral immunogenicity following oral live-attenuated vaccination. This may not hold true for epithelial cell cycle modules rather than blood ones; it could be in this case that we are capturing some differences in maturity between iHO. However, given that samples do not separate by replicate, it would appear that there were similar levels of differentiation of iHO between conditions and replicates. In this scenario, it is likely that interactions of the different encapsulated *S*. Typhi with the iHO epithelium were so similar between serovars, that any differences in these interactions are hidden by more pronounced differences in other transcriptional processes such as cell cycle between samples.

### 6.5.3 Assessing the infectivity of H58 *S*. Typhi in the macrophage model

Given the lack of epithelial transcriptomic difference between the H58 and non-H58 *S.* Typhi, these bacteria were also assessed in the macrophage model, to investigate whether their potential ability to cause severe clinical disease is related to their behaviour within macrophages (**Figure 6.44**). Interestingly, despite its limited invasiveness in the iHO model, Ty101 was phagocytosed more effectively than either of the non-H58 isolates. Ty116 was also recovered intracellularly at higher counts than the non-H58, but not significantly so. It is tempting to suggest that the ability of the H58 *S*. Typhi to cause severe diseases could lie in their ability to survive and replicate within macrophages rather than necessarily being better at invading the intestinal epithelium, although for Ty116, elements of both of these invasion mechanisms may be enhanced. Of course, this is preliminary data and further analysis is required to draw firm conclusions.

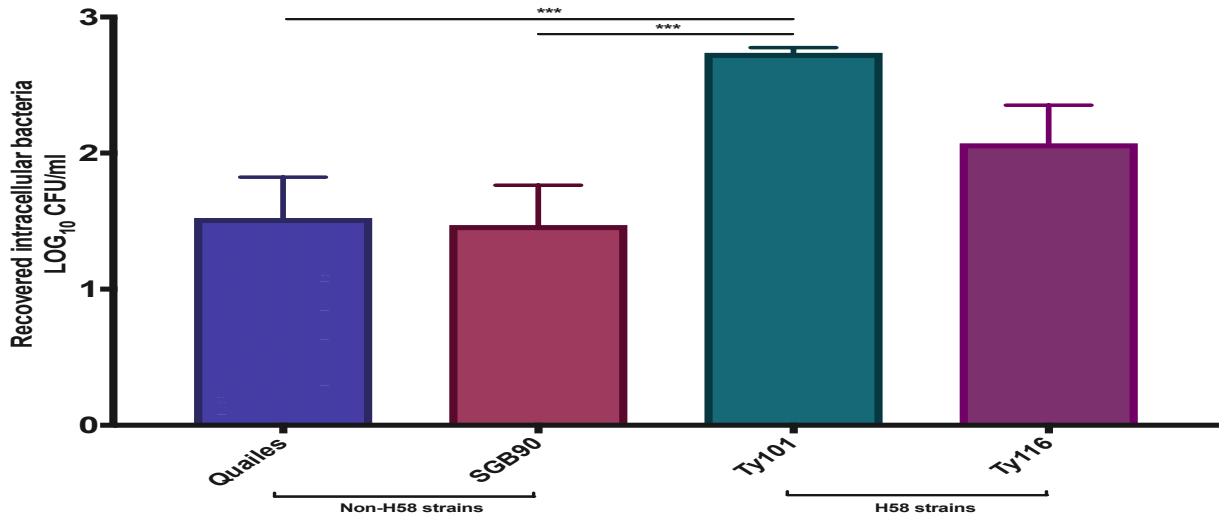


**Figure 6.44: Intracellular bacterial counts for H58 versus non-H58 *S*. Typhi in Kolf2 macrophages.** Kolf2 macrophages were infected with *S*. Typhi Quailes, SGB90, Ty101 or Ty116 strains at MOI of 10 and incubated for 6 hours prior to gentamicin protection assay and recovery of intracellular bacteria. Data presented are for 3 biological replicates (each averaged from 12 technical replicates) +/- SEM. Unpaired Mann-Whitney tests were used for all assays (*** $p < 0.001$). Both of the H58 *S*. Typhi, in particular Ty101, were effectively phagocytosed and able to survive within the macrophage.

### 6.5.4 Transcriptomic changes witnessed during H58 macrophage infection

Kolf2 macrophages were infected for 6 hours with *S*. Typhi Quailes, SGB90, Ty101 or Ty116 at MOI 10, prior to harvesting, RNA extraction and submission for sequencing as outlined in 2.16. QC metrics for all samples are outlined below (**Table 6.7, Figure 6.45**), demonstrating the similarities in terms of depth and alignment of reads for all cell lines and conditions, and increased number of reads versus the earlier macrophage experiments.

| **Stimulation condition:** | **Cell line:** | **Read depth range:** (million reads) | **Read depth mean:** (million reads) | **Read depth median:** (million reads) |
|---|---|---|---|---|
| Quailes | Kolf2 | 26.92 – 33.32 | 30.90 | 32.45 |
| SGB90 | Kolf2 | 27.72 – 37.83 | 31.37 | 28.58 |
| Ty101 | Kolf2 | 25.20 – 27.40 | 26.35 | 26.45 |
| Ty116 | Kolf2 | 24.48 – 30.40 | 27.65 | 28.07 |

**Table 6.7: Summary of raw RNA-Seq reads for each stimulation condition at sample level.** Kolf2 macrophages were infected with *S*. Typhi Quailes, SGB90, Ty101 or Ty116 strains at MOI of 10 and incubated for 6 hours, with 3 biological replicates completed per condition. Data were concatenated from replicate-level reads and demonstrate similarities across groups in terms of depth of sequencing.

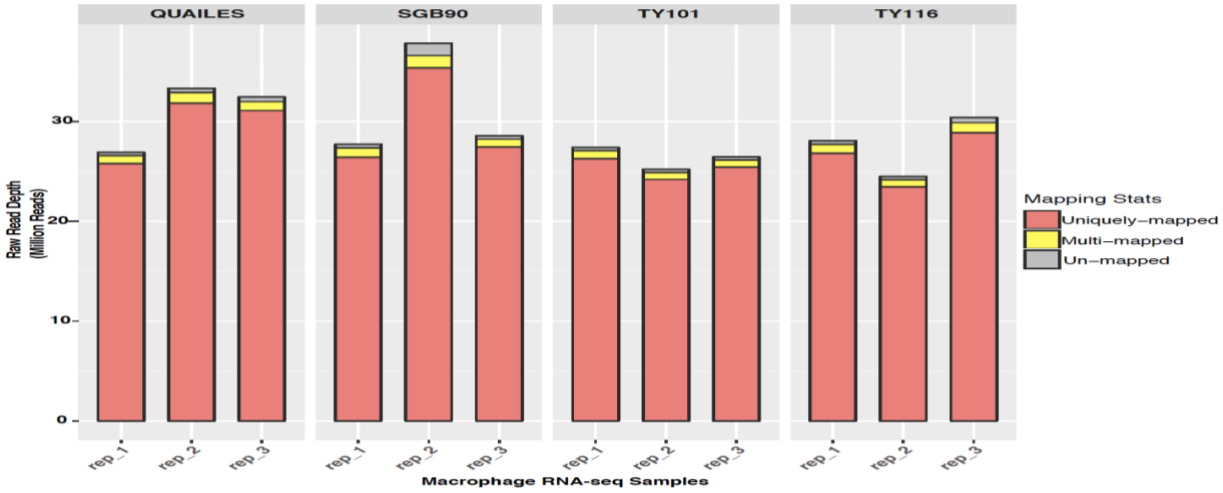


**Figure 6.45: Alignment summary.** Kolf2 macrophages were infected with *S*. Typhi Quailes, SGB90, Ty101 or Ty116 strains at MOI of 10 and incubated for 6 hours, with 3 biological replicates completed per condition. Raw reads were aligned to hg19 genome. 93.47 – 96.17% of the reads uniquely mapped to the hg19 genome. This was consistent for samples across all conditions.

All lowly expressed genes across the 12 samples were removed, leaving 10,583 genes. Samples were then normalised by library size and gene length, FPKM (Fragments Per Kilobase of transcript per Million mapped reads) values obtained and principal component analysis (PCA) performed (**Figure 6.46**). PC1 represents a latent source of variation in the data, as samples do not clearly separate here. However, PC2 separates samples by replicate number, as was seen in the earlier macrophage experiments, and is responsible for 15.23% variation. Excitingly, PC4 separates samples by H58 status, but this is only responsible for 6.3% variation in the data.

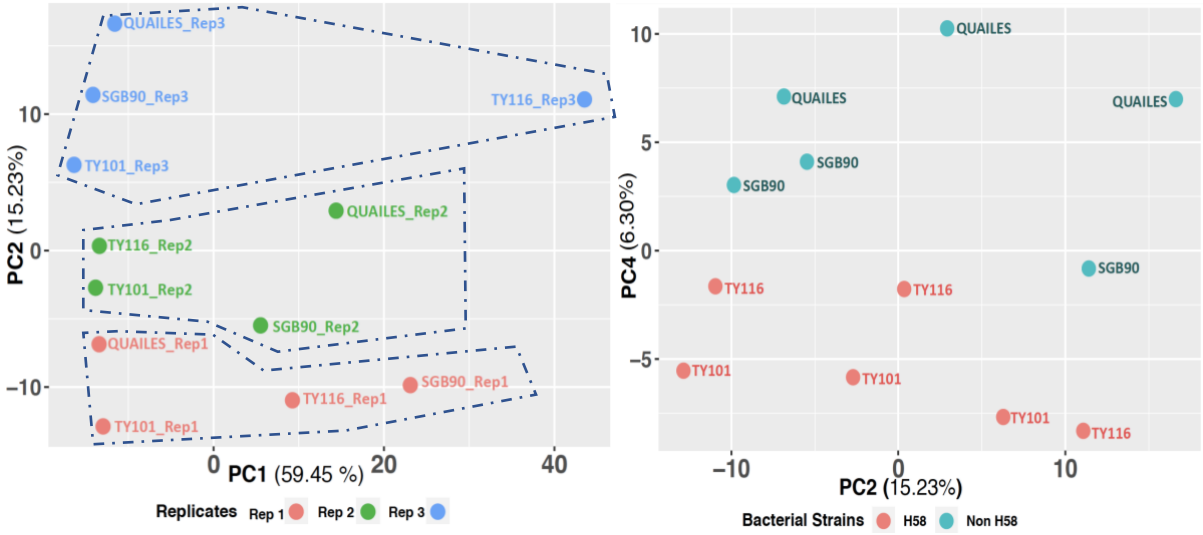


**Figure 6.46: Principal components analysis for H58 and non-H58 macrophage samples.** Kolf2 macrophages were infected with *S*. Typhi Quailes, SGB90, Ty101 or Ty116 strains at MOI of 10 and incubated for 6 hours, with 3 biological replicates completed per condition. Samples separate on PC2 by replicate number (circled) and on PCA4 by H58 status.

Initially, replicates were adjusted for as a batch effect in the differential analysis, but this did not yield any differentially expressed genes. Therefore, the RUV normalization process was again employed. In this case, *k* = 3 was chosen for the analysis. PCA plots were reproduced following RUV (**Figure 6.47**), and demonstrated that PC1 now separated samples both by condition and by H58 status.

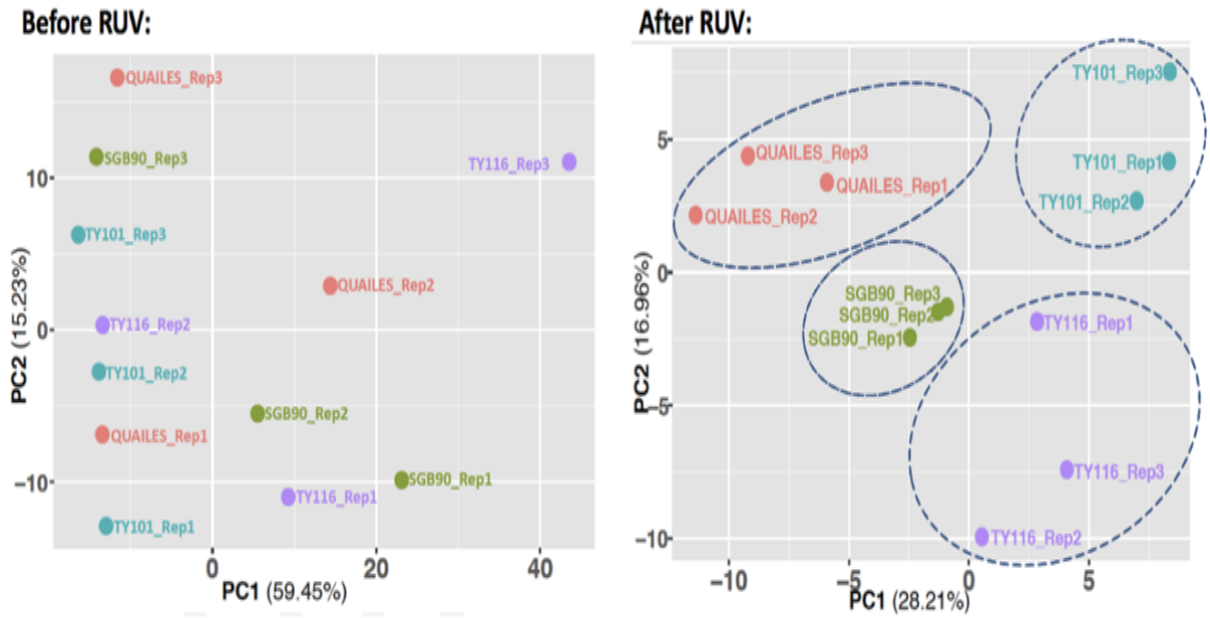


**Figure 6.47: Principal components analysis before and after RUV.** Kolf2 macrophages were infected with *S*. Typhi Quailes, SGB90, Ty101 or Ty116 strains at MOI of 10 and incubated for 6 hours, with 3 biological replicates completed per condition. Following RUV, using *k* = 3, PC1 now separates samples by serovar and by H58 status (circled).

Following these adjustments, differential expression analysis was run for all serovars versus Quailes (control), using the 3 *k* factors obtained from the RUV analysis as covariates in the model. Total number of genes differentially expressed (DE) at a false discovery rate (FDR) < 0.05 are listed. To obtain biologically meaningful genes, this list was further narrowed down to FDR < 0.05 and log2 fold change (log2FC) > ± 0.583 (1.5 fold change) and log2FC > ± 1 (2 fold change) (**Table 6.8**). There were more genes differentially expressed between the H58 strains and Quailes than between SGB90 (non-H58 *S*. Typhi) and Quailes.

| Cell line: | FDR: | SGB90 vs. Quailes (up / down) | Ty101 vs. Quailes (up / down) | Ty116 vs. Quailes (up / down) |
|---|---|---|---|---|
| Kolf2 | < 0.05 | 93 / 62 | 704 / 624 | 419 / 266 |
| | < 0.05<br>log2FC > ± 0.583 | 5 / 3 | 30 / 38 | 18 / 18 |
| | < 0.05<br>log2FC > ± 1 | 1 / 1 | 3 / 0 | 3 / 0 |

**Table 6.8: Summary of the number of genes differentially expressed (DE) in each stimulation comparison.** Kolf2 macrophages were infected with *S*. Typhi Quailes, SGB90, Ty101 or Ty116 strains at MOI of 10 and incubated for 6 hours, with 3 biological replicates completed per condition. Differential expression was calculated for SGB90, Ty101 and Ty116 infections versus Quailes infection.

Differentially expressed (DE) genes for each condition were calculated and compared between in the form of Venn diagrams, volcano plots and a heat map (**Figures 6.48 - 6.50**). Macrophages infected with SGB90 had the fewest genes DE versus infection with Quailes. Interestingly, Ty101 had the most genes DE, which correlates with the fact that it was recovered at the highest counts intracellularly. There is also a good degree of overlap between genes DE for both of the H58 isolates.

Five genes were DE in all conditions versus Quailes, with CXCL11, CXCL9, NCKAP5 and RET being upregulated and TSLP downregulated. CXCL9 and CXCL11 are chemokines, and ligands for CXCR3, whose release is induced by IFNγ. These chemokines are chemotactic for activated T cells. Increased expression of CXCR3 has been demonstrated in T regulatory cells from peripheral blood mononuclear cells (PBMCs) from individuals with acute typhoid infection.[61] In challenge studies, a direct relationship between bacteraemia and enhanced IFNγ response has been noted, with IFNγ primed macrophages able to kill *Salmonella.*[62] NCKAP5 promotes microtubule organisation and stabilisation. *S*. Typhimurium is known to induce accumulation of microtubules around *Salmonella* containing vacuoles in both epithelial cells and macrophages,[63] and as observed on macrophage TEM in this study, *S*. Typhi is able to induce a similar response. RET has a role in controlling cell death / survival balance, and calcium ion binding, which is key to the control of phagolysosomal fusion. TSLP has 2 isoforms, the expression of both of which has been shown to be affected by *Salmonella* infection;[64] an anti-inflammatory short form (expressed at steady state), and a pro-inflammatory long form (expressed during inflammation). In *S*. Typhimurium infections,

the short form is downregulated and the long form upregulated, leading to inflammation. It is not clear here which isoform is being downregulated as either could be biologically feasible.

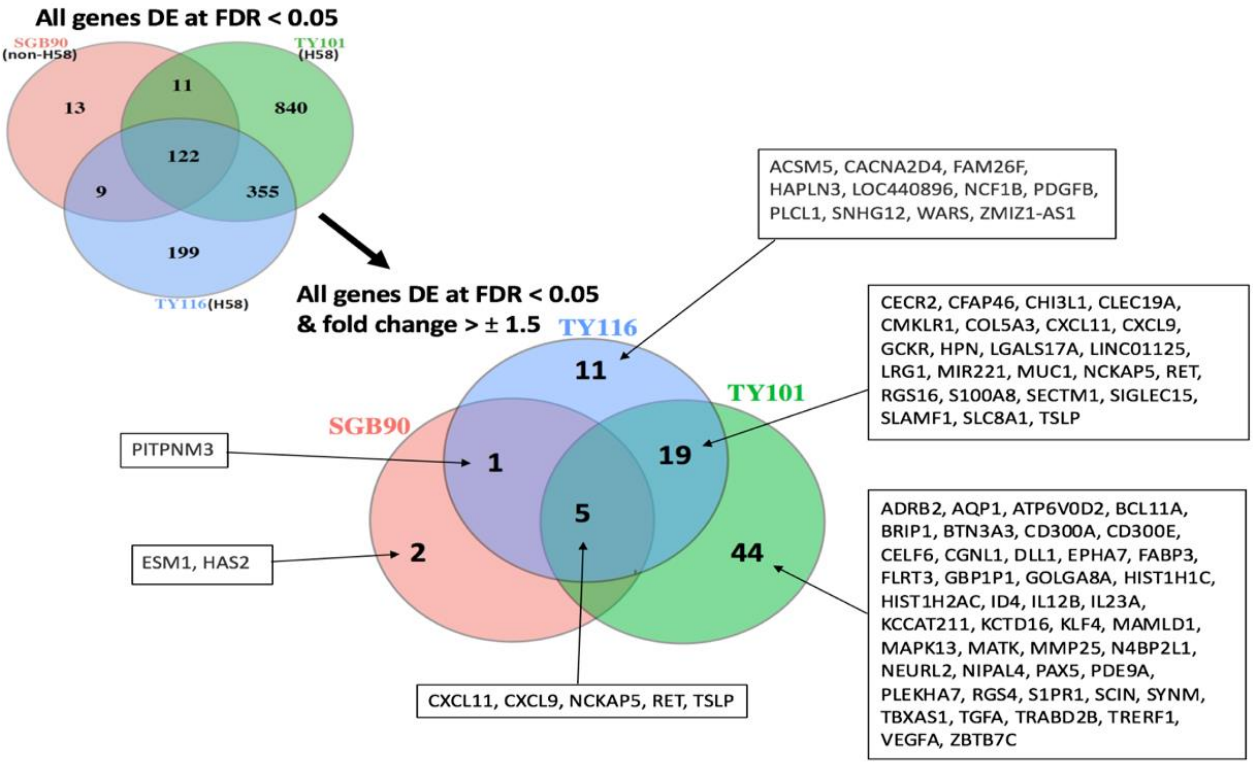


**Figure 6.48: Overlap between differentially expressed genes for each stimulation group.** Kolf2 macrophages were infected with *S*. Typhi Quailes, SGB90, Ty101 or Ty116 strains at MOI of 10 and incubated for 6 hours, with 3 biological replicates completed per condition. Differential expression was calculated for SGB90, Ty101 and Ty116 infections versus Quailes infection. There are fewer genes DE between SGB90 and Quailes than between either of the H58 and Quailes *S*. Typhi. Ty101 has the highest number of DE genes, with a large degree of overlap between those DE in Ty101 and Ty116.

Solely DE in SGB90 was ESM1, or Endocan, a proteoglycan molecule which is a marker of endothelial activation in typhoid fever[65] and the expression of which has been shown to correspond with severity of illness in sepsis.[66] This was comparatively downregulated in SGB90 infected macrophages. HAS2 is a constituent of the extracellular matrix which regulates cell adhesion, differentiation and migration and was also downregulated. PITPNM3, highly upregulated in both SGB90 and Ty116 is thought to catalyse the transfer of phosphatidylinositol between membranes and bind calcium ions, particularly relevant given that maturation of Salmonella containing vacuoles requires formation of phosphatidylinositol 3-phosphate (PI(3)P) on their outer leaflet.[67]

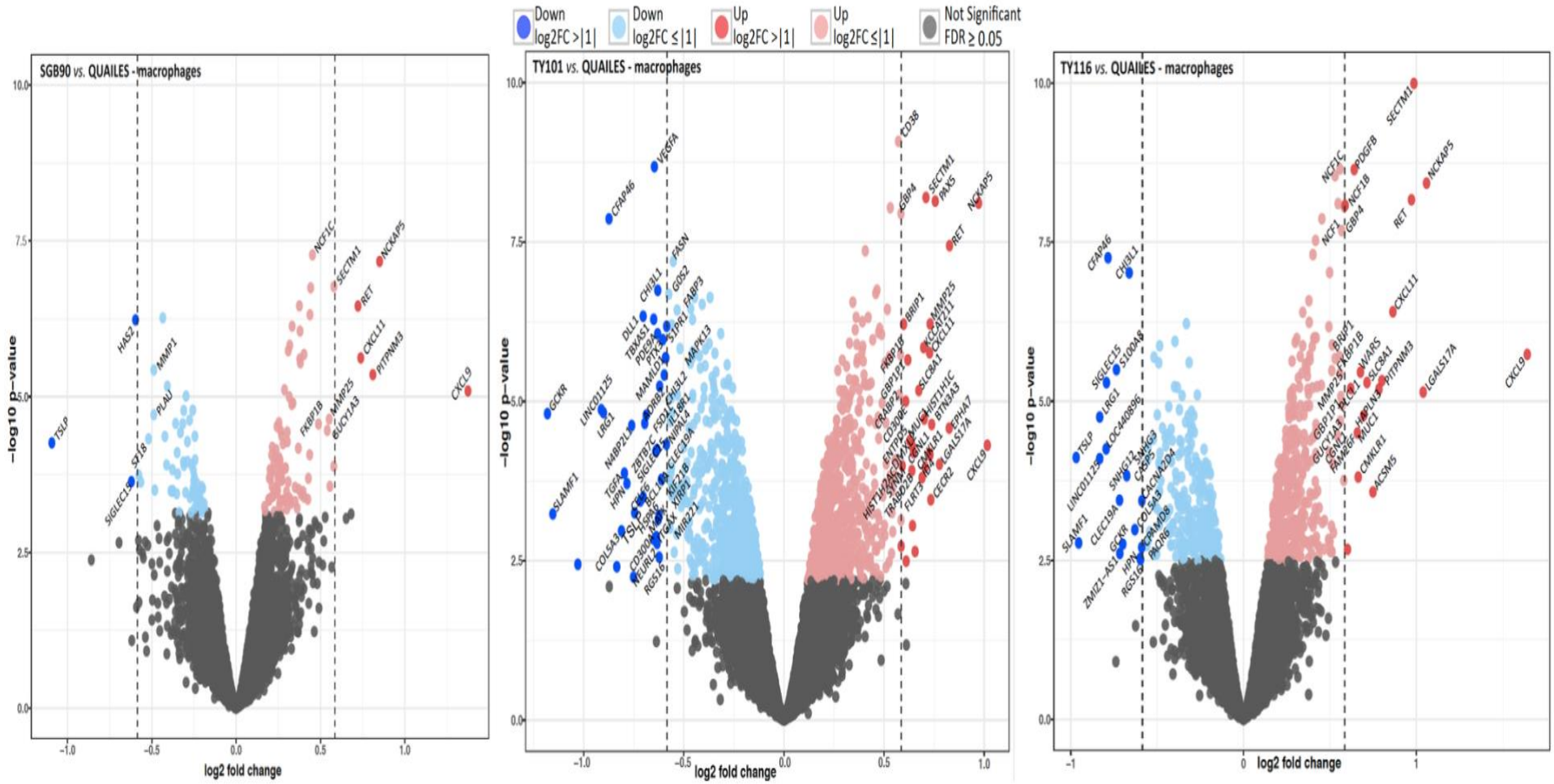


**Figure 6.49: Volcano plots for top genes differentially expressed between each stimulation and control (Quailes strain).** Kolf2 macrophages were infected with *S*. Typhi Quailes, SGB90, Ty101 or Ty116 strains at MOI of 10 and incubated for 6 hours, with 3 biological replicates completed per condition. Differential expression was calculated for SGB90, Ty101 and Ty116 infections versus Quailes infection. There are few differences between SGB90 and Quailes infected macrophages, but larger differences between H58-strain infected macrophages and Quailes, with genes both up and downregulated, implying both activation and suppression of cellular machinery.

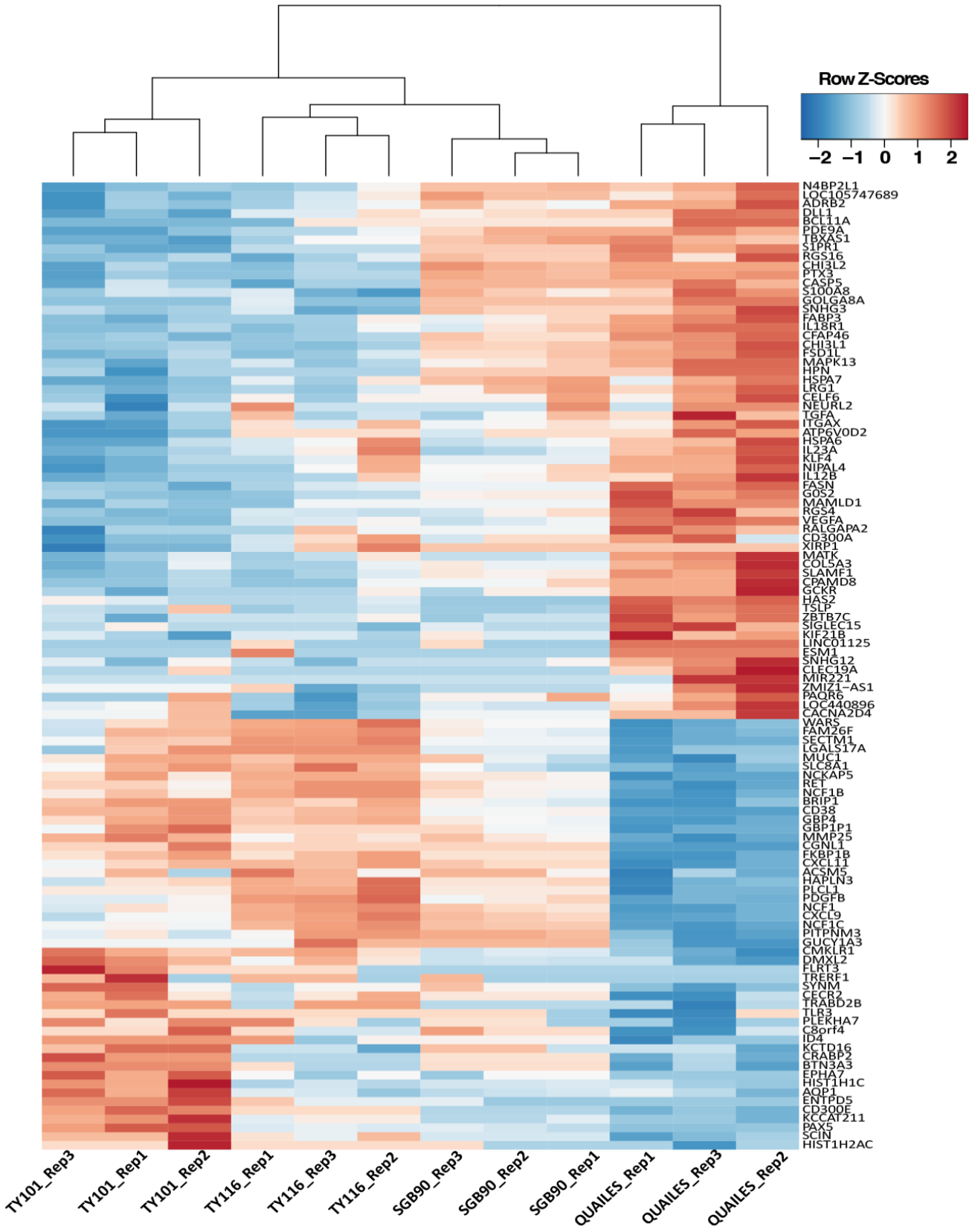


**Figure 6.50: Heatmap of top genes explaining most variance in the transcriptome across all infection conditions.** Kolf2 macrophages were infected with *S*. Typhi Quailes, SGB90, Ty101 or Ty116 strains at MOI of 10 and incubated for 6 hours, with 3 biological replicates completed per condition. Data presented are top genes (logFC > 0.55) differentially expressed in at least one comparison, the colour key shows the expression level differences between Quailes and the other three stimulation conditions, reported as the Z-score (scaled row-wise, mean = 0, SD = 1 ).

Whilst there was no overarching biological process covered by the genes solely upregulated in Ty116 stimulated cells, many of these genes have a clear biological role in the immune response, with CACNA2D4, FAM26f and PLCL1 being associated with calcium channels or calcium binding, NCF1B involved in superoxide production and WARS being induced by IFNγ and involved in tryptophan metabolism, which has recently been shown to have a role in the pathogenesis of typhoid fever.[62]

Similarly, for those genes DE in both of the H58-infected macrophages, there was no single biological process, but a number of these genes are worth highlighting, such as CECR2 (upregulated) and SLAMF1 (downregulated), which play roles in vesicular trafficking and phagosomal maturation, with SLAM1 also inducing IFNγ release. SIGLEC15, RGS16 and SLC8A1 (all downregulated) being involved in calcium ion exchange, and CHI3L1 which is also expressed on the intestinal epithelium and expression of which facilitates bacterial entry into the intestinal mucosa, promotes development of colitis[68] and activation of the IL-6/STAT3 and NFκB signalling pathways[69] also being downregulated. Lastly, in both H58-strains S100A8 was also downregulated. This gene has a number of antibacterial functions, such as calcium binding, activation of NADPH oxidase, induction of apoptosis, cytokine production and TLR4 binding to activate the pro-inflammatory cascade via NFκB pathway. It can exist as a heterodimer with S100A9 (calprotectin), which can inhibit growth of *S*. Typhimurium and *S*. Typhi in vitro and has been found to be markedly elevated in serum and stools of patients with typhoid fever.[70,71] It clearly has the capacity to amplify the inflammatory response engendered by infection, which could either be beneficial or harmful, with studies noting ability to produce S100A8/9 to be associated with endotoxin-induced shock,[52] and levels to be correlated with severity of disease in sepsis.[72] Intriguingly, the fact that both S100A8 and CHI3L1 are downregulated, as well as many of the other genes described above, implies that the H58 strains have methods of dampening the immune response whilst inside of the macrophage.

Finally, looking at genes which are DE in the most invasive H58 *S.* Typhi; Ty101, a couple of patterns emerge. Genes upregulated largely have roles in cytoskeletal structure and maintenance (CGNL1, FLRT3, PLEKHA7, SCIN, SYNM) processes which can be modified by *Salmonella* infection.[73] Many genes involved in DNA repair and replication were highlighted, (BRIP1, CD300E, EPHA7, ID4, TRERF1, HIST1H1C, HIST1H2AC, BCL11A, CELF6, FABP3, KLF4,

MAMLD1, N4BP2L1, ZBTB7C) but were up and down-regulated in equal measure. Signal transduction-related genes were downregulated (MATK, PDE9A, RGS4), as were metal ion binding genes (NIPAL4, TBXAS1) and further genes involved in vesicle production and transport (ATP6V0D2, ADRB2, GOLGA8a, TGFA), suggesting successful replication of Ty101 in cells because of a suppression of phagolysosomal function. Other genes worth highlighting as downregulated are VEGFA, a gene involved in cell migration and inhibitor of apoptosis, which has been shown to be upregulated during *in vivo* Quailes infection,[62] and IL-12B and IL-23A, which together form IL-23, a molecule that stimulates IFN-γ and pro-inflammatory cytokine production.[74] IL-23 also stimulates Th17 cell production and upregulates IL-22 and IL-17 production to form an acute infection response in tissues.[75] Lack of IL-23 is associated with iNTS disease.[75] Overall, these data clearly highlight that there are immunomodulatory processes controlled within the macrophage by H58 *S*. Typhi; in particular the Lineage 2 Ty101, which have led to their success in surviving and replicating within the macrophage and ability to cause disease *in vivo*.

### 6.6 Discussion

Here, the ability of *S*. Typhi and *S*. Paratyphi to interact with iHO was assessed using a variety of assays. It was deemed important to initially perform such assays using iHO derived from cells from a number of stem cell lineages, as this was the first time such data been generated in the hiPSC-derived iHO model. It was thus important not to assume that responses in iHO from one stem cell line were representative of the 'human' response. However, as well as providing valuable data on infection responses, this practice also highlighted that there are numerous potential sources of variance within the data. A previous study on iPSC from 317 cell lines derived from 101 individuals showed that 49.9% of variance at the single gene level was explained by the individual.[44] However, there were also intra-individual sources of variation, including gender, ancestry, age, BMI and even technician completing assays. After eliminating these factors, there was still significant residual variation between cell lines from the same individual. In this study, only one cell line from each donor was used. The HipSci website records a pluripotency and 'novelty' score for each cell line generated. The novelty score represents how closely the line resembles data from other characterised iPSC lines or embryonic stem cell lines.[76] A high

pluripotency and low novelty score are valuable when selecting cell lines. Therefore, for this study, cell lines with these characteristics were chosen. However, there were still some differences between groups in these variables; Kolf2 having a particularly high pluripotency score for example.

In the hiPSC study described above, genes with the highest contribution to variance across individuals were enriched for expression quantitative trait loci (eQTLs) and were associated with metabolic functions. The most varying genes at both high and low expression were those associated with development functions (GO terms included: signal transduction involved in regulation, regionalisation and embryonic morphogenesis). The cell lines chosen for this study varied in terms of demographics, with age, gender and ethnicity varying between lines. This initially seemed a good way to capture a more population-representative response to infection, however it is difficult to know whether the differences detected in the Rayr2 cell line are due to factors such as age (this donor was 75-79, versus 45-49 and 55-59 for the other lines), with number of eQTLs having been shown to decrease with age, whilst variation in expression simultaneously increased[77] or other sources of variation such as iHO differentiation stage. It is well established that the immune system undergoes remodelling and decline with old age, with reduced T cell numbers, impaired cytokine production[78] and reduced pathogen clearance by neutrophils and macrophages.[79] There is also loss of gut bacterial homeostasis with microbiotal diversity declining.[80] The iHO model does not incorporate immune cell function and there is relatively little known about how gut epithelial immunity changes in old age, but studies have shown both that intrinsic ageing of gut stem cells does occur, with impaired response to DNA damage[81] and changes in terms of increased intestinal permeability with remodelling of tight junctions.[82] It is not a huge leap therefore to assume that there may be some age-related contribution to the apparently dampened response and increased *S*. Paratyphi A counts seen in the Rayr2 iHO. It is worth noting however that there are inherently more variables to consider in this study than the iPSC study, given that cells in the iHO will be undergoing differentiation processes, rather than being held in the hiPSC state as in the characterisation study, so it is difficult to draw conclusions based on this limited dataset. If possible, it would be ideal to repeat these experiments on a larger scale with more cell lines, but at present the methods required for iHO growth and microinjection are relatively low throughput techniques.

It is frustrating that despite being able to clearly show *S*. Typhi and *S*. Typhimurium interacting with the epithelium on TEM and demonstrate intracellular counts of bacteria on infection assays, that it has not been possible to produce an image of one of these bacteria inside an IEC. It is possible that the low infectivity of *S*. Typhi at least would require many cells to be imaged before intracellular bacteria could be located, but this issue also raises questions about whether bacteria are definitely invading the epithelium. hiPSC-derived iHO are not known to contain M-cells, a route via which *Salmonella* can cross the intestinal epithelium, however a study using both explanted intestinal biopsies and organoid-derived monolayers which did contain M-cells, was only able to demonstrate invasion into enterocytes,[32] suggesting that lack of M-cells is not a barrier to invasion in this case.

Given the images of both *S*. Typhi and *S*. Paratyphi A dividing in the mucus layer; which is particularly well defined using high pressure freezing (**Figure 6.51**), the question arises of whether bacteria recovered are those sitting in the mucous layer rather than intracellularly.

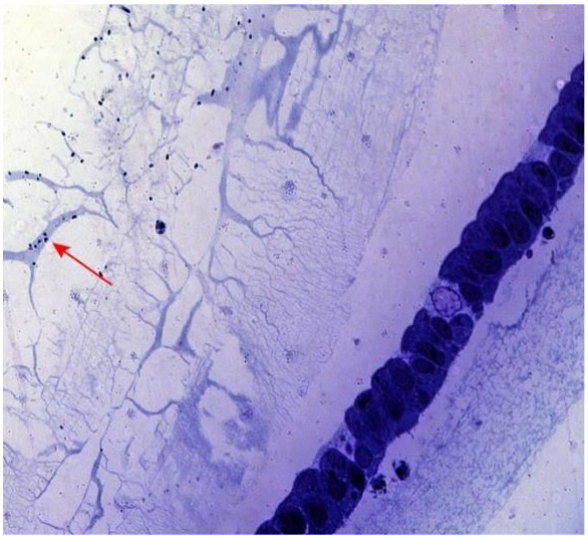

**Figure 6.51: Toluidine blue image of iHO lumen produced by high pressure freezing.** Kolf2 iHO were injected with *S*. Typhi (Quailes) and incubated for 3 hours prior to high pressure freezing. Note the well-preserved mucus layer and presence of *S*. Typhi within this layer.

This is less likely to be the case given that luminal and intracellular counts recovered were both high and similar for *S*. Typhi and *S*. Paratyphi, but low and significantly different for intracellular counts. It has also been demonstrated that gentamicin does penetrate gut epithelial mucus and show killing activity against *S.* Tyhpimurium,[83] and given the antibiotic sensitivities for Quailes and NVGH308 there is no reason why this would not also be the case in this study. The fact that there are significant and different transcriptomic

perturbations between each stimulation condition also suggests that bacteria were located intracellularly. On a wider scale, the ability of *S*. Typhi to survive in the intestinal mucus layer does however raise the idea that it may achieve a similar feat in the mucus lining the gallbladder, perhaps a concept to consider for future studies on *S*. Typhi carriage.

Additional information about behaviour of *S*. Paratyphi A in the intestinal lumen was garnered during this study, with TEM imaging demonstrating the presence of pili radiating from these bacteria in some images. Pili are often used as vessels for DNA transfer between Gram-negative bacterial strains[84] and are able to expand and retract, bringing bacterial cells together and increasing stability of connection prior to DNA transfer.[85] The potential ability of *S*. Paratyphi A to share DNA in this way would be an important topic to investigate, given the current increase in prevalence of *S*. Paratyphi A in some regions,[86] and increasing incidence of MDR *S*. Paratyphi A in Asia.[87-89] Studies describing antimicrobial resistance in *S*. Paratyphi A point to plasmids as a possible mediator of resistance, although molecular studies are limited thus far.[90-92] It has been demonstrated that similar IncHI1 plasmids are able to encode MDR phenotype in both *S*. Typhi and *S*. Paratyphi A. These plasmids share a very well conserved DNA core, but are able to acquire mobile elements encoding antibiotic resistance genes.[93,94] If AMR genes are able to be transferred by *S*. Paratyphi A via pili, this has important implications for the need to increase resources aimed at controlling spread of this pathogen, particularly given the current absence of an effective vaccine against *S*. Paratyphi A.[85]

One other interesting observation regarding *S*. Paratyphi A is that it infected the iHO epithelium at similar levels to S. Typhimurium, yet appeared less invasive than this pathogen in the macrophage model, displaying more gene overlap with *S*. Typhi than *S*. Paratyphi A in this environment. It has been demonstrated that *S*. Paratyphi A expresses lower levels of SPI-1 effector proteins than does *S*. Typhimurium, particularly under aerobic growth conditions.[46] Overexpression of the SPI-1 activator HilA in *S*. Paratyphi A was able to elevate SPI-1 gene expression, increase host cell invasion, pro-inflammatory cytokine release and disruption of epithelial integrity. This suggests that in *S*. Paratyphi A, SPI-1 expression is naturally downregulated, and suppression of SPI-1 components at a higher oxygen tension could be a mechanism to reduce inflammatory response and detection once having passed

through the gut; given that *S*. Paratyphi A causes a similar clinical phenotype to *S*. Typhi but is lacking in SPI-7 to assist in immune evasion. This would fit with the relatively higher oxygen concentration experienced during macrophage infections, but low oxygen concentration in the iHO lumen where *S*. Paratyphi proved most invasive and inflammatory.

Analysis of supernatants of infected iHO revealed some interesting insights into epithelial response to infection. Despite being grown under the same conditions, baseline levels of cytokines tended to be quite variable between replicates within each cell line, perhaps due to differences in seeding density and metabolic status between different plates. Designing the assay was tricky, as cytokines had to be selected to encompass those which could be produced either by epithelial cells or macrophages, those which had been significantly upregulated shortly after human challenge (and thus potentially demonstrating an 'epithelial signature' in response to infection),[62] and those which it was possible to put on the same Luminex assay and to sample at the same timepoint (with 1.5 hours likely being too early to pick up on cytokine which is not released from intracellular stores). One problem with using EGF was that this cytokine is included in iHO base growth medium, so it was not possible to draw any meaningful conclusions about whether an epithelial EGF signature could be picked up in the blood. IECs could be a potential source of the signature, given that stimulation of the EGF receptor has been shown to be involved in internalisation of *S*. Typhimurium into cultured cells.[95] Of interest also, was that a study using intestinal biopsies infected with *S*. Typhi or *S*. Typhimurium found that cytokine release from cells was predominantly apical in cells infected with *S*. Typhi as opposed to bidirectional for *S*. Typhimurium infected cells.[32] This is an intriguing mechanism by which to evade the host inflammatory response by controlling direction of release of cytokines to reduce their effect. It may also explain the limited elevation in some cytokines in the iHO study, as the medium in contact with the basal surface of the iHO was sampled. It would therefore be interesting to break up the structure of the iHO and sample media which also contains luminal contents. Overall, iHO cytokine results were consistent with those for other studies attempting to replicate the gut epithelial response to infection and those possibly constituting the 'epithelial infection signature' in the human challenge model. A model using intestinal cells and fibroblasts, with or without PBMCs demonstrated release of IL-6, TNF$\alpha$, IL-8, IL-1$\beta$ and IL-17A in response to *S*. Typhi infection, with IL-1$\beta$, IL-6 and TNF$\alpha$ secretion

all higher if the model was co-cultured with immune cells, and IL-8 secretion also noted from fibroblasts.[74] IL-6 is thought to have a role in epithelial repair,[96] so it may be that expression of this was higher in *S*. Paratyphi A in this study, given that more *S*. Paratyphi A were invading and potentially damaging the epithelium than were *S*. Typhi. Another human challenge study noted that *S*. Typhi Quailes with toxin gene knockouts were equally able to cause clinical disease as wild type Quailes. Cytokine profiling was done here at the time of diagnosis and showed IL-1RA to be significantly elevated over baseline in both groups. IL-8, IL-2 and IL-1RA levels were noted to be higher in wild type infection, but TNF-$\alpha$ to be higher in toxin negative disease, suggesting that the typhoid toxin may also play a role in modifying host responses to infection.[97]

Cytokine responses observed within the macrophage model were surprisingly uniform across pathogens. For the cytokines of interest as possibly being related to an epithelial infection response (elevated at 12 hours after *S*. Typhi exposure in the human challenge model),[62] EGF, CD40-L, GRO$\alpha$ and IL-1RA were all significantly elevated in supernatants from macrophages within 6 hours of infection, so it could be that macrophages are another source of this signature. Whole blood isolates from participants in challenge studies stimulated with *S*. Typhi also showed large responses in IL-6, IL-8, GRO$\alpha$, TNF$\alpha$ and IL-1RA (Amber Barton, unpublished data), so there appear to be similarities between *S*. Typhi responses in the hiPSC derived macrophage model and those occurring *in vivo*. Again, it would be interesting to study alternative timepoints after infection to determine how rapidly this cytokine response occurs and how long-lasting it is. It could be possible that *S*. Typhi produce a dampened early host response, allowing it to replicate inside of the SCV by 6 hours, at which point a large inflammatory response is more likely. Alternatively, these results may represent a reduced ability of macrophages in culture to kill intracellular pathogens without external stimulation; priming by IFN$\gamma$ may be required to more closely replicate physiological conditions *in vivo*; as levels of IL-1β, TNFα and IL-6 were enhanced in hiPSC derived macrophages pre-treated with IFN$\gamma$ prior to *S.* Typhi BRD948 infection and improved bacterial killing (although of note, this is an attenuated strain).[7] A different hypothesis explaining the similarities in transcriptomic and cytokine responses seen to all pathogens could be that *S*. Typhi is no longer expressing the Vi

capsule once inside of the macrophages. *S*. Typhi not expressing the Vi capsule were demonstrated to induce a higher TNFα response than encapsulated *S*. Typhi.[98] The gene TviA which positively regulates the Vi capsule is repressed in high-osmolarity environments and induced in low-osmolarity environments[46], perhaps the transition from a low osmolarity culture medium to a higher osmolarity intracellular environment after phagocytosis could induce this switch and loss of capsule. Potential evidence for this hypothesis is seen in TEM images of *S*. Typhi within macrophages in this study, as there appeared to be shedding / disintegration of the Vi capsule of some of the *S*. Typhi captured via imaging.

In spite of the differing behaviour exhibited by serovars within the epithelial and macrophage compartments, there were a number of commonalities in the transcriptomic response between the hiPSC-derived macrophages and iHO, with the top 3 KEGG pathways upregulated for all pathogens known to be important early responders to Salmonella infection; namely the TNF signalling pathway, IL-17 pathway and NFκB signalling pathway.

As outlined above there were inherent sources of variation in the transcriptome in iHO between cell lines. What the macrophage studies demonstrated was that this variation is also present within cell line, with batches of macrophages produced a week apart demonstrating transcriptomic responses that were more similar between pathogens than between replicates. These differences could be due to variation in maturation as the embryoid bodies from which their monocyte pre-cursors are harvested age, as well as coming from any number of experimental sources, such as batches of media and cytokines used in macrophage production or the experiment itself, incubator conditions and bacterial cultures on the day of experiment and technician technique (although in this case all experiments were done by the same person, hopefully limiting this factor). Factors such as intracellular bacterial counts and cytokine levels were relatively reproducible between assays, however at the transcriptomic level differences became apparent. It was therefore valuable to be able to tune analyses to incorporate these batch effects, assuming the same bias occurred with each set of replicates. Whilst the Kolf2 cell line is widely used and well phenotyped, had time allowed, it would have been preferable to repeat these assays in a number of different cell lines too, in order to investigate inter-individual as well as intra-individual differences in response to infection.

It was interesting that the transcriptomic response for *S*. Typhi, *S*. Paratyphi A and *S*. Typhimurium within the macrophages was relatively uniform, given the differences seen within the epithelial model. It does however make sense that many of the genes expressed once within the macrophage (e.g. for replication) would be similar between the serovars, thus likely inducing similar responses from the host cell. The most interesting results were seen when looking at the DE genes specific to each pathogen, as these revealed possible insights into alteration of host cell response differing between serovars. It was also intriguing to be able to see clear differences in the macrophage response to the 3 different *S*. Typhi strains versus Quailes, given the genetic similarities between those isolates from different *S.* Typhi clades.

The lack of variability between response to H58 versus non-H58 observed in the iHO model was in stark contrast to that observed in the macrophage model, suggesting that it is the ability of H58 *S*. Typhi to alter host response in this compartment which has led to their successful expansion and potential to cause severe disease. The increased ability of H58 isolates to survive within the macrophage observed in this study, seemingly via dampening of the immune response could be mediated by proteins secreted by the type 3 secretion system (T3SS), as seen with Typhi neutralising the Rab32/Bloc3 pathway,[99] since manifold effects of the *Salmonella* T3SS exist within eukaryotic cells.[100] Studies of invasion and response at different time points would help to learn more about the early and late host cell responses to infection with these pathogens. It would be fascinating to study more of these H58 *S*. Typhi to look for these mechanisms and determine whether changes in invasiveness and ability to survive are widespread. One method would be to look at simultaneous transcriptomic responses during infection in both the bacteria and the host cell. One study has commenced this process in the intestinal compartment, with *S*. Typhi being sequenced following invasion of ileal biopsy samples. Upregulated genes encoded acetyltransferases and serine/threonine kinases, implying modulation of host signalling was taking place.[32]

**References:**


1. Waddington CS, Darton TC, Jones C, et al. An outpatient, ambulant-design, controlled human infection model using escalating doses of Salmonella Typhi challenge delivered in sodium bicarbonate solution. *Clin Infect Dis.* 2014;58(9):1230-1240.
2. Holt KE, Parkhill J, Mazzoni CJ, et al. High-throughput sequencing provides insights into genome variation and evolution in Salmonella Typhi. *Nat Genet.* 2008;40(8):987-993.
3. Levine MM, Tacket CO, Sztein MB. Host-Salmonella interaction: human trials. *Microbes Infect.* 2001;3(14-15):1271-1279.
4. Hornick RB, Greisman SE, Woodward TE, DuPont HL, Dawkins AT, Snyder MJ. Typhoid fever: pathogenesis and immunologic control. *N Engl J Med.* 1970;283(13):686-691.
5. Dobinson HC, Gibani MM, Jones C, et al. Evaluation of the Clinical and Microbiological Response to Salmonella Paratyphi A Infection in the First Paratyphoid Human Challenge Model. *Clin Infect Dis.* 2017;64(8):1066-1073.
6. Crump JA, Mintz ED. Global trends in typhoid and paratyphoid Fever. *Clin Infect Dis.* 2010;50(2):241-246.
7. Hale C, Yeung A, Goulding D, et al. Induced pluripotent stem cell derived macrophages as a cellular system to study salmonella and other pathogens. *PLoS One.* 2015;10(5):e0124307.
8. Roumagnac P, Weill FX, Dolecek C, et al. Evolutionary history of Salmonella typhi. *Science.* 2006;314(5803):1301-1304.
9. Wong VK, Baker S, Pickard DJ, et al. Phylogeographical analysis of the dominant multidrug-resistant H58 clade of Salmonella Typhi identifies inter- and intracontinental transmission events. *Nat Genet.* 2015;47(6):632-639.
10. Klemm EJ, Gkrania-Klotsas E, Hadfield J, et al. Emergence of host-adapted Salmonella Enteritidis through rapid evolution in an immunocompromised host. *Nat Microbiol.* 2016;1:15023.
11. Parry CM, Thompson C, Vinh H, et al. Risk factors for the development of severe typhoid fever in Vietnam. *BMC Infect Dis.* 2014;14:73.

12. Bano-Zaidi M, Aguayo-Romero M, Campos FD, et al. Typhoid fever outbreak with severe complications in Yucatan, Mexico. *Lancet Glob Health.* 2018;6(10):e1062-e1063.
13. Bishop A, House D, Perkins T, Baker S, Kingsley RA, Dougan G. Interaction of Salmonella enterica serovar Typhi with cultured epithelial cells: roles of surface structures in adhesion and invasion. *Microbiology.* 2008;154(Pt 7):1914-1926.
14. Tam CK, Hackett J, Morris C. Salmonella enterica serovar Paratyphi C carries an inactive shufflon. *Infect Immun.* 2004;72(1):22-28.
15. Liao Y, Smyth GK, Shi W. featureCounts: an efficient general purpose program for assigning sequence reads to genomic features. *Bioinformatics.* 2014;30(7):923-930.
16. Wilson RP, Winter SE, Spees AM, et al. The Vi capsular polysaccharide prevents complement receptor 3-mediated clearance of Salmonella enterica serotype Typhi. *Infect Immun.* 2011;79(2):830-837.
17. Wangdi T, Lee CY, Spees AM, et al. The Vi capsular polysaccharide enables Salmonella enterica serovar typhi to evade microbe-guided neutrophil chemotaxis. *PLoS Pathog.* 2014;10(8):e1004306.
18. Zhang Q, Calafat J, Janssen H, Greenberg S. ARF6 is required for growth factor- and rac-mediated membrane ruffling in macrophages at a stage distal to rac membrane targeting. *Mol Cell Biol.* 1999;19(12):8158-8168.
19. Coon C, Beagley KW, Bao S. The role of granulocyte macrophage-colony stimulating factor in gastrointestinal immunity to salmonellosis. *Scand J Immunol.* 2009;70(2):106-115.
20. Dlugosz A, Muschiol S, Zakikhany K, Assadi G, D'Amato M, Lindberg G. Human enteroendocrine cell responses to infection with Chlamydia trachomatis: a microarray study. *Gut Pathog.* 2014;6:24.
21. Zhou D, Chen LM, Hernandez L, Shears SB, Galan JE. A Salmonella inositol polyphosphatase acts in conjunction with other bacterial effectors to promote host cell actin cytoskeleton rearrangements and bacterial internalization. *Mol Microbiol.* 2001;39(2):248-259.
22. Stender S, Friebel A, Linder S, Rohde M, Mirold S, Hardt WD. Identification of SopE2 from Salmonella typhimurium, a conserved guanine nucleotide exchange factor for Cdc42 of the host cell. *Mol Microbiol.* 2000;36(6):1206-1221.

23. Godinez I, Raffatellu M, Chu H, et al. Interleukin-23 orchestrates mucosal responses to Salmonella enterica serotype Typhimurium in the intestine. *Infect Immun.* 2009;77(1):387-398.
24. Forbester JL, Goulding D, Vallier L, et al. Interaction of Salmonella enterica Serovar Typhimurium with Intestinal Organoids Derived from Human Induced Pluripotent Stem Cells. *Infect Immun.* 2015;83(7):2926-2934.
25. Masin M, Vazquez J, Rossi S, et al. GLUT3 is induced during epithelial-mesenchymal transition and promotes tumor cell proliferation in non-small cell lung cancer. *Cancer Metab.* 2014;2:11.
26. Becker KW, Skaar EP. Metal limitation and toxicity at the interface between host and pathogen. *FEMS Microbiol Rev.* 2014;38(6):1235-1249.
27. Darton TC, Blohmke CJ, Giannoulatou E, et al. Rapidly Escalating Hepcidin and Associated Serum Iron Starvation Are Features of the Acute Response to Typhoid Infection in Humans. *PLoS Negl Trop Dis.* 2015;9(9):e0004029.
28. Barquist L, Langridge GC, Turner DJ, et al. A comparison of dense transposon insertion libraries in the Salmonella serovars Typhi and Typhimurium. *Nucleic Acids Res.* 2013;41(8):4549-4564.
29. Santos AJ, Meinecke M, Fessler MB, Holden DW, Boucrot E. Preferential invasion of mitotic cells by Salmonella reveals that cell surface cholesterol is maximal during metaphase. *J Cell Sci.* 2013;126(Pt 14):2990-2996.
30. Botteaux A, Hoste C, Dumont JE, Van Sande J, Allaoui A. Potential role of Noxes in the protection of mucosae: H(2)O(2) as a bacterial repellent. *Microbes Infect.* 2009;11(5):537-544.
31. Grasberger H, Gao J, Nagao-Kitamoto H, et al. Increased Expression of DUOX2 Is an Epithelial Response to Mucosal Dysbiosis Required for Immune Homeostasis in Mouse Intestine. *Gastroenterology.* 2015;149(7):1849-1859.
32. Nickerson KP, Senger S, Zhang Y, et al. Salmonella Typhi Colonization Provokes Extensive Transcriptional Changes Aimed at Evading Host Mucosal Immune Defense During Early Infection of Human Intestinal Tissue. *EBioMedicine.* 2018;31:92-109.
33. Meseguer V, Alpizar YA, Luis E, et al. TRPA1 channels mediate acute neurogenic inflammation and pain produced by bacterial endotoxins. *Nat Commun.* 2014;5:3125.

34. Jung HC, Eckmann L, Yang SK, et al. A distinct array of proinflammatory cytokines is expressed in human colon epithelial cells in response to bacterial invasion. *J Clin Invest.* 1995;95(1):55-65.
35. Klimpel GR, Asuncion M, Haithcoat J, Niesel DW. Cholera toxin and Salmonella typhimurium induce different cytokine profiles in the gastrointestinal tract. *Infect Immun.* 1995;63(3):1134-1137.
36. Vincenz C, Dixit VM. Fas-associated death domain protein interleukin-1beta-converting enzyme 2 (FLICE2), an ICE/Ced-3 homologue, is proximally involved in CD95- and p55-mediated death signaling. *J Biol Chem.* 1997;272(10):6578-6583.
37. Kotlinowski J, Bukowska-Strakova K, Koppolu A, et al. A Novel Monoallelic Nonsense Mutation in the NFKB2 Gene Does Not Cause a Clinical Manifestation. *Front Genet.* 2019;10:140.
38. Fiorentino M, Lammers KM, Levine MM, Sztein MB, Fasano A. In vitro Intestinal Mucosal Epithelial Responses to Wild-Type Salmonella Typhi and Attenuated Typhoid Vaccines. *Front Immunol.* 2013;4:17.
39. Hedstrom L. Serine protease mechanism and specificity. *Chem Rev.* 2002;102(12):4501-4524.
40. Xia L, Li S, Liu Y, et al. NDNF inhibits the migration and invasion of human renal cancer cells through epithelial-mesenchymal transition. *Oncol Lett.* 2019;17(3):2969-2975.
41. Lappin TR, Grier DG, Thompson A, Halliday HL. HOX genes: seductive science, mysterious mechanisms. *Ulster Med J.* 2006;75(1):23-31.
42. Yasuno K, Bakircioglu M, Low SK, et al. Common variant near the endothelin receptor type A (EDNRA) gene is associated with intracranial aneurysm risk. *Proc Natl Acad Sci U S A.* 2011;108(49):19707-19712.
43. Brockdorff N, Duthie SM. X chromosome inactivation and the Xist gene. *Cell Mol Life Sci.* 1998;54(1):104-112.
44. Carcamo-Orive I, Hoffman GE, Cundiff P, et al. Analysis of Transcriptional Variability in a Large Human iPSC Library Reveals Genetic and Non-genetic Determinants of Heterogeneity. *Cell Stem Cell.* 2017;20(4):518-532 e519.

45. Weinstein DL, O'Neill BL, Metcalf ES. Salmonella typhi stimulation of human intestinal epithelial cells induces secretion of epithelial cell-derived interleukin-6. *Infect Immun.* 1997;65(2):395-404.
46. Elhadad D, Desai P, Grassl GA, McClelland M, Rahav G, Gal-Mor O. Differences in Host Cell Invasion and Salmonella Pathogenicity Island 1 Expression between Salmonella enterica Serovar Paratyphi A and Nontyphoidal S. Typhimurium. *Infect Immun.* 2016;84(4):1150-1165.
47. Yeung ATY, Hale C, Lee AH, et al. Exploiting induced pluripotent stem cell-derived macrophages to unravel host factors influencing Chlamydia trachomatis pathogenesis. *Nat Commun.* 2017;8:15013.
48. Baldassarre M S-CV, Balci A, Wilson H, Mukhopadhyay S, Dougan G, Spano S. Salmonella Typhi survives in human macrophages by neutralizing the RAB32/BLOC-3 host-defence pathway. *bioRxiv* 2019;570531.
49. Risso D, Ngai J, Speed TP, Dudoit S. Normalization of RNA-seq data using factor analysis of control genes or samples. *Nat Biotechnol.* 2014;32(9):896-902.
50. Withanage GS, Kaiser P, Wigley P, et al. Rapid expression of chemokines and proinflammatory cytokines in newly hatched chickens infected with Salmonella enterica serovar typhimurium. *Infect Immun.* 2004;72(4):2152-2159.
51. Parween F, Yadav J, Qadri A. The Virulence Polysaccharide of Salmonella Typhi Suppresses Activation of Rho Family GTPases to Limit Inflammatory Responses From Epithelial Cells. *Front Cell Infect Microbiol.* 2019;9:141.
52. Billker O, Popp A, Brinkmann V, et al. Distinct mechanisms of internalization of Neisseria gonorrhoeae by members of the CEACAM receptor family involving Rac1- and Cdc42-dependent and -independent pathways. *EMBO J.* 2002;21(4):560-571.
53. Daniwijaya EW, Murata Y, Kotani T, et al. Tyrosine Phosphorylation of Carcinoembryonic Antigen-related Cell Adhesion Molecule 20 and Its Functional Role. *Kobe J Med Sci.* 2013;59(5):E172-E183.
54. Feuillet V, Medjane S, Mondor I, et al. Involvement of Toll-like receptor 5 in the recognition of flagellated bacteria. *Proc Natl Acad Sci U S A.* 2006;103(33):12487-12492.

55. Dunstan SJ, Hawn TR, Hue NT, et al. Host susceptibility and clinical outcomes in toll-like receptor 5-deficient patients with typhoid fever in Vietnam. *J Infect Dis.* 2005;191(7):1068-1071.

56. Ma J, Zhang YG, Xia Y, Sun J. The inflammatory cytokine tumor necrosis factor modulates the expression of Salmonella typhimurium effector proteins. *J Inflamm (Lond).* 2010;7:42.

57. Mayuzumi H, Inagaki-Ohara K, Uyttenhove C, Okamoto Y, Matsuzaki G. Interleukin-17A is required to suppress invasion of Salmonella enterica serovar Typhimurium to enteric mucosa. *Immunology.* 2010;131(3):377-385.

58. Simon R, Samuel CE. Activation of NF-kappaB-dependent gene expression by Salmonella flagellins FliC and FljB. *Biochem Biophys Res Commun.* 2007;355(1):280-285.

59. Jin C, Gibani MM, Moore M, et al. Efficacy and immunogenicity of a Vi-tetanus toxoid conjugate vaccine in the prevention of typhoid fever using a controlled human infection model of Salmonella Typhi: a randomised controlled, phase 2b trial. *Lancet.* 2017;390(10111):2472-2480.

60. Blohmke CJ, Hill J, Darton TC, et al. Induction of Cell Cycle and NK Cell Responses by Live-Attenuated Oral Vaccines against Typhoid Fever. *Front Immunol.* 2017;8:1276.

61. McArthur MA, Fresnay S, Magder LS, et al. Activation of Salmonella Typhi-specific regulatory T cells in typhoid disease in a wild-type S. Typhi challenge model. *PLoS Pathog.* 2015;11(5):e1004914.

62. Blohmke CJ, Darton TC, Jones C, et al. Interferon-driven alterations of the host's amino acid metabolism in the pathogenesis of typhoid fever. *J Exp Med.* 2016;213(6):1061-1077.

63. Guignot J, Caron E, Beuzon C, et al. Microtubule motors control membrane dynamics of Salmonella-containing vacuoles. *J Cell Sci.* 2004;117(Pt 7):1033-1045.

64. Fornasa G, Tsilingiri K, Caprioli F, et al. Dichotomy of short and long thymic stromal lymphopoietin isoforms in inflammatory disorders of the bowel and skin. *J Allergy Clin Immunol.* 2015;136(2):413-422.

65. de Jong HK, Parry CM, van der Vaart TW, et al. Activation of coagulation and endothelium with concurrent impairment of anticoagulant mechanisms in patients with typhoid fever. *J Infect.* 2018;77(1):60-67.

66. Scherpereel A, Depontieu F, Grigoriu B, et al. Endocan, a new endothelial marker in human sepsis. *Crit Care Med.* 2006;34(2):532-537.
67. Mallo GV, Espina M, Smith AC, et al. SopB promotes phosphatidylinositol 3-phosphate formation on Salmonella vacuoles by recruiting Rab5 and Vps34. *J Cell Biol.* 2008;182(4):741-752.
68. Mizoguchi E. Chitinase 3-like-1 exacerbates intestinal inflammation by enhancing bacterial adhesion and invasion in colonic epithelial cells. *Gastroenterology.* 2006;130(2):398-411.
69. Tran HT, Lee IA, Low D, et al. Chitinase 3-like 1 synergistically activates IL6-mediated STAT3 phosphorylation in intestinal epithelial cells in murine models of infectious colitis. *Inflamm Bowel Dis.* 2014;20(5):835-846.
70. De Jong HK, Achouiti A, Koh GC, et al. Expression and function of S100A8/A9 (calprotectin) in human typhoid fever and the murine Salmonella model. *PLoS Negl Trop Dis.* 2015;9(4):e0003663.
71. Vogl T, Tenbrock K, Ludwig S, et al. Mrp8 and Mrp14 are endogenous activators of Toll-like receptor 4, promoting lethal, endotoxin-induced shock. *Nat Med.* 2007;13(9):1042-1049.
72. van Zoelen MA, Vogl T, Foell D, et al. Expression and role of myeloid-related protein-14 in clinical and experimental sepsis. *Am J Respir Crit Care Med.* 2009;180(11):1098-1106.
73. Fiskin E, Bionda T, Dikic I, Behrends C. Global Analysis of Host and Bacterial Ubiquitinome in Response to Salmonella Typhimurium Infection. *Mol Cell.* 2016;62(6):967-981.
74. Salerno-Goncalves R, Galen JE, Levine MM, Fasano A, Sztein MB. Manipulation of Salmonella Typhi Gene Expression Impacts Innate Cell Responses in the Human Intestinal Mucosa. *Front Immunol.* 2018;9:2543.
75. Godinez I, Keestra AM, Spees A, Baumler AJ. The IL-23 axis in Salmonella gastroenteritis. *Cell Microbiol.* 2011;13(11):1639-1647.
76. Muller FJ, Brandl B, Loring JF. Assessment of human pluripotent stem cells with PluriTest. In: *StemBook.* Cambridge (MA)2008.

77. Vinuela A, Snoek LB, Riksen JA, Kammenga JE. Genome-wide gene expression regulation as a function of genotype and age in C. elegans. *Genome Res.* 2010;20(7):929-937.
78. Simon AK, Hollander GA, McMichael A. Evolution of the immune system in humans from infancy to old age. *Proc Biol Sci.* 2015;282(1821):20143085.
79. Weiskopf D, Weinberger B, Grubeck-Loebenstein B. The aging of the immune system. *Transpl Int.* 2009;22(11):1041-1050.
80. Biagi E, Candela M, Turroni S, Garagnani P, Franceschi C, Brigidi P. Ageing and gut microbes: perspectives for health maintenance and longevity. *Pharmacol Res.* 2013;69(1):11-20.
81. Kirkwood TB. Intrinsic ageing of gut epithelial stem cells. *Mech Ageing Dev.* 2004;125(12):911-915.
82. Tran L, Greenwood-Van Meerveld B. Age-associated remodeling of the intestinal epithelial barrier. *J Gerontol A Biol Sci Med Sci.* 2013;68(9):1045-1056.
83. Dupont A, Kaconis Y, Yang I, et al. Intestinal mucus affinity and biological activity of an orally administered antibacterial and anti-inflammatory peptide. *Gut.* 2015;64(2):222-232.
84. Curtiss R, 3rd. Bacterial conjugation. *Annu Rev Microbiol.* 1969;23:69-136.
85. Clarke M, Maddera L, Harris RL, Silverman PM. F-pili dynamics by live-cell imaging. *Proc Natl Acad Sci U S A.* 2008;105(46):17978-17981.
86. Ochiai RL, Wang X, von Seidlein L, et al. Salmonella paratyphi A rates, Asia. *Emerg Infect Dis.* 2005;11(11):1764-1766.
87. Chandel DS, Chaudhry R, Dhawan B, Pandey A, Dey AB. Drug-resistant Salmonella enterica serotype paratyphi A in India. *Emerg Infect Dis.* 2000;6(4):420-421.
88. Maskey AP, Day JN, Phung QT, et al. Salmonella enterica serovar Paratyphi A and S. enterica serovar Typhi cause indistinguishable clinical syndromes in Kathmandu, Nepal. *Clin Infect Dis.* 2006;42(9):1247-1253.
89. Sood S, Kapil A, Dash N, Das BK, Goel V, Seth P. Paratyphoid fever in India: An emerging problem. *Emerg Infect Dis.* 1999;5(3):483-484.
90. Mandal S, Mandal MD, Pal NK. Antibiotic resistance of Salmonella enterica serovar Paratyphi A in India: emerging and reemerging problem. *J Postgrad Med.* 2006;52(3):163-166.

91. Hasan Z, Rahman KM, Alam MN, et al. Role of a large plasmid in mediation of multiple drug resistance in Salmonella typhi and paratyphi A in Bangladesh. *Bangladesh Med Res Counc Bull.* 1995;21(1):50-54.
92. Zhou Z, McCann A, Weill FX, et al. Transient Darwinian selection in Salmonella enterica serovar Paratyphi A during 450 years of global spread of enteric fever. *Proc Natl Acad Sci U S A.* 2014;111(33):12199-12204.
93. Holt KE, Thomson NR, Wain J, et al. Multidrug-resistant Salmonella enterica serovar paratyphi A harbors IncHI1 plasmids similar to those found in serovar typhi. *J Bacteriol.* 2007;189(11):4257-4264.
94. Sun P, Pan C, Zeng M, et al. Design and production of conjugate vaccines against S. Paratyphi A using an O-linked glycosylation system in vivo. *NPJ Vaccines.* 2018;3:4.
95. Galan JE, Pace J, Hayman MJ. Involvement of the epidermal growth factor receptor in the invasion of cultured mammalian cells by Salmonella typhimurium. *Nature.* 1992;357(6379):588-589.
96. Kuhn KA, Manieri NA, Liu TC, Stappenbeck TS. IL-6 stimulates intestinal epithelial proliferation and repair after injury. *PLoS One.* 2014;9(12):e114195.
97. Gibani MM, Jones E, Barton A, et al. Investigation of the role of typhoid toxin in acute typhoid fever in a human challenge model. *Nat Med.* 2019;25(7):1082-1088.
98. Hirose K, Ezaki T, Miyake M, et al. Survival of Vi-capsulated and Vi-deleted Salmonella typhi strains in cultured macrophage expressing different levels of CD14 antigen. *FEMS Microbiol Lett.* 1997;147(2):259-265.
99. Spano S, Galan JE. A Rab32-dependent pathway contributes to Salmonella typhi host restriction. *Science.* 2012;338(6109):960-963.
100. Ramos-Morales F. Impact of Salmonella enterica Type III Secretion System Effectors on the Eukaryotic Host Cell. *ISRN Cell Biology.* 2012;2012:787934.